15105

APPLICATION OF K-Ar AND FISSION-TRACK DATING TO THE METALLOGENY OF PORPHYRY AND RELATED MINERAL DEPOSITS IN THE CANADIAN CORDILLERA

by

PETER ALLEN CHRISTOPHER

B.Sc., State University of New York at Fredonia, 1966

M.A., Dartmouth College, Hanover, New Hampshire, 1968

A THESIS SUBMITTED IN PARTIAL FULFILMENT OF

THE REQUIREMENTS FOR THE DEGREE OF

DOCTOR OF PHILOSOPHY

in the Department

of

Geological Sciences

We accept this thesis as conforming to the

required standard

THE UNIVERSITY OF BRITISH COLUMBIA

May, 1973

Department of Geology

The University of British Columbia
Vancouver 8, Canada

Date April 27

ABSTRACT

This study evaluates the concept of metallogenic epochs as it applies to porphyry mineral deposits of the Canadian Cordillera, extends the study of the age of porphyry mineral deposits into northern British Columbia and the Yukon Territory, evaluates the usefulness of the fission-track dating method in determining the age and history of porphyry mineral deposits, and demonstrates the usefulness of an Ar^{40} total vs %K isochron plot.

Samples were obtained from six areas in the Canadian Cordillera: the Syenite Range and Burwash Landing area in the Yukon Territory and Cassiar area, Adanac Property, Granisle Mine, and Copper Mountain area in British Columbia. Apatite was separated from the samples for use in fission-track analysis, and co-genetic biotite or hornblende was separated in order to obtain K-Ar checks on the fission-track ages.

A comparison of fifteen apatite fission-track ages with K-Ar ages demonstrates that the apatite fission-track method can be used to age date porphyry mineral deposits, however the K-Ar method is generally more suitable in terms of cost and reliability. Discordant apatite fission-track and biotite K-Ar ages obtained from the Copper Mountain area and Granisle Mine suggest that apparent apatite fission-track ages from highly altered rocks or thermally complex areas should be checked by using another dating method (e.g. K-Ar).

Radiometric dating of the Cassiar Molybdenum, Adanac, Mt. Reed and Mt. Haskin porphyry mineral deposits in northern British Columbia suggests that the Early Tertiary metallogenic epoch for porphyry deposits in central British

Columbia and south-eastern Alaska, can be extended through northern British Columbia.

Post-Eocene intermittent subduction of the Juan de Fuca plate below Vancouver Island and transverse motion along the Fairweather-Queen Charlotte-Shakwak-Denali Fault system with subduction into the Aleutian Trench are consistent with present plate-tectonic theory and the distribution of post-Eocene calc-alkaline igneous rocks in the Canadian Cordillera. If porphyry mineral deposits form in calc-alkaline igneous rocks above active subduction zones, then the youngest porphyry deposits in the Canadian Cordillera should occur west of the Fairweather-Queen Charlotte-Shakwak-Denali fault system, on Vancouver Island and in the Cascade Mountains. The relatively young 26.2 m.y. biotite K-Ar age determined for the Burwash Creek porphyry west of the Shakwak Trench in the Yukon Territory is consistent with the evolution of porphyry mineral deposits above an active subduction zone.

Comparison of K-Ar ages obtained for this study with published K-Ar ages suggests that metallogenic epochs for porphyry mineral deposits in the Canadian Cordillera occurred at approximately 195 m.y. and 150 ± 10 m.y. for deposits of the plutonic and volcanic porphyry classes; and at approximately 100 m.y., 80 m.y., 65 m.y., 50 m.y., 35-40 m.y. and 26 m.y. for deposits of the phallic porphyry class.

ACKNOWLEDGMENTS

Support for this study was provided through grants to Drs. A.J. Sinclair and W.H. White from the National Research Council of Canada and the Geological Survey of Canada. The writer was supported by teaching assistantships and a university fellowship from the University of British Columbia.

The writer appreciates the assistance and co-operation of mining companies involved in exploration in northern British Columbia and the Yukon Territory. G. Brett (Brettland Mines), R. Oddy (Imperial Oil), W. Sirola (Kerr Addison Mines), G. Lamont (Della Mines), and G. LeCheminant (Amax Exploration Inc.) were especially helpful.

Several geologists employed by the British Columbia Department of Mines and by the Geological Survey of Canada provided helpful discussions of the geological settings of porphyry deposits in the Canadian Cordillera. Dr. V.A. Preto and N.C. Carter (B.C. Dept. Mines) and Drs. H. Gabrielse and J.W.H. Monger (Geological Survey of Canada) were especially helpful.

The late Drs. J.A. Gower and W.H. White were instrumental in stimulating the writers interest in porphyry mineral deposits of the Canadian Cordillera. Their advice and encouragement contributed greatly to this study.

Drs. A.J. Sinclair, H.R. Wynne-Edwards, A.E. Soregaroli and W.F. Slawson made suggestions for improvement of the original manuscript. Drs. A.J. Sinclair and H.R. Wynne-Edwards supervised the study.

Numerous members of the Departments of Geological Sciences and

Geophysics helped with useful discussion and advice. Miss Yvonne Colasanti, Mr. G. Cargill, Mr. B. Ryan, and Mr. J. Blenkinsop were especially helpful. Mr. J.E. Harakal supervised the potassium and argon analyses.

CONTENTS

LIST OF TABLES

LIST OF FIGURES

LIST OF FIGURES (Cont.)

LIST OF PLATES

LIST OF PLATES (Cont.)

1. INTRODUCTION

1.1 SCOPE

The purpose of this study is to investigate the age of porphyry mineral deposits in northern British Columbia and southwestern Yukon Territory, and wherever possible, to compare the relatively new fission-track method with the well-known potassium-argon method.

In addition to dating samples from northern British Columbia and the Yukon Territory, where only reconnaissance radiometric dating is available, samples previously dated by the potassium-argon method were obtained from the Copper Mountain area, Brenda Mine and Granisle Mine to compare apatite and (or) sphene fission track ages for these samples.

The isochron method is applied to potassium-argon data obtained for this study and published potassium-argon data from the Topley Intrusions and Guichon Batholith to evaluate the effect of excess initial argon on potassium-argon age determinations. A new Ar^{40} total vs %K, method of plotting isochrons is presented and evaluated.

Finally, the concept of metallogenic epochs is evaluated for porphyry and related mineral deposits in the Canadian Cordillera in the light of the age determinations reported and the new global tectonics.

Six samples from the Burwash Landing area and six samples from the Cassiar area were collected by the writer during the 1969 field season. A sample from the Granisle Mine and ten samples from the Copper Mountain area were obtained from the British Columbia Department of Mines. A sample of coarse alaskite from the Adanac Mine was obtained from W. Sirola of Kerr Addison Mines and two samples of quartz monzonite from the Syenite Range were collected for the writer by C. Godwin and K. Dawson of Atlas Exploration.

Biotite, hornblende, apatite, sphene and zircon were separated from the samples for dating. A sphene concentrate from quartz diorite at Brenda Mines was provided by Dr. W.H. White. Fifteen biotite K-Ar ages, two hornblende K-Ar ages and fifteen apatite fission-track ages were determined by the writer at the University of British Columbia in geochronology laboratories of the Departments of Geological Sciences and Geophysics.

Parts of this study have been published:

Christopher, P.A., White, W.H., and Harakal, J.E., 1972a. K-Ar dating of the 'Cork' (Burwash Creek) Cu-Mo prospect, Burwash Landing area, Yukon Territory. Can. J. Earth Sci., 9, pp. 918-921.

____ , 1972b. Age of molybdenum and tungsten mineralization in northern British Columbia. Can. J. Earth Sci., 9, pp. 1727-1734.

Christopher, P.A., 1972. Metallogenic epochs for "porphyry type" mineral deposits in the Canadian Cordillera (Abstr.). In Proceedings of the 9th. Annual Western Inter-University Geological Conference, Vancouver, B.C. p. 15.

________________ , 1973. Application of apatite fission-track dating to the study of porphyry mineral deposits. Can. J. Earth Sci., 10, May, in press.

1.2 PORPHYRY MINERAL PROPERTIES STUDIED

The term porphyry copper refers to large low-grade copper deposits that are spatially, temporally and genetically related to porphyritic intrusive rocks. Porphyry mineral deposits in the Canadian Cordillera include mineral deposits of copper, molybdenum and (or) tungsten with one or more of these metals of economic interest.

Sutherland Brown (1972) suggested that the porphyry deposits of the Canadian Cordillera have the following unifying characteristics:

1) Porphyry deposits consist of pervasive primary mineralization sparsely distributed in fracture or veinlet stockworks, breccias, or disseminations that are intimately related to porphyritic plutons.
2) Mineralization and alteration are distributed in porphyry or host in zonal patterns.
3) Plutons may be formed from magma of either granitic or syenitic affiliations.

Sutherland Brown used variation within these unifying characteristics to classify porphyry deposits as: 1) phallic, 2) volcanic and 3) plutonic porphyry deposits. The criteria used to classify a porphyry deposit are: 1) size and shape of pluton, 2) position and distribution of mineralization and alteration, 3) stage in orogenic cycle, and 4) age relationship of deposit and host. The first two criteria can be evaluated from careful empirical observation and routine laboratory investigation. The last two criteria require sophisticated isotopic analysis of samples of the intrusive and host rocks. These later criteria, the evaluation of the age and geologic setting of porphyry mineral deposits, were investigated during this study.

The K-Ar method is extremely useful in age dating igneous rocks of Mesozoic and Cenozoic age. Porphyry mineral deposits in the Canadian Cordillera are of Mesozoic and Cenozoic age, and therefore, the K-Ar method is suitable for dating the age of porphyry mineral deposits. The apatite fission-track method is also useful for dating Mesozoic and Cenozoic rocks, and this method of dating porphyry mineral deposits is evaluated in sections 3.3 and 3.5.

Areas studied by K-Ar and fission-track dating methods are located on Figure 1-1. The Burwash Landing area, Syenite Range, Cassiar area, and Adanac property were selected to extend the dating of porphyry mineral deposits into northern British Columbia and the Yukon Territory. Samples previously dated by the biotite K-Ar method were obtained from the Copper Mountain area (Preto et al., 1971) and the Granisle Mine (Carter, 1972b) to compare biotite K-Ar ages with apatite fission-track ages. Table 1-1 is an application of Sutherland Brown's (1972) porphyry classication to the deposits studied.

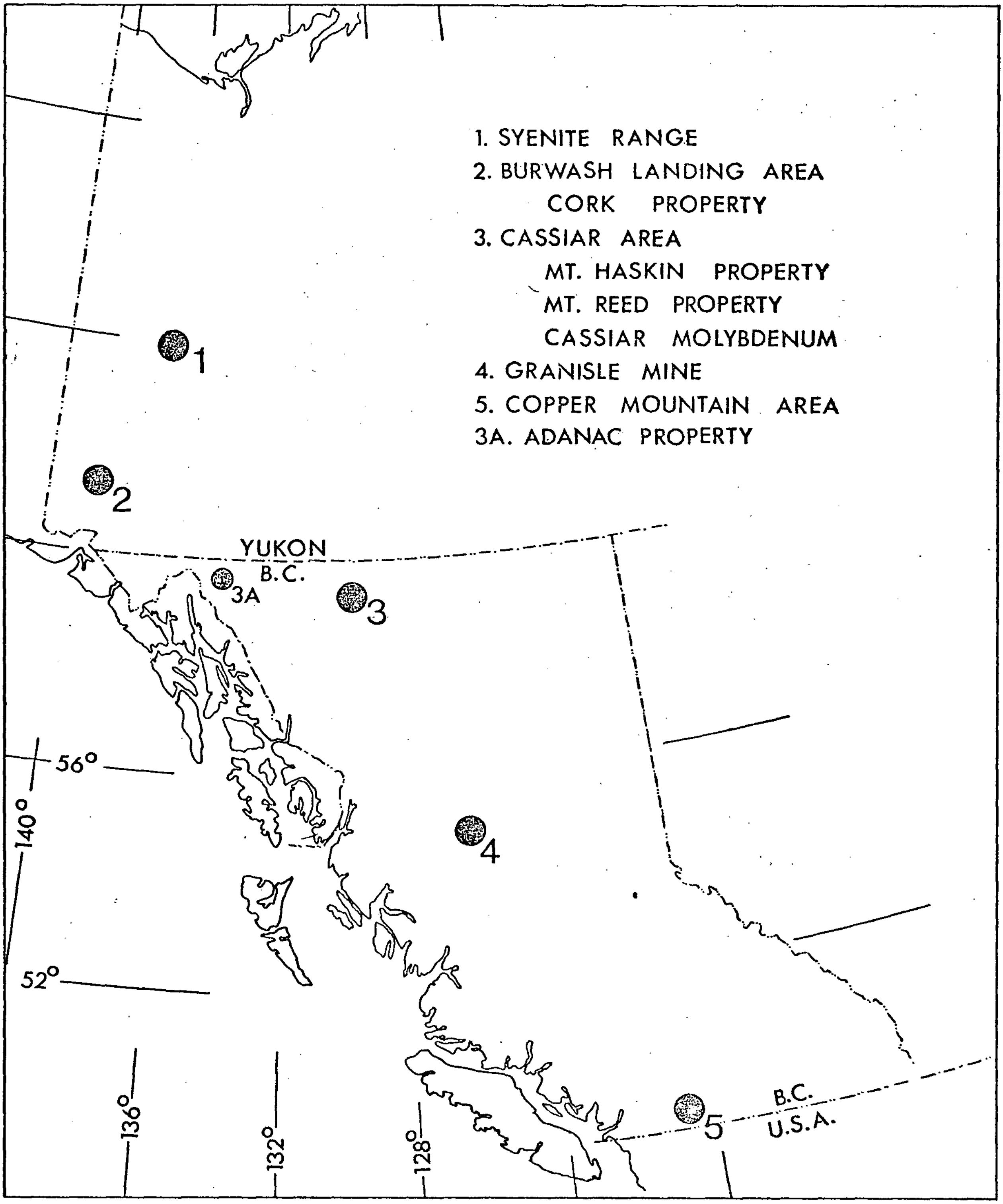

Figure 1-1. Location map for areas studied.

Table 1-1. Classification of deposits studied

Deposit	Tectonic Belt	Shape	Pluton Composition	Age m.y.	Host Age	Mineralization	Stage	Type
Burwash Creek	Insular	3000' x 1000'?	Qtz. latite	26.2	Permian & Triassic	Cu, Mo in stock and host	late	Phallic
Adanac	Intermontane	6000' x 3500'?	Alaskite	62.0	Permo-Pennsylvanian & Jurassic	Mo, W in stock	late	Phallic(?)
Mt. Haskin	Omineca	4000' x 4000'	Granite porphyry	50.1	Cambrian	Mo in stock and host	late	Phallic
Mt. Reed	Omineca	1000' x 3000'?	Granite porphyry	49.5	Cambrian	Mo, W in stock and host	late	Phallic
Cassiar Molybdenum	Omineca	2000' x 500'	Latite	less 70.0	Cretaceous 70.0 m.y.	Mo, Cu in stock and host	late	Phallic
Granisle	Intermontane	2000' x 1500'	Bio.-Feld. porphyry	51.2	Triassic & Jurassic	Cu in stock and host	late	Phallic
Copper Mountain & Ingerbelle	Intermontane	complex	Syenite to Diorite	193	Late Triassic	Cu in stock and host	early	Volcanic

2. POTASSIUM-ARGON DATING

2.1 INTRODUCTION

The K-Ar method has been reviewed by Hamilton (1965), Damon (1968), Dalrymple and Lanphere (1969) and York and Farquhar (1972). York and Farquhar (1972) and York (1970) reviewed recent developments in K-Ar dating that include the K-Ar isochron method.

The problem of radiometric dating of porphyry mineral deposits in the Canadian Cordillera involves the dating of events that occurred during Mesozoic and Cenozoic time. The K-Ar method has been extensively used for this purpose because:

1) It is suitable for dating events that occurred during the time span being investigated.
2) Most porphyry deposits contain mineral or whole-rock samples suitable for K-Ar dating.
3) The precision and accuracy required is obtained at a reasonable cost.

K-Ar ages obtained for this study are used to extend the study of age of porphyry mineral deposits into northern British Columbia and the Yukon Territory and as a reference for comparing fission-track ages.

In this chapter the K-Ar data is presented and examined by using the isochron method and a new Ar^{40} total vs %K isochron plot is suggested and evaluated. Application of the Ar^{40} rad. vs %K isochron method (section 2.3) to published K-Ar data from the Topley Intrusions and Guichon Batholith are presented in Appendix B.

2.2 K-Ar METHOD

The K-Ar method of dating depends upon the decay of K^{40} to Ar^{40}, both of which must be measured for an age to be calculated. Standard analytical techniques used for measuring potassium and argon have been described in detail by Hamilton (1965), Dalrymple and Lanphere (1969) and York and Farquhar (1972).

In the present study, biotite and hornblende apparent ages were determined in K-Ar laboratories operated jointly by the Departments of Geophysics and Geological Sciences, University of British Columbia, using procedures and equipment previously described (White et al., 1967). In addition to the normal procedure, the sample and entire fusion system were baked at 130°C for 16 hours which effectively eliminates atmospheric argon contamination in the system (Roddick and Farrar, 1971). Isotopic ages of the seventeen analyzed samples are plotted on Figures 4-1 to 4-7 and analytical data given in Table 2-1.

Isotopic abundances of potassium and atmospheric argon normally used for K-Ar dating were determined by Neir (1950) and are listed in Table 2-2. The assumptions made in using isotopic values have been reviewed by Dalrymple and Lanphere (1969).

TABLE 2-1 Potassium-Argon Analytical Data (ages obtained for this study)

Specimen No.	Location	Unit	Rock Type	Mineral	%K±s*	A^{40}rad** / A^{40}total	A^{40}rad. (10^{-5}cc STP/g)	A^{40}rad. / K^{40} $x10^{-3}$	K^{40} / Ar^{36} $x10^{5}$	Ar^{40} / Ar^{36} $x10^{3}$	Apparent Age (m.y.)
PC1	Lat. 61°22'18" Long. 139°18'20"	Tertiary plug?	Qtz. latite porphyry	Biotite	7.06±0.05	0.81	0.733	1.534	8.1274	1.535	26.0±1.0
PC2	Lat. 61°22'17" Long. 139°18'10"	Tertiary plug?	Qtz. latite porphyry	Biotite	6.75±0.05	0.85	0.717	1.570	10.4016	1.915	26.7±1.2
PC3	Lat. 61°22'30" Long. 139°25'55"	Tertiary plug?	Qtz. latite porphyry	Biotite	7.44±0.03	0.85	0.776	1.541	10.3722	1.885	26.2±1.0
PC4	Lat. 61°22'30" Long. 139°26'08"	Tertiary plug?	Qtz. latite porphyry	Biotite	7.30±0.03	0.83	0.757	1.533	9.2347	1.704	26.0±1.0
PC5	Lat. 61°22'00" Long. 139°25'09"	Kluane Range Intrusions	Gabbro	Hbl.	0.404±.001	0.56	0.190	6.943	0.5344	0.6619	115 ±4.0
PC6	Lat. 61°22'05" Long. 139°25'09"	Kluane Range Intrusions	Gabbro	Hbl.	0.379±.002	0.36	0.181	7.038	0.2343	0.4590	117 ±4.0
PC7	Lat. 61°32'36" Long. 138°32'38"	Ruby Range batholith	Biotite Granodiorite	Biotite	6.51±0.02	0.75	1.357	3.081	2.7009	1.111	51.9±2.0
PC8	Lat. 61°32'36" Long. 138°45'30"	Ruby Range batholith	Bio.-Hbl. Granodiorite	Biotite	7.24±0.03	0.90	1.584	3.232	7.5150	2.711	54.5±2.0
PC9	Lat. 59°20'25" Long. 129°30'22"	Mt. Haskin porphyry	Granite porphyry	Biotite	7.51±0.02	0.93	1.508	2.944	11.8377	3.764	49.7±1.5
PC10	Lat. 59°22'42" Long. 129°30'39"	Mt. Haskin porphyry	Granite porphyry	Biotite	7.31±0.01	0.93	1.483	2.996	11.9294	3.853	50.5±1.5
PC11	Lat. 59°17'58" Long. 129°25'18"	Mt. Reed porphyry	Granite porphyry	Biotite	7.78±0.05	0.84	1.521	2.888	5.0408	1.740	48.7±1.9
PC12	Lat. 59°18'00" Long. 129°25'19"	Mt. Reed porphyry	Granite porphyry	Biotite	7.75±0.03	0.89	1.491	2.979	8.0373	2.679	50.2±1.6
PC13	Lat. 59°12'12" Long. 129°50'23"	Cassiar batholith	Qtz. Monzonite	Biotite	6.52±0.01	0.83	1.886	4.274	3.1785	1.644	71.7±2.6
PC14	Lat. 59°13'29" Long. 129°50'10"	Cassiar batholith	Qtz. Monzonite	Biotite	7.60±0.03	0.85	2.093	4.068	4.1202	1.963	68.3±2.7
PC15	Lat. 59°42'30" Long. 133°23'24"	Mt. Leonard Boss	coarse Alaskite	Biotite (5% Chl.)	5.16±0.04	0.89	1.287	3.685	6.2809	2.597	62.0±2.2
PC16	Lat. 63°58'10" Long. 137°18'10"	Syenite Range Intrusions	Qtz. Monzonite	Biotite	6.92±0.03	0.94	2.391	5.104	8.0164	4.364	85.3±2.7
PC17	Lat. 63°57'55"	Syenite Range Intrusions	Qtz. Monzonite	Biotite	7.10±0.03	0.96	2.576	5.361	11.0437	6.183	89.5±2.7

* Potassium analyses by P. Christopher, J.E. Harakal and V. Bobik using KY and KY-3 flame photometers, s-standard deviation of quadruplicate analyses.

** Argon analyses by J.E. Harakal and P. Christopher using MS-10 mass spectrometer.
Constants used in model age calculations: $\lambda_e = 0.585 \times 10^{-10} y^{-1}$, $\lambda_\beta = 4.72 \times 10^{-10} y^{-1}$, $^{40}K/K = 1.181 \times 10^{-4}$.

Table 2-2. Isotopic abundance of potassium and atmospheric argon (Data from Neir, 1950).

Isotope	Relative atomic abundance (per cent)
Ar^{40}	99.600
Ar^{38}	0.063
Ar^{36}	0.337
K^{41}	6.91 $\pm$ 0.04
K^{40}	0.0119 $\pm$ 0.0001
K^{39}	93.08 $\pm$ 0.04

In order to determine the absolute age of a single mineral or rock sample, it is necessary to assume that all argon in the rock or mineral is either radiogenic or argon with the present atmospheric ratio (i.e. Ar^{40} total = Ar^{40}rad.+ Ar^{40} with Atm. ratio). Because the Ar^{40}/Ar^{36} atmospheric ratio is 295.5 (Neir, 1950), the conventional method of correcting for 'atmospheric argon' is to assume that Ar^{40}rad.= Ar^{40}total - 295.5 (Ar^{36}). However, subsequent workers have shown variation in the initial Ar^{40}/Ar^{36} ratio and an alternative graphical approach to determine the initial argon ratio has been suggested. This method is outlined below.

2.3 GRAPHICAL INTERPRETATION OF K-Ar DATA

Investigation of argon content of biotite (Wanless, Stevens and Loveridge, 1969; Giletti, 1971), hornblende (Roddick and Farrar, 1971), pyroxene (Hart and Dodd, 1962), plagioclase feldspar (Laughlin, 1966; Livingston et al., 1967), and nepheline (Macintyre, York and Gittens, 1969) shows that excess initial Ar^{40} can occur in most datable minerals. Thus samples must be treated in a manner that does not assume that initial argon has the present atmospheric ratio if the K-Ar method is to be of use in establishing trends in age of intrusions and age of mineral deposits. The K-Ar isochron method (York et al., 1969; McDougall et al., 1969; Roddick and Farrar, 1971; Hayatsu and Carmichael, 1970) provides a method of determining the initial argon ratio.

The data necessary for determining isochron ages is essentially the same as the data needed for the conventional K-Ar age calculation. The isochron method requires that for each rock unit dated at least two and preferably a minimum of three analyses are available from phases or minerals differing by at least 50 per cent in potassium content. In addition to the added analyses required, the entire fusion system must be baked overnight at a temperature that will remove loosely held atmospheric argon, but will not cause loss of initial or radiogenic argon. The temperature required to clean samples properly has been empirically determined to be 130°C for 16 hours (Roddick, 1970; Roddick and Farrar, 1971).

Ar^{40}/Ar^{36} vs K^{40}/Ar^{36} and Ar^{40} radiogenic vs per cent potassium diagrams are plotted and the method of least squares (York, 1966) is used to fit the best straight line to the points. The lines produced are called isochrons and the slope of the line is used to calculate an isochron age.

The (Ar^{40}/Ar^{36}) vs (K^{40}/Ar^{36}) isochron equation is:

$$\left(\frac{Ar^{40}}{Ar^{36}}\right)_T = \frac{\lambda e}{\lambda_\beta + \lambda e} \cdot (e^{\lambda t} - 1)\frac{K^{40}}{Ar^{36}} + \left(\frac{Ar^{40}}{Ar^{36}}\right)_I \qquad (2.1)$$

Where

$\left(\frac{Ar^{40}}{Ar^{36}}\right)_T$ = the total Ar^{40} to total Ar^{36} ratio found in the mineral at present.

$\left(\frac{Ar^{40}}{Ar^{36}}\right)_I$ = the initial value of the ratio at t=0.

$\left(\frac{K^{40}}{Ar^{36}}\right)$ = present-day ratio of K^{40} to Ar^{36} in the mineral

$\lambda = \lambda e + \lambda_\beta$

λe = decay constant for electron capture by K^{40} $(0.585 \times 10^{-10} yr^{-1})$.

λ_β = decay constant for beta emission by K^{40} $(4.72 \times 10^{-10} yr^{-1})$.

For equation 2.1 to be applicable to a set of samples, the samples must have: 1) the same age, 2) the same initial argon ratio and 3) essentially no atmospheric argon contamination.

The Ar^{40} rad. vs %K isochron equation is:

$$Ar^{40}rad. = 6.835 \times 10^{-4}\ m\ (\%K) + Ar^{36}_i\ (I - 295.5) \qquad (2.2)$$

Where

$Ar^{40}rad.$ = radiogenic argon 40 expressed in cc/gm at S.T.P. and calculated assuming $(Ar^{40}_i + Ar^{40}_{Atm.})/(Ar^{36}_i + Ar^{36}_{Atm.}) = 295.5$

$m = \frac{\lambda e}{\lambda_e + \lambda_\beta}(e^{\lambda t} - 1)$

slope = 6.835×10^{-4} m, (Roddick, 1970, p. 59)

I = initial Ar^{40}/Ar^{36} ratio, and

Ar^{36}_i; Ar^{40}_i = initial concentration.

For equation 2.2 to be applicable to a set of samples, the following criteria must apply: 1) samples have the same age, 2) samples have the same initial argon ratio, and 3) samples have the same amount of initial argon. An exception to criterion three occurs when the initial argon ratio is 295.5.

Roddick and Farrar (1971) refer to the Ar^{40}rad. vs %K diagram as an initial argon diagram and Roddick (1970) suggested that: "Minerals having different crystal structures will probably incorporate different amounts of initial argon. Therefore, only the same type of minerals can be plotted on an initial argon diagram".

Because Ar^{40}rad. is calculated assuming $(Ar^{40}{}_i + Ar^{40}{}_{Atm.})/(Ar^{36}{}_i + Ar^{36}{}_{Atm.}) = 295.5$, the y-intercept of the Ar^{40}rad. vs %K diagram is $Ar^{36}{}_i$ (I - 295.5) (Roddick and Farrar, 1971) and not initial Ar^{40}rad. as the Ar^{40} rad. vs %K plot seems to suggest. A positive intercept occurs on the Ar^{40} axis when I>295.5 and a negative intercept occurs when I<295.5.

Roddick and Farrar (1971) suggest that unlike the Ar^{40}/Ar^{36} vs K^{40}/Ar^{36} isochron, the Ar^{40} rad. vs %K isochron yields the correct age of the mineral when atmospheric argon is present in the system. However, the presence of atmospheric argon in the system eliminated any possibility of obtaining quantitative information on the initial argon ratio and the initial concentration of argon in the sample.

The assumptions necessary for a complete K-Ar isochron determination (both Ar^{40}/Ar^{36} vs K^{40}/Ar^{36} and Ar^{40} rad. vs %K) are:

1) the baking procedure essentially eliminates atmospheric argon from the system, and
2) the absolute amount of $Ar^{40}{}_i$ = initial Ar^{40}/Ar^{36} ratio and age of the samples are the same.

If these assumptions hold, then an Ar^{40} total vs %K plot will be a valid isochron plot.

The Ar^{40} total vs %K isochron equation is:

$$Ar^{40} \text{ total} = 6.835 \times 10^{-4}\, m\, (\%K) + Ar^{40}{}_i \qquad (2.3)$$

Where

Ar^{40} total = total Ar^{40} measured by mass spectrometry.

slope = 6.835×10^{-4} m

$Ar^{40}{}_i$ = initial Ar^{40} in sample at t=0 = intercept on y axis.

The y-intercept for this diagram yields the absolute amount of initial Ar^{40}.

2.4 APPLICATION OF ISOCHRON METHOD

Ages shown in table 2-1 were calculated assuming that Ar^{40} total = Ar^{40} radiogenic + Ar^{40} with atmospheric ratio. Four samples from quartz latite porphyry near Burwash Creek (PC1 to PC4) and four samples from granite porphyry on the Mt. Reed and Mt. Haskin properties provided independent checks on the age of these units. Isochron plots were constructed for these samples to check the initial Ar^{40}/Ar^{36} ratio and to compare isochron results with conventional determinations obtained using the assumed 295.5 initial argon ratio.

Isochron ages for these units have large uncertainties due to the small spread in potassium content of analyzed biotite concentrates. Isochron ages shown for samples PC1 to PC4 in Figure 2-1 and PC9 to PC13 in Figure 2-2 show much greater uncertainty than the respective mean ages of 26.2 $\pm$ 0.3 m.y. and 49.8 $\pm$ 0.7 m.y. for the samples. Initial argon ratios obtained for these samples both overlap the 295.5 value within the limits of error and therefore, the isochron result is consistent with the use of the 295.5 value.

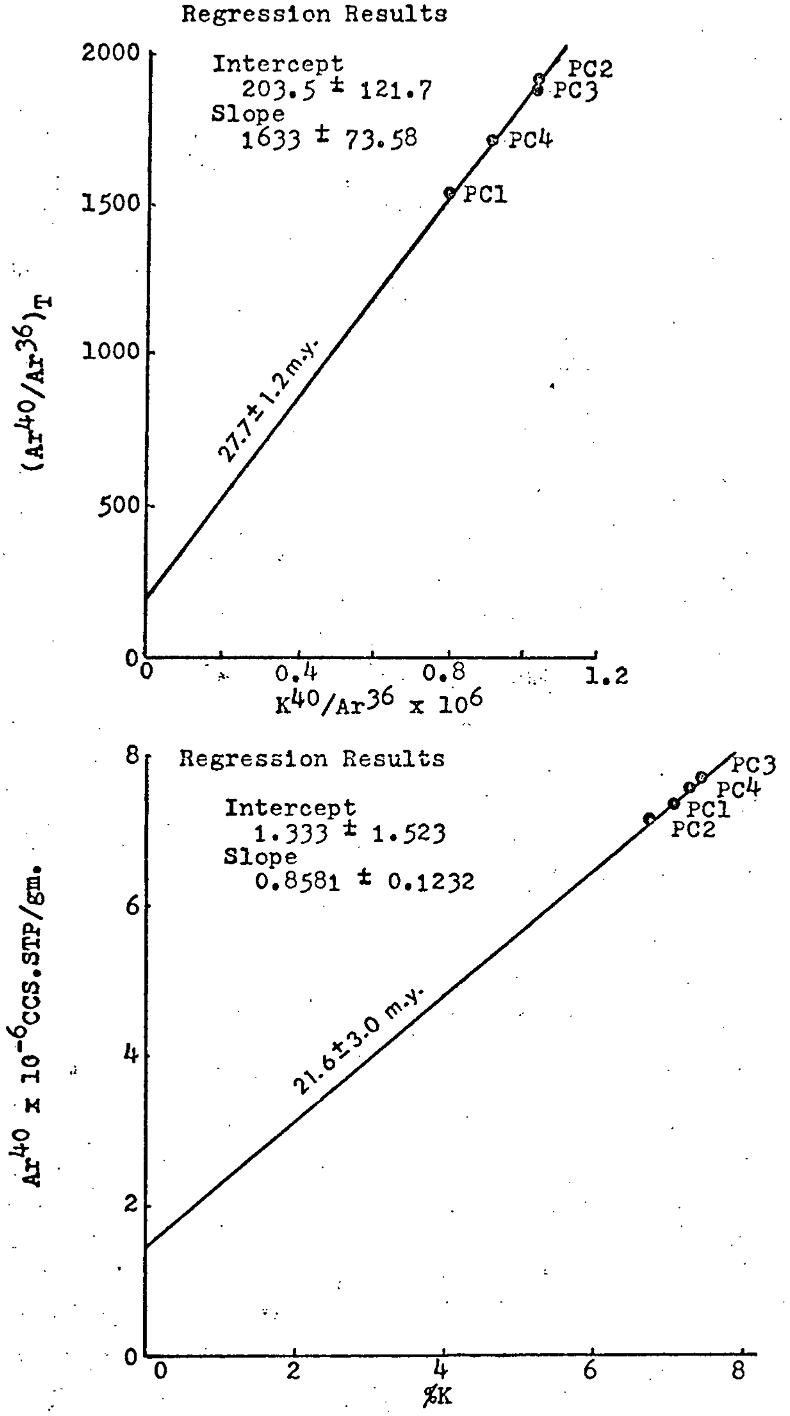

Fig. 2-1 Isochron plots for quartz latite porphyry near Burwash Creek, Yukon Territory.

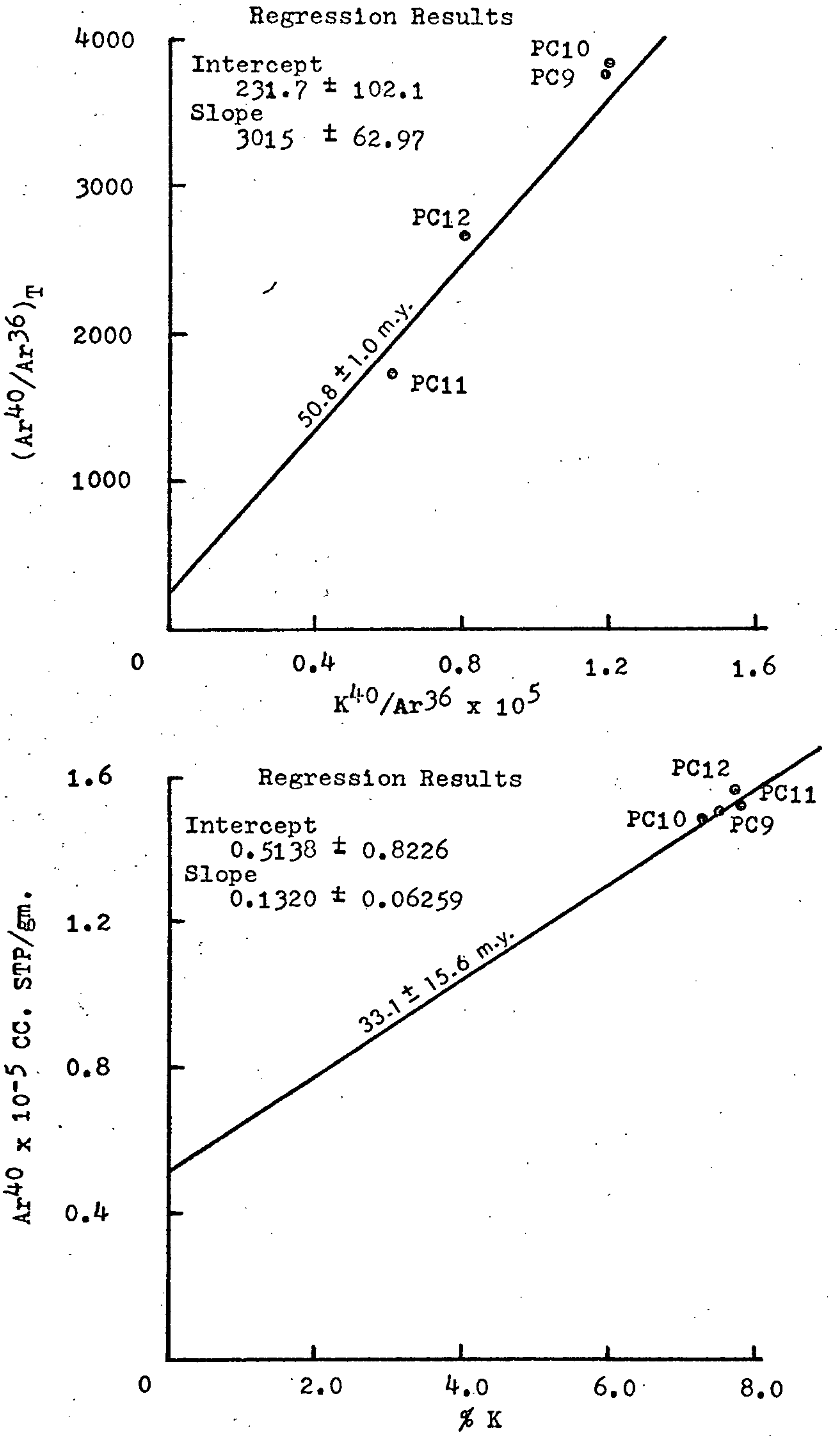

Fig. 2-2 Isochron plots for Mt. Reed and Mt. Haskin porphyries.

2.4.1 Ar^{40} total vs %K Isochrons

The Ar^{40} total vs %K isochron approach was checked by using published data from Hayatsu and Carmichael (1970) and Roddick and Farrar (1971) that was unsuitable for Ar^{40}rad. vs %K plots.

<u>Case I</u> Cape Breton Whole-Rock Samples

A recalculated isochron for whole-rock K-Ar data obtained by Hayatsu and Carmichael (1970) is compared with a plot of total Ar^{40} vs %K. Argon measurements have been converted from moles/gm. to CC.STP/gm. in order to allow comparison. Data is presented in Table 2-3 and the isochron plots are shown in Figure 2-3. Discordant whole-rock K-Ar data yielded a concordant Ar^{40} rad. vs %K isochron age of 391 $\pm$ 5 m.y. for samples from Cape Breton Island, Nova Scotia (see Hayatsu and Carmichael, 1970) with a positive intercept on the Y axis that indicated an initial Ar^{40}/Ar^{36} ratio greater than 295.5. An Ar^{40} total vs %K plot yields an isochron parallel to the Ar^{40} corrected vs %K plot and an isochron age of 391 $\pm$ 7 m.y. The total Ar^{40} plot also has a positive intercept on the Ar^{40} axis and this value is the absolute amount of initial Ar^{40} plus a small increment of atmospheric Ar^{40} (less than 10%).

This example shows that an Ar^{40} total vs. %K isochron can correct for discordant whole-rock K-Ar data and provides a one step method of obtaining the initial Ar^{40} content of a set of samples.

<u>Case II</u> Tulameen Complex Hornblende Samples

A recalculated isochron for hornblende K-Ar data obtained by Roddick and Farrar (1971) is compared with a plot of total Ar^{40}. Data is presented in Table 2-4 and the isochron plots are shown in Figure 2-4. Discordant hornblende K-Ar data yields a concordant Ar^{40} rad. vs %K isochron

TABLE 2-3 Analytical data and ages of Cape Breton whole rock samples (data from Hayatsu Carmichael, 1970). Units for Ar^{40} were converted from moles/gm to cc. STP/gm.

Sample No.	Rock Type	K (%)	^{40}Ar total* ($x10^{-6}$ cc. STP/gm.)	^{36}Ar** ($x10^{-13}$ moles/gm.)	^{40}Ar rad ($x10^{-6}$ cc. STP/gm.)	Age+ (m.y.)
CB-18	Basalt	0.066	3.611	2.39	2.148	680
17	Basalt	0.363	9.677	2.72	8.019	485
12	Red felsite	0.777	16.442	3.54	14.246	412
9	Crystal lithic tuff	0.931	19.219	3.54	17.024	411
8	Greywacke	1.52	28.582	1.49	27.686	409
7	Red felsite (quartz keratophyre?)	0.040	3.237	2.30	1.830	891
1A	Greywacke	1.64	30.598	2.05	29.322	402
1B	Greywacke	1.57	29.277	2.08	28.000	401
2	Amygdaloidal basalt	0.098	4.771	2.47	3.024	644
3	Basalt	0.270	6.406	1.38	5.555	456
4	Basalt	0.261	6.406	1.43	5.533	455
5	Red felsite	0.595	14.381	3.22	12.365	460

*^{40}Ar spike.

**^{36}Ar spike subtracted.

+Values of constants used are $\lambda_\beta = 0.566$, $^{40}K/K = 1.18 \times 10^{-4}$(4).

TABLE 2-4 Analytical data and ages of hornblende from Tulameen Complex (data from Roddick and Farrar, 1971). Ar^{40} total was calculated using the values for Ar^{40} rad. and percent atmospheric argon reported by Roddick and Farrar.

Sample No.	K (%)	^{40}Ar total* ($x10^{-6}$ cc. STP/gm.)	^{40}Ar rad ($x10^{-6}$ cc. STP/gm.)	% Atmos.	$(^{40}Ar/^{36}Ar)_T$	Age and Error (m.y.)
2H-2	1.63	13.55	13.14	3.0	9803	191.5 ± 2.9
2H-3	1.63	13.61	13.15	3.5	8330	191.6 ± 2.9
5H-3	1.19	9.16	9.86	3.4	8631	196.6 ± 3.0
5H-4	1.19	10.22	9.99	3.8	7682	199.1 ± 3.0
8H-2	1.016	10.37	8.731	4.8	6152	203.5 ± 3.1

$\lambda_e = 0.584 \times 10^{-10} yr^{-1}$; $\lambda_\beta = 4.72 \times 10^{-10} yr^{-1}$; $^{40}K = 1.22 \times 10^{-4}$ g/g K.

* Calculated assuming $(^{40}Ar_I + {}^{40}Ar_A) / (^{36}Ar_I + {}^{36}Ar_A) = 295.5$.

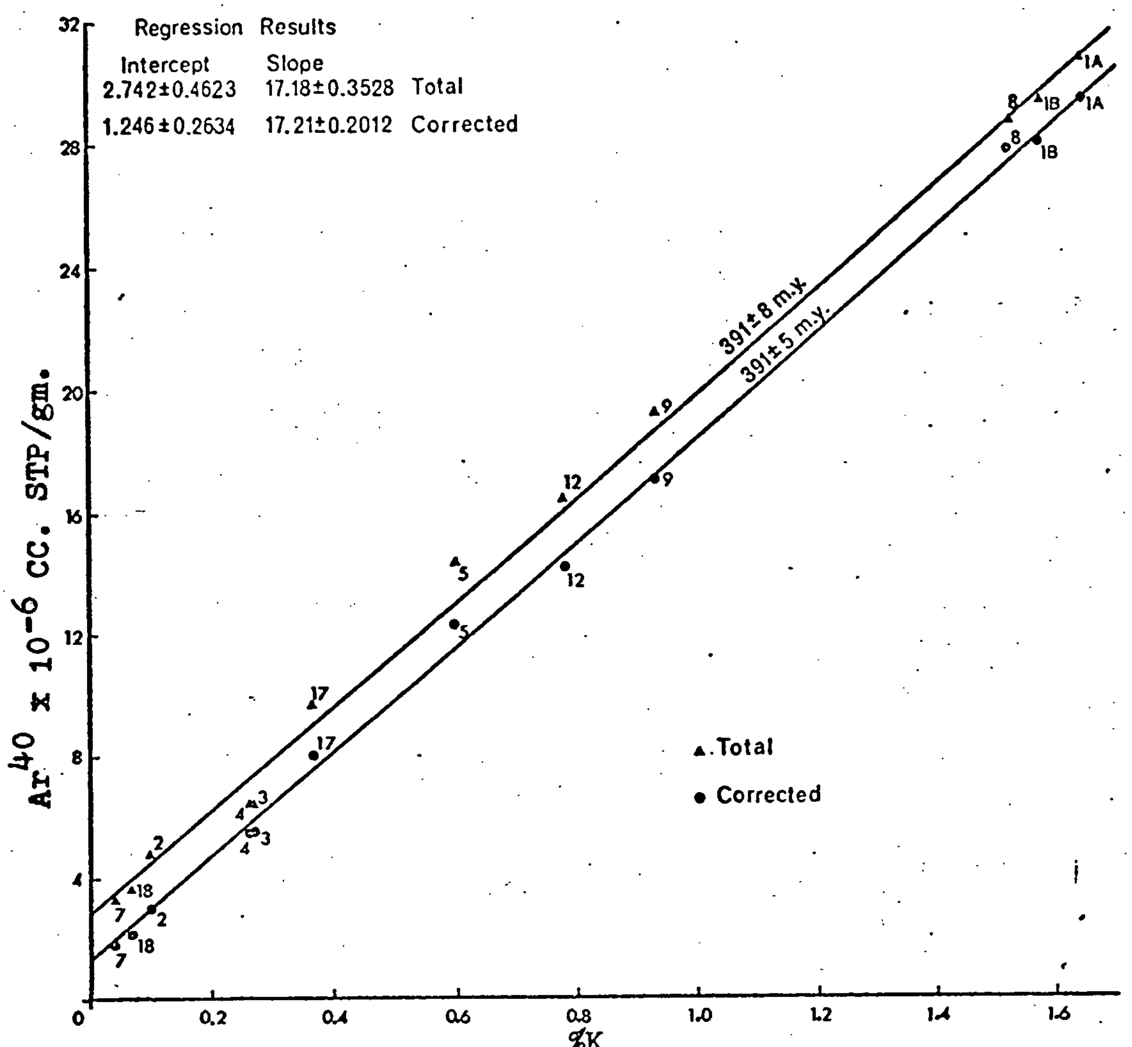

Fig. 2-3 Total and corrected Ar^{40} vs %K isochrons for whole-rock K-Ar data. Corrected isochron is recalculated from Hayatsu and Carmichael's (1970) data.

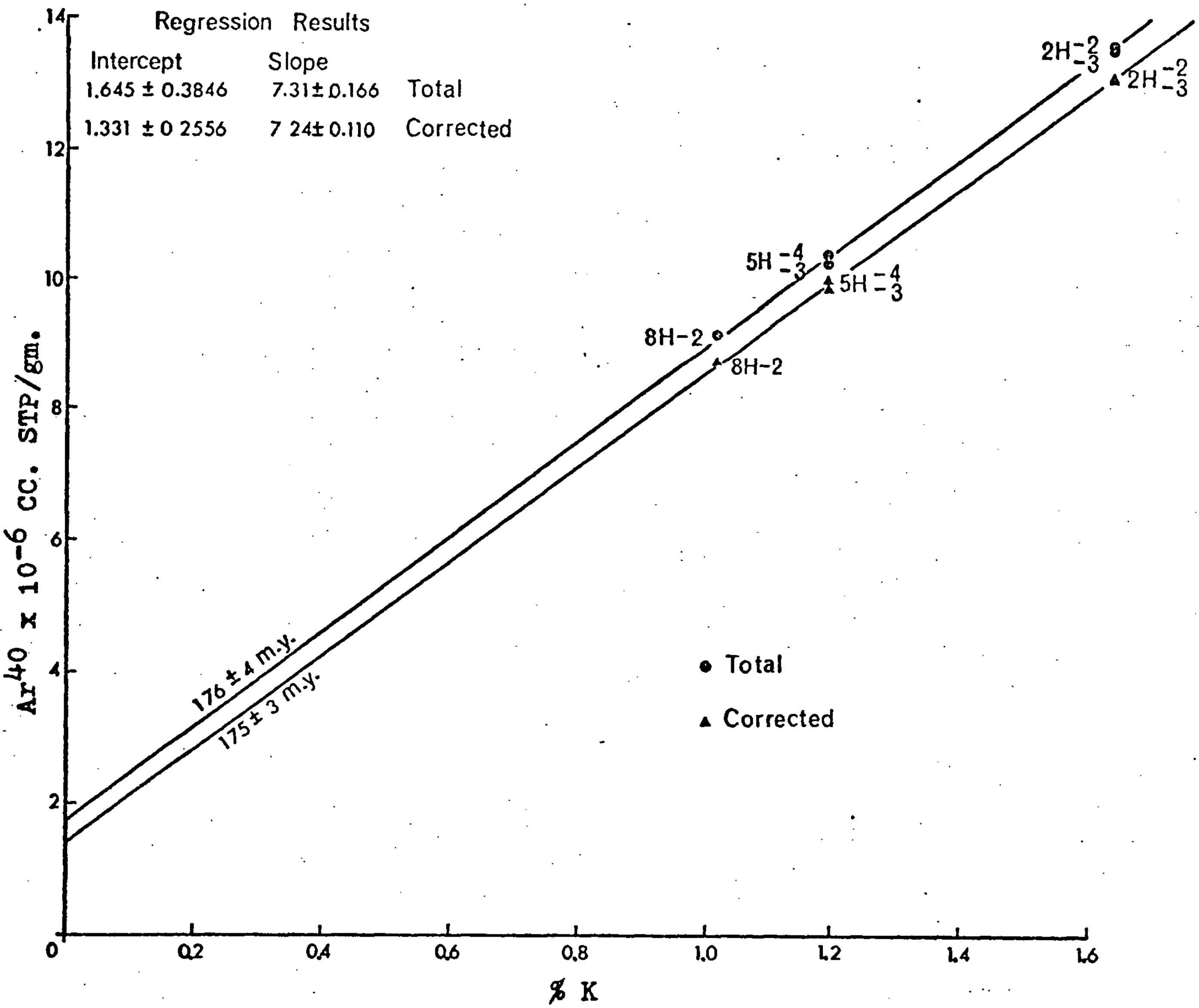

Fig. 2-4 Comparison of Ar^{40} total isochron with Ar^{40} corrected isochron diagram for K-Ar hornblende data from the Tulameen Complex, British Columbia (data from Roddick and Farrar, 1971).

age of 175 $\pm$ 3 m.y. for samples from the Tulameen Complex, British Columbia (see Roddick and Farrar, 1971) and an Ar^{40} total vs %K plot yields an isochron parallel to the Ar^{40} rad. vs %K plot and an isochron age of 176 $\pm$ 4 m.y. The y-intercept for the Ar^{40} total isochron is the absolute amount of initial Ar^{40} plus a small increment of atmospheric Ar^{40}.

This example suggests that the total argon plot yields essentially the same results as the Ar^{40} rad. vs %K plot, and that the absolute amount of initial Ar^{40} is obtained directly by using the Ar^{40} approach. Both plots yield $Ar^{40}{}_i$ values of 1.6 x 10^{-6} CC.STP/gm. for the Tulameen hornblende samples, but the Ar^{40} total vs %K plot does not require the plotting of an Ar^{40}/Ar^{36} vs K^{40}/Ar^{36} isochron in order to obtain the $Ar^{40}{}_i$ value.

2.5 SUMMARY

Hayatsu and Carmichael (1970) and Roddick and Farrar (1971) have shown that the K-Ar isochron method corrects for excess initial Ar^{40} in a mineral sample. Since the isochron method can yield more meaningful ages, an attempt should be made to apply the method to K-Ar data.

At least three samples from a single igneous event are necessary in order to establish an isochron. Samples PC1 to PC4 and PC9 to PC13 were analyzed in a manner suitable for isochron determinations (Roddick and Farrar, 1971), but the narrow range of potassium values for the samples leads to isochron ages with large uncertainties (Figure 2-1 and 2-2).

Isochron plots of Ar^{40} total vs %K yield the same age as Ar^{40} rad. vs %K plots, and in addition, the Ar^{40} total vs %K plot provides a one step approach to obtaining the absolute value of initial Ar^{40} (Figures 2-3 and 2-4).

2.6 EVALUATION OF ISOCHRON METHOD

The graphical approach to potassium-argon age dating provides a new approach to data treatment and interpretation. Advantages of the graphical approach are:

1) In order to obtain meaningful ages for minerals of low K content and (or) young age, the initial argon ratio of the minerals must be determined. In theory, the Ar^{40}/Ar^{36} vs K^{40}/Ar^{36} plot will yield the initial argon ratio of properly treated samples of related age and history.
2) Isochron plots are useful visual and interpretative aids, these diagrams emphasize irregularities and trends in K-Ar data.
3) As information on initial argon accumulates, it will add to our understanding of the argon retentivity of various minerals and the origin of excess argon (Hayatsu and Carmichael 1970).
4) Provides a method of correcting for high initial argon ratios (e.g. Hayatsu and Carmichael, 1970 and Roddick and Farrar, 1971).

Disadvantages of the graphical approach are:

1) Several samples must be analyzed in order to determine the initial argon ratio.
2) Mineral samples that are from the same intrusive phase often contain similar potassium content and therefore are not suitable for isochron plots. (e.g Samples PC1 to PC4 and samples PC9 to PC13 section 2.4).
3) For an Ar^{40} vs %K plot to apply, samples must contain the same amount of excess argon. It is unlikely that this assumption will generally hold for more than one mineral phase.

3. FISSION TRACK DATING

3.1 INTRODUCTION

Recent work has established the feasibility of using the fission-track technique for dating common accessory minerals (Fleischer and Price, 1964a; Naeser, 1967b; Wagner, 1968; Christopher, 1969; Naeser and Dodge, 1969; Naeser and McKee, 1970); however, most of the studies to date have been carried out on samples that are from unaltered rocks that yield clean concentrates of datable major and accessory minerals. These studies have shown that the fission-track method can be used as a dating tool and does provide information on the age and crystallization history of a mineral or rock unit.

The Canadian Cordillera has been established as a porphyry copper and molybdenum mineral province (Sutherland Brown et al., 1971; Sutherland Brown, 1969a) with low grade (porphyry type) mineral deposits of the 'paramagmatic class' (White, Harakal and Carter, 1968). Most examples of porphyry copper deposits exhibit a characteristic sulfide and alteration zoning that was formed in an epizonal to mesozonal environment during Mesozoic and Cenozoic times (Lowell and Guilbert, 1970; Rose, 1970). Naeser (1967a) concluded that: "...apatite, because of its property of low temperature track annealing is a very sensitive temperature monitor. It is most useful in looking at events in the Mesozoic and Cenozoic, where effects of burial are minimal". Porphyry deposits of the Canadian Cordillera should provide an ideal setting for fission track age determinations on apatite.

In this chapter the fission-track method is reviewed, and the application of apatite fission-track dating to the study of porphyry mineral deposits is evaluated by comparing apatite fission-track and K-Ar ages for co-genetic minerals.

3.2 FISSION-TRACK METHOD

Following the discovery by K.A. Petrzhak and G.N. Flervo in the U.S.S.R. in 1940 that uranium undergoes spontaneous fission, many scientists looked for tracks of radiation damage recorded in crystal structures. Fission-tracks were first detected in irradiated flakes of the mineral muscovite by Silk and Barnes (1959). The most direct method for observing tracks is to examine irradiated solids with an electron microscope at high magnification (50,000x). This method of observing fission-tracks limited their utility until the discovery of chemical etching techniques by P.B. Price and R.W. Walker (1962) permitted the study of fission-tracks with the optical microscope.

The discovery of etch techniques for revealing fission-tracks was followed by the development of the fission-track technique for dating minerals and glass (Price and Walker, 1963, p. 4847; Fleischer and Price, 1964a, p. 331 and 1964d. p. 1705). Spontaneous fission-tracks can be produced by the fission decay of U^{238}, U^{235}, and Th^{232}, but Price and Walker (1963) calculated that in most cases spontaneous fission of U^{238} is the only likely source of fission-tracks. Therefore, the parent material for the fission-track method is U^{238} and the daughter products of a spontaneous decay are represented by a damaged trail (fission-track). The increase in the spontaneous fission-track density is a measure of the build-up of the daughter products and the spontaneous fission-track density is directly related to the age and U^{238} content of a mineral or material.

The fission-track method has been applied to the dating of metamorphic and igneous events ranging in age from historic times to the Precambrian. Minerals suitable for fission-track dating include: biotite, hornblende, apatite, zircon, muscovite (Fleischer and Price, 1964b), sphene (Naeser, 1967b) and epidote (Naeser, Engels, and Dodge, 1970). Glass (Brill et al., 1964; Fleischer and Price, 1964a and b) can also be dated and most plastics are excellent track detectors.

3.2.1 Procedure

The procedure for determining fission-track ages involves:

a) determining the spontaneous fission-track density on an etched interior surface of a mineral.
b) using the calculated value for spontaneous fission decay constant (λ F),
c) determining the U^{238} content.

An accurate, indirect determination of the U^{238} content can be made by exposing an annealed portion of the sample to a known dose of thermal neutrons (Fleischer et al., 1964). Thermal neutron induced fission takes place in U^{235}, but not in U^{238}, and therefore, the induced track density (ρi) will be a function of the thermal neutron flux, the cross section capture area of U^{235} for thermal neutrons, and the concentration of U^{235}. Once the values necessary for determination of the U^{235} content are obtained, the U^{238} content can be found by using the constant isotope ratio (U^{235}/U^{238} = 1/137.7). From an induced track count, a spontaneous track count, and a flux determination, the age of a mineral can be obtained from the following equation (Fleischer et al., 1965a, p. 389):

$$A = \frac{1}{\lambda D} \quad \ln \left[1 + \left(\frac{\rho s \lambda D \sigma I \phi}{\rho i \lambda F}\right)\right]$$

Where A = age in years;

ρs = spontaneous track density (natural tracks from spontaneous decay of U^{238});

ρi = induced track density (tracks caused by neutron induced fission of U^{235});

λD = total decay constant for U^{238} ($1.54 \times 10^{-10} yr^{-1}$);

σ = thermal neutron cross section for fission of U^{235} (582×10^{-24} cm^2);

ϕ = total thermal neutron dose (nvt);

I = 1/137.7 = isotope ration U^{235}/U^{238} (7.26×10^{-3});

λF = fission decay constant for U^{238} ($6.85 \times 10^{-17} yr^{-1}$) (Fleischer and Price, 1964a, p. 63).

By substituting values for the constants, the equation reduces to (Naeser, 1967b, p. 1523):

$$A = 6.49 \times 10 \quad \ln \left[1 + \left(9.45 \times 10^{-18} \frac{\rho s}{\rho i}\right)\right] \text{ yr.}$$

The various steps involved in a fission-track age determination are outlined in detail in Appendix C.

The reader is referred to descriptions of the analytical procedure presented by Lahoud et al. (1966), Naeser (1967a and b) and Christopher (1969).

3.2.2 Flux Determination

The largest analytical uncertainty in determining a fission-track age generally involves the determination of the neutron flux obtained during sample irradiation. The reactor irradiation is used for determining uranium content of samples and a neutron flux in the order of 10^{15} to 10^{17} nvt* is required for the uranium determination. The most accurate method for determining the flux obtained during a reactor run is to include a calibrated standard with either a known uranium content or known fission-track age and count fission-tracks produced in the standard. A glass standard calibrated by Dr. C.W. Naeser of the United States Geological Survey to contain 0.4 ppm uranium was included in the reactor run along with standard apatite Me/G-1 that has concordant 120 m.y. biotite potassium-argon and 119 m.y. apatite fission-track ages.

Three independent checks were used to determine the flux obtained:

1) a flux of 1.31×10^{15} nvt was determined for the standard glass;
2) a flux of 1.31×10^{15} nvt was obtained by comparing track density produced in the U.B.C. reactor run with the track density of the same standard glass included in the Dartmouth reactor run 1 (Christopher 1968 and 1969); and
3) a flux of 1.30×10^{15} nvt was calibrated by using 120 m.y. as the age of standard apatite Me/G-1.

Although the standard deviation of three independent checks of the flux is less than one per cent, an error of 5% was assigned to the 1.31×10^{15} nvt flux because of uncertainty in the track density produced in the standard.

* nvt = total thermal neutron dose.

3.3 EVALUATION OF THE FISSION TRACK METHOD

Several assumptions must be made in calculation of fission-track ages, many of which cannot be assigned an absolute error. Possible sources of error in each fission-track age include determination of (1) fossil track density, (ρs), (2) induced track density (ρi), and (3) neutron dose (ϕ). In addition, incomplete knowledge of the physical and geochemical properties of uranium may also be a source of error.

The ability to distinguish tracks from inclusions, dislocations, and other imperfections in crystals has been discussed by Fleischer and Price (1964 d). The five characteristics used in identification of fission-tracks are: 1) they form line defects, 2) they are straight, 3) they are randomly oriented, 4) they are of limited length (typically of the order of 5 to 20 microns or 5 to 20 x 10^{-3} mm), and 5) they can be caused to disappear by suitable heating (Fleischer and Price, 1964 d; Wagner, 1968; Naeser and Faul, 1969). The spontaneous and induced track counts are substituted in the dating equation as a ratio, and therefore, consistent application of the above 5 criteria in the counting of both the natural and induced tracks will help eliminate counting error.

In natural mineral samples, the uranium isotope U^{238} is the only element for which spontaneous fission is significant. Spontaneous fission of U^{235} and Th^{232} also occur, but U^{235} would account for less than 0.5 per cent of the spontaneous fission tracks in a mineral and Th^{232} would make a 50 per cent contribution only in a substance in which it was approximately 100,000 time more abundant than uranium (Faul, 1966). Cosmic-ray interaction could produce radiation damage similar to fission-tracks, but the effect of the cosmic ray flux on buried terrestrial samples is considered to be negligible because of strong attenuation by rock or soil

(Price and Walker, 1963).

Uranium in nature is predominately composed of two radioactive isotopes U^{235} and U^{238}. These two isotopes have always been found to occur together in nature with the phases intimately mixed and in a fixed proportion ($U^{235}/U^{238} = 1/137.7 \pm 0.3$) (Senftle et al., 1957). U^{235} and U^{238} also decay by alpha emission with half lives of 7.13×10^{8} yrs. and 4.51×10^{9} yrs. respectively. Price and Walker (1963) calculated that the effect of parent reduction because of alpha decay is significant when the time involved is greater than approximately 10^{9} yrs.

The value of the fission decay constant for U^{238} directly controls the accuracy of ages calculated by the fission-track method (Price and Walker, 1963). Fleischer and Price (1964 a and c) determined a weighted average value of $6.85 \pm 0.20 \times 10^{-17} yr^{-1}$ for the decay constant for spontaneous fission of U^{238} (λF). This average value was obtained by using two track counting methods that gave concordant results. The first value, $\lambda F = 6.9 \times 10^{-17} yr^{-1}$, was obtained by requiring that ages of a large number of minerals determined by using the fission-track method agree with ages determined by decay of K^{40} and Rb^{87}. The second value, $\lambda F = 6.6 \pm 0.8 \times 10^{-17} yr^{-1}$, was determined by counting fission-tracks recorded in mica SSTR held against a sheet of uranium foil for six months. Fleischer and Price's weighted average value for $\lambda F = 6.85 \pm 0.20 \times 10^{-17} yr^{-1}$ is supported by a value of $\lambda F = 7.03 \pm 0.11 \times 10^{-17} yr^{-1}$ (Roberts et al., 1968) determined using standard mica SSTR against uranium foil, and a value of $6.8 \pm 0.6 \times 10^{-17} yr^{-1}$ (Kleeman and Lovering, 1971) determined by accumulating fission fragment tracks in Lexan plastic held adjacent to uranium metal for one year. Values for λ_F ranging from 8.27 to 8.42 $\times 10^{-17} yr^{-1}$ have been determined by Spadavecchia and Hahn (1967) and Galliker et al. (1970), using a 'spinner' apparatus. The larger values are not commonly used for fission-track dating and the weighted average value of $\lambda_F = 6.85 \pm 0.20 \times 10^{-17} yr^{-1}$ (Fleischer and Price, 1964 a and c) was used in this study.

A closed system for uranium is assumed. This assumption can be checked by careful observation of the position of natural and induced tracks in a substance. Irregularities in the uranium distribution are also detectable during fission-track counting. If extreme irregularities are found (e.g. sphene sample JH5 from Brenda Mine), the sample cannot be age dated by random counting methods.

The accuracy of the flux determination has been discussed by Fleischer, Price and Walker (1964). A value of $1.31 \pm 0.07 \times 10^{15}$ nvt was determined for the reactor run used for irradiating samples studied by the writer. Fleischer, Price and Walker (1964) showed that flux variation over a 5 cm length is about 10% and they estimated that the total error in the flux determination is about 15%. Samples used in this study were irradiated over a tube length of less than 2 centimeters and therefore flux variation should be about 3%. Error in the flux determination is caused by uncertainty in the uranium content of the standard, variation of the flux within the reactor, counting error, and uncertainty in constants assigned to isotope ratios and capture cross sections.

Naeser (1967b) suggested that the number of tracks counted provided the major source of error in a fission-track age determination. If a minimum of 400 fossil and induced tracks are counted, the error for each slide is ± 5%, a value obtained by assuming a Poisson distribution. (i.e. the standard deviation of the track counts is the square root of the number of tracks counted).

Empirically, Naeser and Dodge (1969) determined that ± 10 per cent is a good estimate of the standard deviation of a fission-track age, assuming at least 250 counts of both fossil and induced tracks. For this study an error of ± 10 per cent is considered to be a good estimate of the standard deviation of a fission-track age when at least 400 counts of both fossil and induced tracks are obtained. When total counts are less than 400, the standard deviation was calculated by taking the square root of the sum of the squares of the estimated error (10%) and the standard deviations of counting error for natural and induced tracks.

3.4 PRESENTATION OF DATA

Analytical data and the calculated fission-track ages measured on fifteen apatite concentrates from five localities (Figure 1-1) in the Canadian Cordillera are shown in Table 3-1. Analytical data for standard apatite samples Me/G-1 and Me/N-1 are also presented (see Christopher 1968 and 1969). K-Ar ages obtained at the University of British Columbia on co-genetic biotite are shown for comparison. The biotite K-Ar ages are believed to represent the time at which the rock cooled to a temperature at which biotite retains argon (about 150°C), and for high-level epizonal and mesozonal igneous bodies, the time of emplacement and time of setting of the biotite K-Ar clock should be relatively close.

Seven sphene and two zircon samples were also prepared for fission-track dating but etched grain mounts revealed extreme irregularities in uranium content, and the sphene and zircon samples could not be dated by using random track counting methods. An alternate procedure for dating minerals with non-uniform uranium content has been described by Naeser (1967 a and b), but samples were not irradiated in a manner suitable for treating samples with non-uniform uranium content.

TABLE 3-1 FISSION TRACK ANALYTICAL DATA AND AGES (thermal neutron flux = 1.31 x 10^{15})

Sample No.	Unit	Minerals Dated	Tracks Counted	Track Density ρ_s (counts/cm^2) x10^5	Tracks Counted	Track Density ρ_i (counts/cm^2) x10^5	Uranium Content in ppm	Etch Time (sec.)	Fission Track Age (m.y.)	K-Ar Age (m.y.)
				BURWASH LANDING AREA						
PC1	Tertiary plug?	Apatite	86	1.08	296	2.04	5.6	15	42±7	
		Biotite								26.0±1.0
PC2	Tertiary plug?	Apatite	385	1.53	466	2.27	6.3	10	54±6	
		Apatite	94	0.91	301	2.10	5.8	15	35±5	
		Biotite								26.7±1.2
PC3	Tertiary plug?	Apatite	419	2.03	428	3.48	9.6	10	47±5	
		Biotite								26.2±1.0
PC8	Ruby Range batholith	Apatite	170	1.94	411	3.17	8.7	10	49±7	
		Biotite								54.5±2.0
				CASSIAR AREA						
PC9	Mt. Haskin porphyry	Apatite	416	2.58	310	4.28	11.8	15	48±6	
		Apatite	316	2.92	336	3.89	10.7	12	60±8	
		Biotite								49.7±1.5
PC12	Mt. Reed porphyry	Apatite	144	2.71	593	4.04	11.1	13	54±7	
		Biotite								50.2±1.6
PC13	Cassiar intrusions	Apatite	880	4.90	1094	5.87	16.2	10	67±7	
		Biotite								71.7±2.6
PC14	Cassiar intrusions	Apatite	660	3.59	734	4.85	13.4	10	60±6	
		Biotite								68.3±2.7
				SYENITE RANGE						
PC16	Syenite Range intrusions	Apatite	702	7.74	934	8.18	22.5	10	76±8	
		Biotite								85.3±2.7
PC17	Syenite Range intrusions	Apatite	187	9.92	468	6.48	17.9	15	121±16	
		Biotite								89.5±2.7
				COPPER MOUNTAIN AREA						
KA1	Lost Horse intrusion	Apatite	616	9.17	472	6.25	17.2	10	117±12	
		Biotite								194±8
KA4	Verde Creek qtz. monz.	Apatite	571	7.50	52	4.64	12.8	10	129±23	
		Biotite								101±4
KA9	Lost Horse (dike)	Apatite	326	3.27	428	2.67	7.4	12	101±12	
		Biotite								197±8
KA10	Lost Horse intrusion	Apatite	381	5.02	271	3.97	10.9	10	101±13	
		Apatite	292	6.02	151	3.77	10.4	15	127±18	
		Biotite								195±8
				GRANISLE MINE						
NC-69-8	apatite bearing vein	Apatite	231	3.09	191	8.39	23.1	10	30±4	
		Biotite								50.2±2.1
				STANDARD APATITE						
Me/G-1		Apatite	859	7.46	606	4.95	13.6	10	120±12	
		Apatite*	1120	9.12	816	6.40	15.1	10	133±20	
		Apatite*	2087	9.61	1588	7.52	17.7	13-15	119±18	
		Biotite								120
		Apatite**							113	
Me/N-1		Apatite	761	6.38	456	3.34	9.2	10	152±15	
		Apatite	504	5.45	434	3.79	10.4	15	115±12	
		Apatite*	558	7.27	579	5.71	13.4	15	119±18	
		Apatite*	879	5.58	588	3.89	9.6	15	134±13	
		Apatite**							101	

* Ages determined by the writer at Dartmouth College (Christopher 1968 and 1969).
** Ages determined at Dartmouth College (personal communication J.B. Lyons 1971).

3.5 DISCUSSION OF FISSION TRACK RESULTS

Figure 3-1 is a graphical comparison of the results obtained for biotite K-Ar and apatite fission-track methods. It demonstrates that fission-track ages for apatite from the Burwash Landing area, Cassiar area and Syenite Range are consistent and in general concordant with K-Ar ages determined on co-genetic biotite; and that one sample from a mineralized potassic-zone vein at the Granisle Mine and four samples from the Copper Mountain area show discordant results.

Thin section investigation revealed that co-genetic minerals obtained from weakly altered (potassic zone) rocks give concordant results and that discordant results are obtained from strongly altered propylitic and potassic zone rocks. Alteration of apatite makes track distinguishing more difficult, thus eliminating the possibility of using several of the apatite concentrates prepared for this study from the Copper Mountain intrusions.

Thermal events have been suggested by Naeser (1967a), Naeser and McKee (1970), and Wagner and Reimer (1972) to explain apatite fission-track ages that are younger than the biotite K-Ar age for the sample. Annealing studies on apatite by Naeser (1967a), Naeser and Faul (1969) and Wagner (1968) show that fission-tracks in apatite are very sensitive to thermal events, and that a temperature of less than 75°C is necessary for complete track retention. Concordant apatite fission-track and biotite K-Ar ages suggest that the rock unit cooled from greater than 150°C (Damon 1968) to less than 75°C (Naeser and Faul 1969; Wagner, 1968) within a length of time less than the experimental error of the techniques. An apatite fission-track age younger than a biotite K-Ar age for a unit

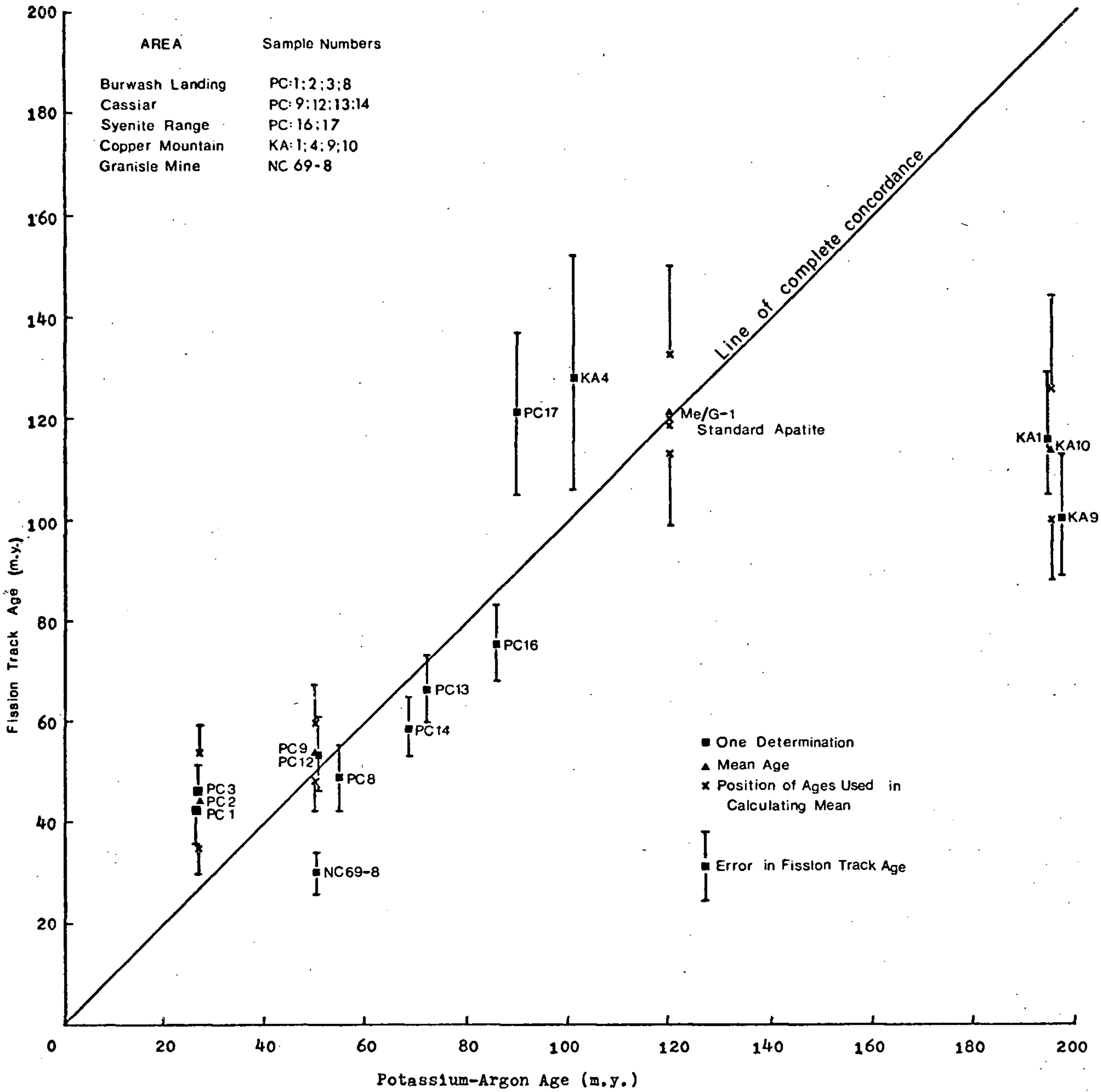

Fig. 3-1 Graphical comparison of apatite fission-track and biotite pottasium-argon apparent ages. Potassium-argon ages determined at the University of British Columbia have been shown to be accurate within 3 per cent (J. Harakal personal communication).

indicates that either slow cooling or mild reheating in the temperature range 150°C to 75°C annealed fission-tracks from apatite while argon was being retained by biotite. If apatite fission track ages are older than K-Ar ages on co-genetic biotite, the discrepancy is difficult to explain.

A mean apatite fission-track age of 111 $\pm$ 7 m.y. from samples KA1, KA9, and KA10 from the Copper Mountain intrusions is considerably younger than the mean biotite K-Ar age of 195 $\pm$ 2 m.y. for the samples. The consistently low ages obtained for apatite from the Copper Mountain intrusions suggest a thermal event that was strong enough to reset the apatite fission-track clocks but not the biotite K-Ar clocks. A temperature between 150°C and 75°C associated with a Cretaceous thermal event would account for the difference in apparent apatite fission-track and biotite K-Ar ages.

Concordance of apatite fission-track and biotite or hornblende K-Ar ages increases the reliability of an absolute age determination. Samples from the Cassiar area, Syenite Range, and Burwash Landing area generally have concordant biotite K-Ar and apatite fission-track ages. These findings suggest that the apatite fission-track method is a suitable absolute age dating method for late Mesozoic and Cenozoic igneous events in the Cassiar area, Burwash Landing area and Syenite Range.

3.6 COMPARISON OF K-Ar AND FISSION-TRACK DATING TECHNIQUES

Apatite fission-track ages of samples dated in this study are both concordant and discordant with K-Ar dates on co-genetic biotite or hornblende from the same sample. Young apatite fission-track ages have been attributed to the sensitive annealing character of fission-tracks in apatite (Naeser, 1967 a and b; Wagner, 1968; Christopher, 1969; Engels and Crowder, 1971). Apatite maintained at a temperature in excess of 50°C for a million years will lose 10 per cent of its tracks, and if the temperature is maintained in excess of 175°C, all accumulated fission-tracks will be annealed (Naeser and Faul, 1969).

Each mineral suitable for fission-track dating has a different temperature range for track annealing (Fleischer et al., 1965b; Naeser and Faul, 1969; Wagner, 1968). Figure 3-2 is a summary of annealing studies. In principle, dating a suite of minerals from the same site allows a thermal history to be constructed (e.g. Naeser, 1967 a and b; Engels and Crowder, 1971).

Lowering of K-Ar ages can also be caused by heating, but for biotite and hornblende, the loss of argon does not begin until a temperature of approximately 150°C is reached (Damon, 1968). Hornblende is more resistant to argon loss than biotite, but for either mineral, essentially all argon will be retained when fission-tracks are being annealed from apatite at temperatures between 75 and 175°C. K-Ar ages, obtained in conjunction with apatite or other fission-track ages, help resolve the thermal history of an area.

The simplicity of the apatite fission-track method is an appealing

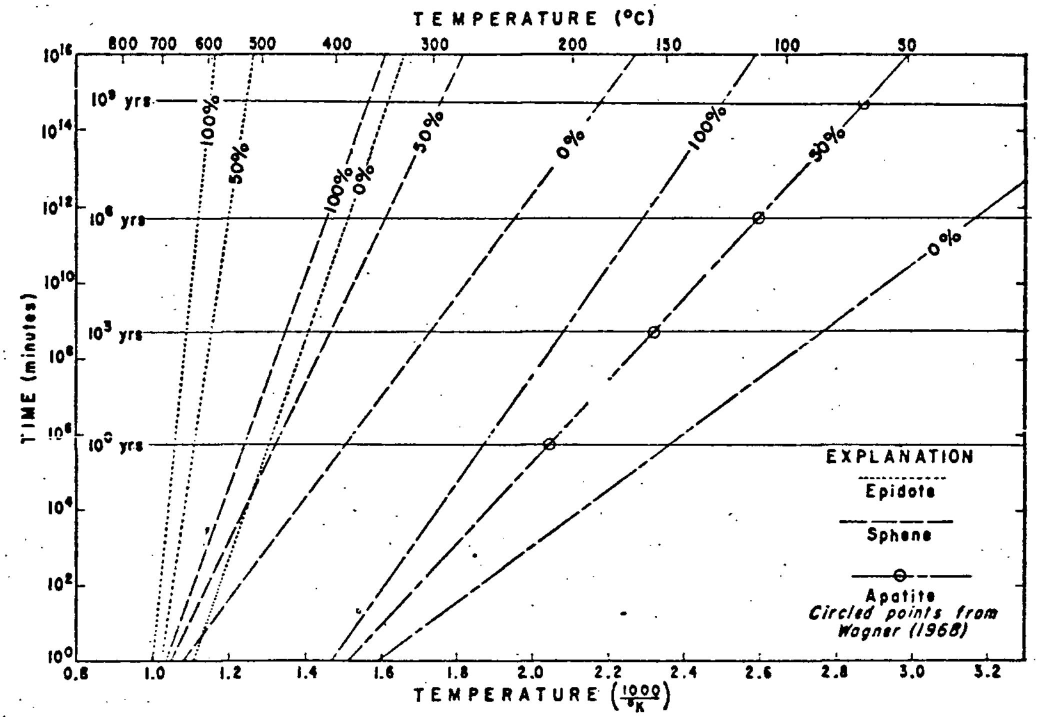

Fig. (3-2). Track-loss curves for epidote, sphene, and apatite (from Naeser and Dodge, 1969).

feature. Because normal laboratory equipment is used for fission-track dating, the experimental costs are minimal. The main cost of a fission-track determination involves the thermal neutron irradiation. Neutron irradiation services are commerically available, and by including several samples in a reactor run, the cost per sample is less than ten dollars.

After obtaining mounted and polished thin sections for normal and irradiated sample portions, the time needed for making a fission-track age determination will depend upon the fission-track density. An apatite fission-track age determination should take between 2 and 6 hours (Naeser and McKee, 1970) if between 10 and 20 grains are examined. For this study, track counting time was between 4 and 8 hours. The time necessary for a complete K-Ar analysis, including both potassium and argon analysis, is about 6 to 10 hours. In addition, the K-Ar analysis must be spread over several days.

Because only a few grains of sample are necessary for a fission-track determination, the mineral separation time is short and mineral concentrates can be obtained as by-products of mica and amphibole mineral separations. Rocks that are poor in micas and amphiboles are not easily dated by K-Ar and Rb-Sr methods, but should be datable by the fission-track method.

For samples with less than 50% atmospheric argon contamination, the precision of replicate K-Ar age determinations in the University of British Columbia K-Ar laboratory is within 1% and the accuracy within 3% (J.A. Harakal, personal communication, 1972). The amount of analytical uncertainty is greater for fission-track age determinations. Empirically, Naeser and Dodge (1969) have determined that ± 10% is a good estimate of 1 standard deviation in a fission-track age determination. Accuracy estimates for fission-track age determination cannot be made because of lack of interlaboratory comparison.

3.7 SUMMARY AND CONCLUSIONS

Fifteen apatite fission-track ages were obtained for apatite concentrates from six areas in British Columbia and the Yukon Territory. Apatite fission-track ages obtained from epizonal and mesozonal intrusions with porphyry mineral deposit affinity are consistent and generally concordant with biotite K-Ar ages where alteration is weak. Apatite samples from the Copper Mountain area and from the Granisle Mine were difficult to date using the fission-track method because of the altered nature of the apatite.

Three apatite fission-track ages from the Copper Mountain intrusions have a mean age of 111 ± 7 m.y. This mean age is interpreted to reflect a heating event that is related to Early to Middle Cretaceous granitic intrusion. Because biotite K-Ar ages in the Copper Mountain area are affected only by contact thermal events, and apatite fission-track ages appear to be regionally reset, temperatures between the minimum annealing temperature of apatite (approximately 75°C) and the minimum temperature for argon loss from biotite (approximately 150°C) are suggested for a regional thermal event of Cretaceous age.

Without additional geologic and geochronologic evidence, apatite fission-track ages from the Copper Mountain area and the Granisle Mine give misleading results with resulting misinterpretation of thermal history. Therefore, in cases where alteration is involved or thermal events are suspected, apatite fission-track ages should be checked by using another more refractory mineral or another radiometric clock.

A comparison of fifteen apatite fission-track ages with K-Ar ages (Figure 3-1) demonstrates that the apatite fission-track method can be used to age date porphyry mineral deposits, however the K-Ar method is generally more suitable in terms of cost and reliability.

4. AREAS STUDIED

4.1 INTRODUCTION

Areas studied are located on Figure 1-1. This chapter outlines the geologic setting and age of the areas studied. In addition the K-Ar and fission-track methods are compared for these areas.

4.2 SYENITE RANGE, YUKON TERRITORY

4.2.1 Introduction

Syenite Range is located about 60 miles southeast of Dawson City, Yukon Territory and 50 miles west-northwest of Mayo, Yukon Territory in the Yukon Plateau near the northeast flank of the Tintina Trench. Along the Tintina Trench and near its northeast flank are many bodies of course light grey granite commonly containing abundant feldspar phenocrysts (Bostock, 1948). These granitic bodies have been mapped by Bostock (1964) as Jurassic and (or) Cretaceous Coast Intrusions. The Syenite Range is composed of a composite stock of these coarse-grained granitic and syenitic rocks arranged in concentric zones with an outer zone of porphyritic syenite and a core of porphyritic granite (Bostock, 1948).

4.2.2 General Geology and Geochronology

Figure 4-1 shows the general geology and geochronology of the Syenite Range. Granitic rocks that compose the Syenite Range intrude Paleozoic sedimentary rocks. Similar granitic rocks of Cretaceous age occur in the Mayo Lake, Scougale Creek and McQuesten Lake map areas (Green, 1971).

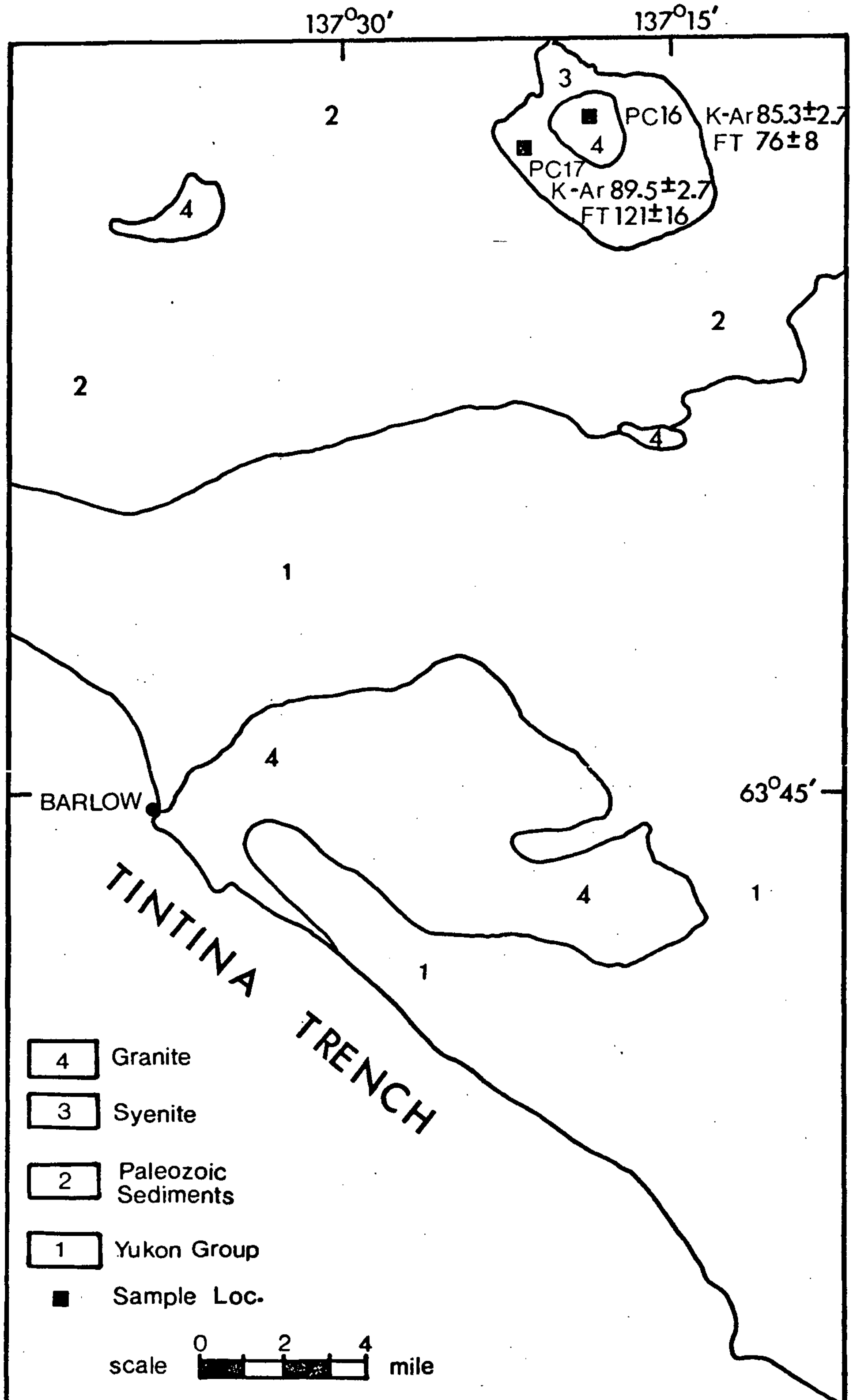

Figure 4-1. General geology and geochronology of the Syenite Range, Yukon Territory (geology after Bostock, 1964).

A Cretaceous age for granitic rocks of the Syenite Range is supported by field relationships and a number of radiometric age determinations. To the north and east of the Syenite Range, similar granitic rocks intrude the Keno Hill Quartzite of probable Early Cretaceous age (Green, 1971) and about 50 miles west of the Syenite Range in the Tintina Trench, similar granitic debris is present in Tertiary conglomerates (Green, 1972).

4.2.3 Radiometric Dating

Table 4-1 summarizes fission-track and K-Ar ages obtained for co-genetic biotite and apatite samples PC16 and PC17. Both rock samples contain about 5% biotite that is weakly altered along cleavage edges and grain boundaries to chlorite. Biotite K-Ar ages of 85.3 ± 2.7 m.y. and 89.5 ± 2.7 m.y. were obtained for specimens PC16 and PC17 respectively. These ages are similar to biotite K-Ar ages of 85 ± 7 m.y. (GSC 65-50) from a quartz monzonite stock about 25 miles south of the Syenite Range and 81 ± 5 m.y. (GSC 65-49) from quartz porphyry in the Keno Hill area about 50 miles northeast of the Syenite Range.

An apatite fission-track age of 76 ± 8 m.y. for sample PC16 is concordant with the 85.3 ± 2.7 m.y. biotite K-Ar age for the sample. An apatite fission-track age of 121 ± 16 m.y. for sample PC17 is discordant with the 89.5 ± 2.7 m.y. biotite K-Ar age for the sample. The large uncertainty for the apatite fission-track age (16 m.y.) is caused by the small number (187) of spontaneous fission-tracks counted.

4.2.4 Conclusions

The biotite K-Ar ages (85.3 ± 2.7 and 89.5 ± 2.7 m.y.) and apatite fission-track ages (76 ± 8 and 121 ± 16 m.y.) are mainly Late Cretaceous as defined in Wanless et al. (1972). These ages are in agreement with others (Gabrielse, 1967, p. 286) obtained from an arc of relatively small granitic intrusions strung out along the northeast side of the Tintina Trench.

Table 4-1 Fission-track and K-Ar ages obtained for granitic rocks in the Syenite Range, Yukon Territory.

Sample Number	Unit	Rock Type	Mineral dated	Fission-track age* (m.y.)	K-Ar age** (m.y.)
PC16	Syenite Range intrusions	Qtz. monz.	apatite	76 ± 8	
			biotite		85.3 ± 2.7
PC17	Syenite Range intrusions	Qtz. monz.	apatite	121 ± 16	
			biotite		89.5 ± 2.7

* Fission-track analyses by P.A. Christopher. Constants used in model age calculations: λ_F for U^{238} = $6.85 \times 10^{-17} yr^{-1}$; λ_D for U^{238} = $1.54 \times 10^{-10} yr^{-1}$; σ for U^{235} = $582 \times 10^{-24} cm^2$.

** Argon analyses by J.E. Harakal and P.A. Christopher using MS-10 mass spectrometer. Constants used in model age calculations: $\lambda_e = 0.585 \times 10^{-10} yr^{-1}$; $\lambda_\beta = 4.72 \times 10^{-10} yr^{-1}$; 40K/K = 1.181×10^{-4}.

4.3 CORK (BURWASH CREEK) Cu-Mo PROSPECT

4.3.1 Introduction

Eight K-Ar and four apatite fission-track ages were obtained from granitic and porphyritic textured intrusive rocks in the Burwash Landing area of southwestern Yukon Territory. Six of the samples were selected because of their spatial relationship to a porphyry Cu-Mo prospect on Burwash Creek, and two samples were collected to check the age of the Ruby

Range batholith to the east of Burwash Landing.

Figures 4-2 and 4-3 show sample locations and outline the geology in the Burwash Landing area. The Cork property lies in the northern segment of the Insular tectonic belt (Sutherland Brown et al., 1971). The area is part of the St. Elias Fold Belt, and consists of an eugeosynclinal assemblage of sedimentary, volcanic and intrusive rocks with ages ranging from Devonian to Tertiary.

High level porphyritic intrusive rocks near Burwash Creek have been mapped as Tertiary age by Muller (1967) on the basis of their chemical and textural similarity to sills, dikes, and small stocks that cut Tertiary sediments in the St. Elias Fold Belt. The Cork Cu-Mo prospect occurs in and around a body of quartz latite porphyry that intrudes sedimentary and volcanic rocks of late Paleozoic (Cache Creek Group) and early Mesozoic age (Mush Lake Group). An unmineralized gabbroic stock, mapped as part of the Cretaceous (?) Kluane Range intrusions (Muller, 1967), occurs along the southern margin of the Cork property.

Shakwak Trench, a major transcurrent fault zone, separates mainly volcanic and sedimentary rocks of the St. Elias Mountains to the southwest (Insular Belt) from mainly granitic and metamorphic rocks of the Yukon Plateau to the northeast (Coast Crystalline Belt). The Yukon Complex and the Ruby Range batholith are the major components of the Coast Crystalline Belt in the Burwash Landing area. The Ruby Range batholith is considered by Muller(1967) as part of the Coast Intrusions. The age of the Ruby Range batholith cannot be determined directly by its relationship to fossiliferous beds (Muller, 1967). Biotite K-Ar age determinations on quartz monzonite

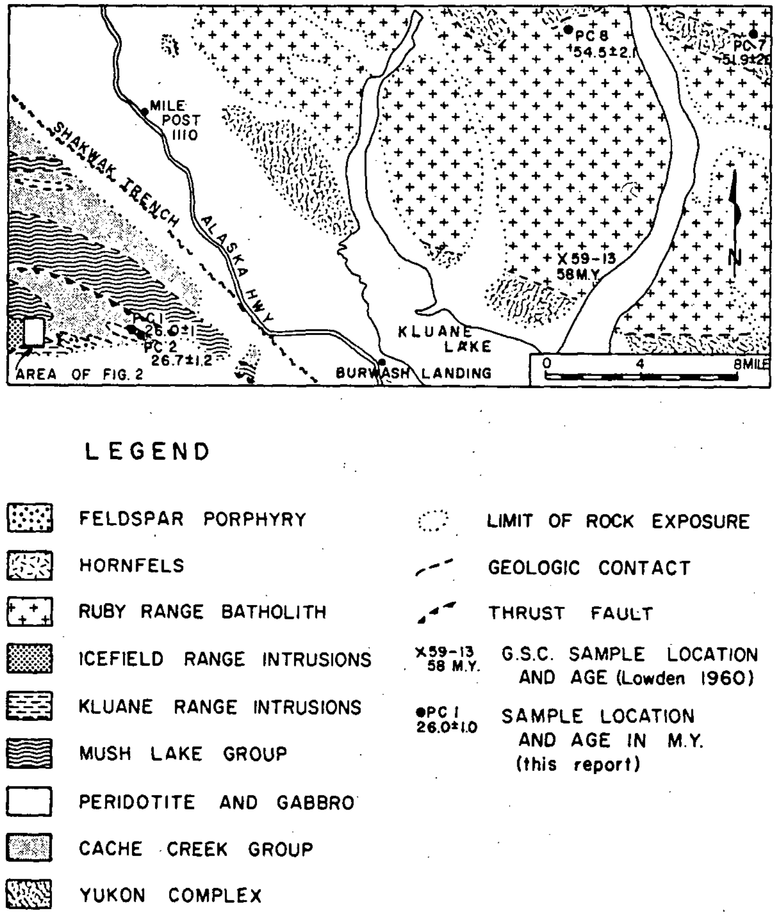

FIG.4-2 General geology and geochronology in the Burwash Landing area, Yukon Territory. Geology after Muller (1967).

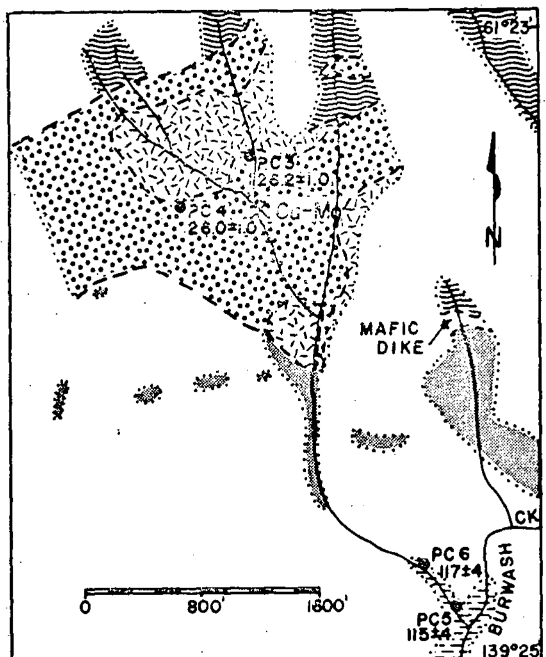

FIG. 4-3 General geology and geochronology of the Cork prospect (for legend see Fig.2-2).

and granodiorite from the Ruby Range batholith have yielded early Tertiary and Jurassic ages (Lowden, 1960; 1961). A 58 m.y. biotite K-Ar age was obtained from gneissic biotite granodiorite east of Burwash Landing.

4.3.2 Potassium-Argon Results

Isotopic age of the 8 analyzed samples are plotted on Figures 4-2 and 4-3. Table 4-2 summarizes K-Ar and apatite fission-track aged obtained for granitic rocks from the Burwash Landing area.

Specimens PC3 and PC4 were collected from a mineralized quartz latite porphyry stock located on the Cork property. Specimens PC1 and PC2 were collected from a chemically and texturally similar but unmineralized stock 3 miles east of the Cork property. These porphyritic rocks contain from 1 - 4% biotite as phenocrysts with minor chlorite alteration along cleavage planes and crystal boundaries. Unaltered hornblende concentrates were obtained from gabbro specimens PC5 and PC6 from the Cork property, and unaltered biotite concentrates were obtained from granodiorite specimens PC7 and PC8 from the Ruby Range batholith.

4.3.3 Fission-Track Results

Apatite concentrates were obtained from samples PC1, PC2, PC3, and PC8. The 48.9 $\pm$ 6.6 m.y. apatite fission-track age determined for sample PC8 from the Ruby Range batholith is concordant with and provides support for the 54.5 $\pm$ 2.0 m.y. biotite K-Ar age determined for this sample. Apatite fission-track ages ranging from 42.4 to 46.6 m.y. (PC1 to PC3) were obtained for the porphyritic rocks near Burwash Creek. These age are

Table 4-2. Fission-track and K-Ar ages obtained for granitic rocks in the Burwash Landing area, Yukon Territory.

Sample Number	Unit	Rock Type	Mineral dated	Fission-track age* (m.y.)	K-Ar age** (m.y.)
PC1	Tertiary stock (?)	Qtz. latite porphyry	apatite	42 ± 7	
			biotite		26.1 ± 1.0
PC2	Tertiary stock (?)	Qtz. latite porphyry	apatite	54 ± 6	
			apatite	35 ± 5	
			biotite		26.7 ± 1.2
PC3	Tertiary stock (?)	Qtz. latite porphyry	apatite	47 ± 5	
			biotite		26.2 ± 1.0
PC4	Tertiary stock (?)	Qtz. latite porphyry	biotite		26.0 ± 1.0
PC5	Kluane Range Intrusions	Gabbro	hbl.		115 ± 4.0
PC6	Kluane Range Intrusions	Gabbro	hbl.		117 ± 4.0
PC7	Ruby Range batholith	Bio. granodiorite	biotite		51.9 ± 2.0
PC8	Ruby Range batholith	Bio.-Hbl. granodiorite	apatite	49 ± 7	54.5 ± 2.0
			bio.		

Note: Porphyritic latite sample CKD-1 from the Cork property has a K-Ar age of 26.2 ± 0.4 m.y. and hornblende diorite sample JCD-1 from the Kluane Range intrusions on the Cork property has a K-Ar age of 111.7 ± 2 m.y. (D.C. Way written communication, December 1972). Samples CKD-1 and JCD-1 were analysed by Dr. E. Farrar of the Department of Geological Sciences, Queen's University, Kingston, Ontario.

* Fission-track analyses by P.A. Christopher. Constants used in model age calculations: λ_F for $U^{238} = 6.85 \times 10^{-17} yr^{-1}$; λ_D for $U^{238} = 1.54 \times 10^{-10} yr^{-1}$; σ for $U^{235} = 582 \times 10^{-24}$ cm^2.

** Argon analyses by J.E. Harakal and P.A. Christopher using MS-10 mass spectrometer. Constants used in model age calculations: $\lambda_e = 0.585 \times 10^{-10} yr^{-1}$; $\lambda_\beta = 4.72 \times 10^{-10} yr^{-1}$; $^{40}K/K = 1.181 \times 10^{-4}$.

consistently older than the mean 26.2 ± 0.3 m.y. biotite K-Ar age determined for samples PC1 to PC4, but both methods support the Tertiary age assigned to this unit by Muller (1967).

The reason for consistently older apatite fission-track ages is not clear. Older apatite fission-track apparent ages relative to biotite K-Ar apparent ages are difficult to explain because argon is retained in biotite at a temperature that will cause annealing of fission-tracks in apatite (Naeser, 1967a; Naeser and Faul, 1969). It is unlikely that secondary biotite could have formed without the annealing of primary apatite grains and the discrete biotite grains and books appear to be primary biotite. If weathering was important in lowering the K-Ar age, it is not indicated by the small deviation in the four biotite K-Ar apparent ages, in thin section examination of rocks, or microscopic examination of biotite concentrates. The most likely explanation for the discrepancy is a slight bias in counting which might result because of the extremely low spontaneous track density and the small spontaneous to induced track density ratio. A consistent bias could explain the older ages.

4.3.4 Discussion

The 26.2 ± 0.3 m.y. mean biotite K-Ar age determined for quartz latite porphyry (PC1 - PC4) is the best age for emplacement of this unit. Samples were analyzed in a manner suitable for isochron determinations (Roddick and Farrar, 1971), but the narrow range of potassium values for the samples leads to isochron ages with large uncertainties (see section 2.4).

The 115 ± 4 m.y. and 117 ± 4 m.y. hornblende K-Ar ages determined for Kluane Range Intrusions on the Cork property agree with the Cretaceous age assigned to this unit by Muller (1967). The 51.9 ± 2.0 m.y. and 54.5 ± 2.0 m.y. biotite K-Ar ages determined for the Ruby Range batholith are slightly younger than the Geologic Survey of Canada age of 58 m.y. (Lowdon, 1961).

Tertiary apatite fission-track ages determined for quartz latite porphyry near Burwash Creek and for one sample (PC8) from the Ruby Range batholith are consistent with biotite K-Ar ages and the Tertiary ages suggested for these units by Muller (1967).

Both mineralized and barren quartz latite porphyry near Burwash Creek yield ages which are identical within the limits of detection and precision of the K-Ar method. This agrees with the findings of White et al. (1968) that for many British Columbia porphyry mineral deposits, mineralization is an integral feature of a magmatic event.

The Cork prospect is in a large belt of Tertiary volcanic and intrusive rocks which extend through the St. Elias Mountains and adjacent Alaska Range (Muller, 1967 p. 102). This belt may contain other similar Tertiary porphyry type mineral deposits.

4.4. NORTHERN BRITISH COLUMBIA

4.4.1 Introduction

Seven biotite K-Ar ages and four apatite fission-track ages (Table 4-3) were determined for porphyritic intrusions in northern British Columbia (Figures 4-4 and 4-5). Samples were selected because of their spatial and temporal relationship to Mo and Mo-W deposits in the Cassiar and Atlin areas. Sutherland Brown et al. (1971) suggested that an area extending from the Coast Crystalline Belt-Intermontane Belt boundary in the Atlin area across

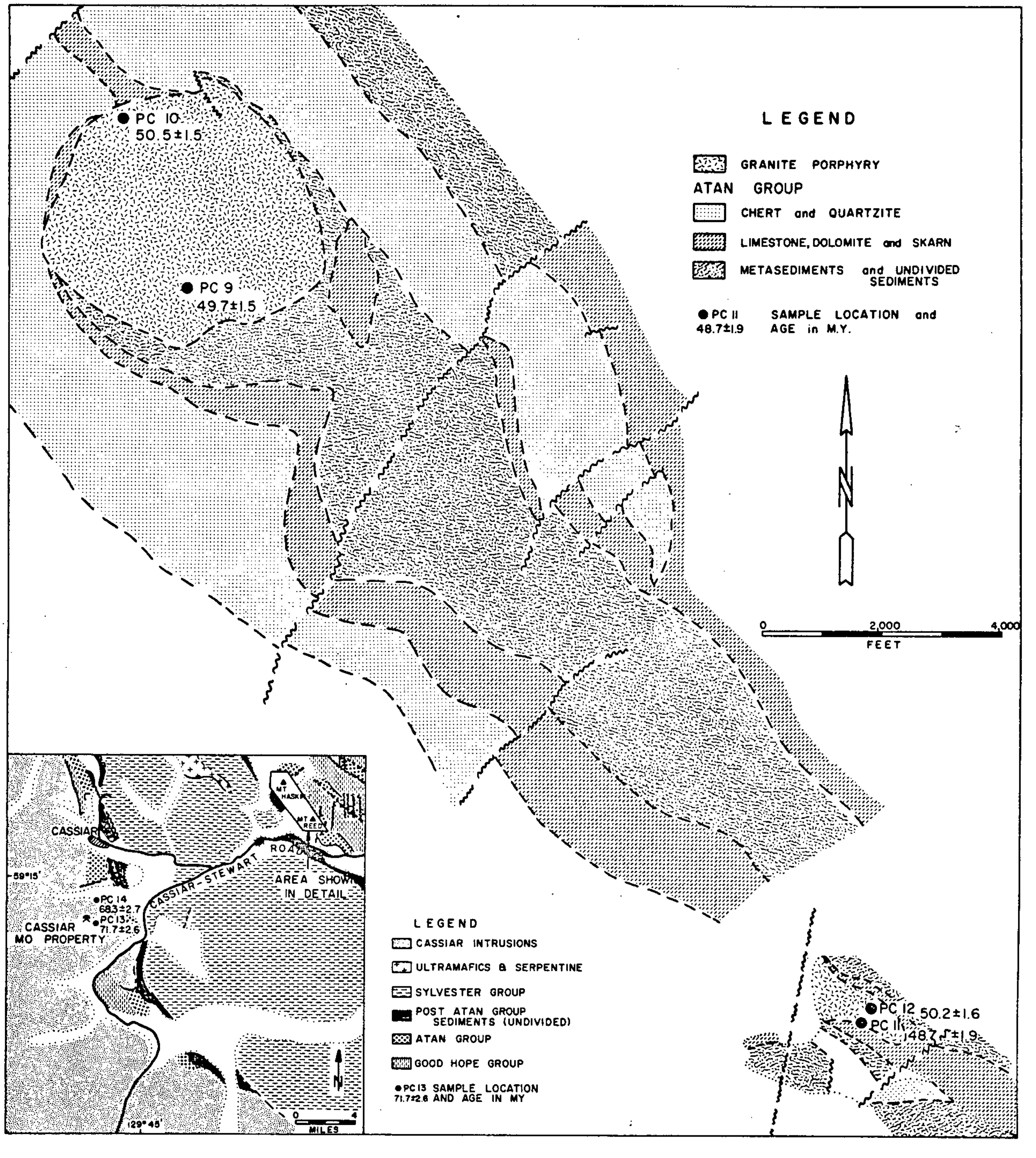

Figure 4-4. General geology and geochronology in the Cassiar area, B.C. (after Gabrielse, 1963), Mt. Haskin Mo Property (after G. Lamont, 1971, unpublished mapping) and Mt. Reed Mo-W property (after P. Hirst, 1969, unpublished mapping).

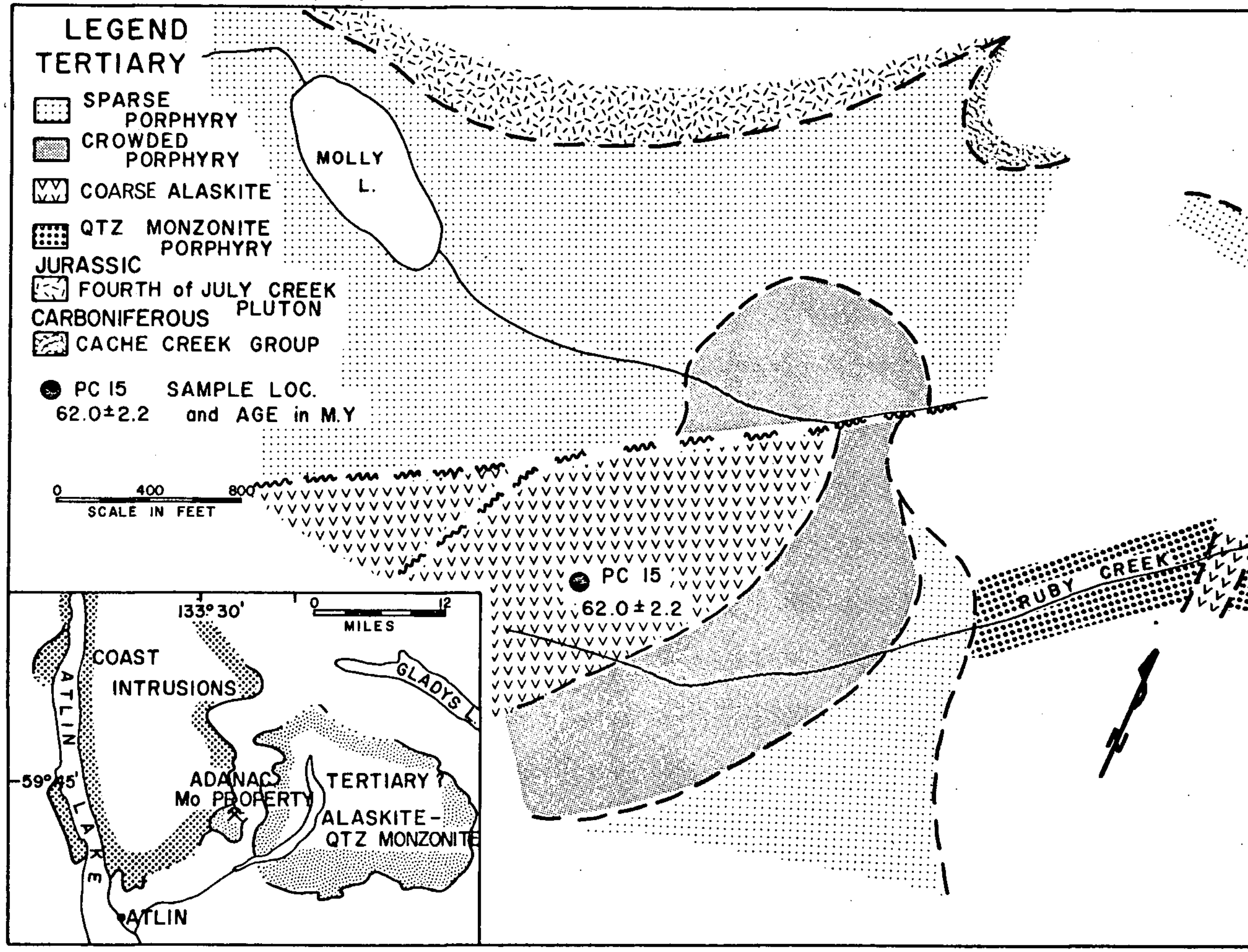

Figure 4-5. General geology and geochronology in the Atlin Area (after Aitken, 1959) and of the Adera Claims - Adanac Mo property (after Sutherland Brown, 1969b).

Table 4-3. Fission-track and K-Ar ages of granitic rocks in northern British Columbia.

Sample Number	Unit	Rock Type	Mineral dated	Fission-track age* (m.y.)	K-Ar age** (m.y.)
		CASSIAR AREA			
PC9	Mt. Haskin porphyry	Granite porphyry	apatite	48 ± 6	
			apatite	60 ± 8	
			biotite		49.7 ± 1.5
PC10	Mt. Haskin porphyry	Granite porphyry	biotite		50.5 ± 1.5
PC11	Mt. Reed porphyry	Granite porphyry	biotite		48.7 ± 1.9
PC12	Mt. Reed porphyry	Granite porphyry	apatite	54 ± 7	
			biotite		50.2 ± 1.6
PC13	Cassiar intrusions	Quartz monzonite	apatite	67 ± 7	
			biotite		71.7 ± 2.6
PC14	Cassiar intrusions	Quartz monzonite	apatite	60 ± 6	68.3 ± 2.7
			biotite		
		ATLIN AREA			
PC15	Mt. Leonard Boss	coarse Alaskite	biotite		62.0 ± 2.2

* Fission-track analyses by P.A. Christopher. Constants used in model age calculations: λ_F for $U^{238} = 6.85 \times 10^{-17} yr^{-1}$; λ_D for $U^{238} = 6.85 \times 10^{-17} yr^{-1}$; λ_D for $U^{238} = 1.54 \times 10^{-10} yr^{-1}$; σ for $U^{235} = 582 \times 10^{-24}$ cm^2.

** Argon analyses by J.E. Harakal and P.A. Christopher using MS-10 mass spectrometer. Constants used in model age calculations: $\lambda_e = 0.585 \times 10^{-10} yr^{-1}$; $\lambda_\beta = 4.72 \times 10^{-10} yr^{-1}$; $40K/K = 1.181 \times 10^{-4}$.

the Stikine Arch into the Omineca Belt in the Cassiar area contains one of the three major molybdenum concentrations in the Canadian Cordillera. The general geology of the Cassiar and Atlin areas is described below.

4.4.2 Cassiar Area *

The Cassiar Batholith (Figure 4-4) has a mean K-Ar age of 102 ± 3 m.y. Late Cretaceous igneous activity along the western margin of the Cassiar Batholith is indicated by mean ages of 96 ± 3 m.y. from the Seagull Batholith and 76.5 ± 4 m.y. from the Glundebery Batholith, and by K-Ar ages of 78 ± 4 m.y. from the Parallel Creek Batholith and 71 m.y. from a quartz monzonite north of Dease Lake. Early Tertiary igneous activity to the west of the Cassiar Batholith is indicated by concordant K-Ar ages of 48 ± 4 m.y. on hornblende and 46 ± 2 m.y. on biotite from a small quartz diorite pluton that intrudes the Christmas Creek Batholith.

A young stock, that occurs within the Cassiar Batholith to the northwest of the area shown in Figure 4-4 has yielded biotite K-Ar ages of 58 ± 3 m.y. and 53 ± 3 m.y. The Blue Light property, located in this young quartz monzonite body, contains tungsten and beryllium minerals (Mulligan, 1969).

A muscovite K-Ar age of 57 m.y. was obtained from granitized terrain exposed about 10 mi. northeast of Mt. Haskin in the Horse Ranch Range. Gabrielse (in Lowdon et al., 1963b) suggested that this age might date the emplacement of post-tectonic plutons and metamorphic rocks recrystallized to some extent at that time.

Because the youngest rocks intruded by the Cassiar intrusions in the area shown in Figure 4-4, are of Devono-Mississippian age (Gabrielse, 1963),

* See Appendix D (Table D-1) for review of ages cited

time of intrusion cannot be dated accurately by stratigraphic methods.

Samples PC9 to PC14 (Figure 4-4) were collected from:

(1) a quartz monzonite porphyry stock that intruded Paleozoic sedimentary and volcanic rocks to the east of the Cassiar Batholith and

(2) small granite porphyry stocks, sills and dikes that intruded sedimentary and metasedimentary rocks of the Atan Group.

Cassiar Molybdenum Property

The Cassiar Molybdenum property (Figure 4-4) occurs within a young quartz monzonite that cuts the Cassiar Batholith along its eastern border (Campbell, 1968). Stockwork and disseminated molybdenite are related spatially and probably genetically to a late, fine-grained phase of the young quartz monzonite.

Samples PC13 and PC14 were collected from the early, pre-mineralization phase of the quartz monzonite stock. Biotite concentrates from these samples contain less than 2% chlorite as alteration along cleavage planes. Quartz monzonite samples PC13 and PC14 have consistent biotite K-Ar ages of 71.7 ± 2.6 m.y. and 68.3 ± 2.7 m.y.

Mt. Haskin Mo and Mt. Reed Mo-W Properties

Granite porphyry intruded sedimentary and metasedimentary rocks of the Atan Group on both the Mt. Haskin Mo and Mt. Reed Mo-W properties (areas shown in detail on Figure 4-4). Stockwork and disseminated molybdenum and tungsten bearing minerals are found in both the granite porphyry and contact altered metasedimentary rocks. Mineralization is believed to be temporally related to the granite porphyry.

Granite porphyry samples PC9 and PC10 are from a small stock on the Mt. Haskin property and granite porphyry samples PC11 and PC12 are from a texturally and chemically similar stock on the Mt. Reed property. Biotite contents of samples PC9-PC12 range from 1 to 4%. Chlorite content of the analyzed biotite concentrates is less than 5%.

Granite porphyry samples PC9 to PC12 from Mt. Haskin Mo and Mt. Reed Mo-W properties have biotite K-Ar ages ranging from 48.7 to 50.5 m.y. and a mean K-Ar age of 49.8 $\pm$ 0.7 m.y. Reliable isochron ages could not be obtained from the granite porphyry (see section 2.4) because of the small differences in potassium content of the biotite concentrates PC9 to PC12.

Discussion

Ages obtained for quartz monzonite and granite porphyry in the Cassiar area suggest that molybdenum and associated tungsten mineralization occurred after the emplacement of the Cassiar Batholith (102 $\pm$ 3. m.y.). The 71.7 $\pm$ 2.6 m.y. and 68.3 $\pm$ 2.7 m.y. ages obtained for a young phase of the Cassiar intrusions place an upper limit on the age of mineralization on the Cassiar Molybdenum property. Because both mineralized and barren granite porphyry samples from the Mt. Reed and Mt. Haskin properties yield the same age within analytical limits, mineralization on these properties is considered to be an integral part of an early Tertiary magmatic event. The Late Cretaceous and early Tertiary ages obtained for quartz monzonite porphyry and granite porphyry phases of the Cassiar intrusions are consistent with a trend from older, more basic, granitic phases to younger, more acid, porphyritic bodies.

Apatite fission-track ages obtained from the Cassiar area are in good agreement with K-Ar ages for cogenetic biotite. Figure 3-1 demonstrates the K-Ar ages and apatite fission-track ages for samples PC8, PC12, PC13 and PC14 are the same within analytical limits. Because apatite fission-track and biotite K-Ar ages are concordant, the apatite fission-track method is considered to be useful in age dating Late Cretaceous and Tertiary units in the Cassiar area.

4.4.3. Atlin Area

No radiometric ages are available for intrusive rocks in the Atlin area. Ages ranging from 54 m.y. to 70 m.y. were reported from the Bennett area to the west and adjacent parts of the Alaska Panhandle (Cristie in Lowdon et al., 1963a), and an age of 69 m.y. was obtained from quartz monzonite in the Tulsequah area to the south. Souther (in Lowdon et al., 1963b) reported that discordant quartz monzonite stocks along the eastern contact of the Coast Crystalline Belt in western British Columbia and southeastern Yukon are part of the youngest phase of the Coast Intrusions.

More recently, K-Ar whole-rock and biotite ages ranging from 46.9 to 52.8 m.y. were obtained from quartz monzonite of the East Marginal Pluton of the Coast Intrusions in the Juneau Ice Field area (Forbes and Engles, 1970). These data reinforce the early Tertiary K-Ar ages for granitic rocks along the eastern margin of the Coast Intrusions.

Adanac Mo Property

Figure 4-5 shows the location and general geology of the Adanac area. The Adanac Mo property is on upper Ruby Creek, and molybdenum with minor tungsten is found in granitic rocks that are part of the Mt. Leonard Boss mapped by Sutherland Brown (1969b). The Mt. Leonard Boss intrudes a sequence of rocks ranging in age from Permo-Pennsylvanian Cache Creek metavolcanic rocks to the Fourth of July Batholith which has been assigned a Jurassic (?) age (Aitken, 1959). Sutherland Brown (1969b) suggested that the mid-Cretaceous (?) Mt. Leonard Boss is in all probability connected to the main Suprise Lake Batholith and that all phases of the stock are as closely related in age as they are in chemistry.

One sample (provided by W. Sirola) was available from the Mt. Leonard Boss. This sample contained about 1% biotite with 15% chlorite alteration. A biotite concentrate containing about 5% chlorite was obtained from the sample. Low potassium content of the biotite (5.16 $\pm$ 0.04%) is caused by chlorite alteration. A 62.9 $\pm$ 2.2 m.y. K-Ar age was obtained for the biotite concentrate.

The 62.9 $\pm$ 2.2 m.y. age for the alaskite phase of the Mt. Leonard Boss is consistent with the young age of discordant quartz monzonite stocks along the eastern contact of the Coast Crystalline Belt (Souther in Lowdon et al., 1963a; Forbes and Engles, 1970).

4.4.4 Conclusions

Late Cretaceous and early Tertiary ages obtained for the Adanac Mo property, Cassiar Mo property, Mt. Haskin Mo property, and Mt. Reed Mo-W property, and early Tertiary ages reported for quartz monzonite and pegmatite associated with the Blue Light tungsten property (Wanless et al., 1970) indicate a Late Cretaceous to early Tertiary metallogenic epoch for molybdenum and tungsten in northern British Columbia. The existence of a

Late Cretaceous to early Tertiary metallogenic epoch for porphyry mineral deposits has previously been suggested for central British Columbia (Carter, 1970; 1972a) and for southeastern Alaska (Reed and Lanphere, 1969).

4.5 GRANISLE MINE, BABINE LAKE AREA, BRITISH COLUMBIA

4.5.1 Introduction

Copper deposits of the Babine Lake area are related to small, high-level, subvolcanic porphyritic intrusions of early Tertiary age that intrude Mesozoic volcanic and sedimentary rocks of the Hazelton Group (see Carter, 1972b, Fig. 12, page 28; Carter, 1970). The intersection of northwesterly and northeasterly striking faults may have controlled emplacement of Tertiary intrusions. Porphyry copper deposits are associated with dykes and plugs of biotite-feldspar porphyry of quartz diorite composition. Biotite K-Ar ages obtained for 10 samples from porphyries have yielded a mean age of 51.2 $\pm$ 2 m.y. (Carter 1972b).

The Granisle Mine has been classified as an elaborate porphyry deposit (Sutherland Brown, 1969a) because of the several phases and pulses of biotite-feldspar porphyry that are spatially and temporally associated with copper mineralization. An oval zone of potassic alteration is roughly coincident with the ore zone and a number of north 50° east striking bornite-chalcopyrite-quartz-biotite-apatite veins occur in the potassic zone (Carter, 1972b).

4.5.2. Potassium-Argon Dating

A mean biotite potassium-argon age of 51.2 $\pm$ 2 m.y. was determined for

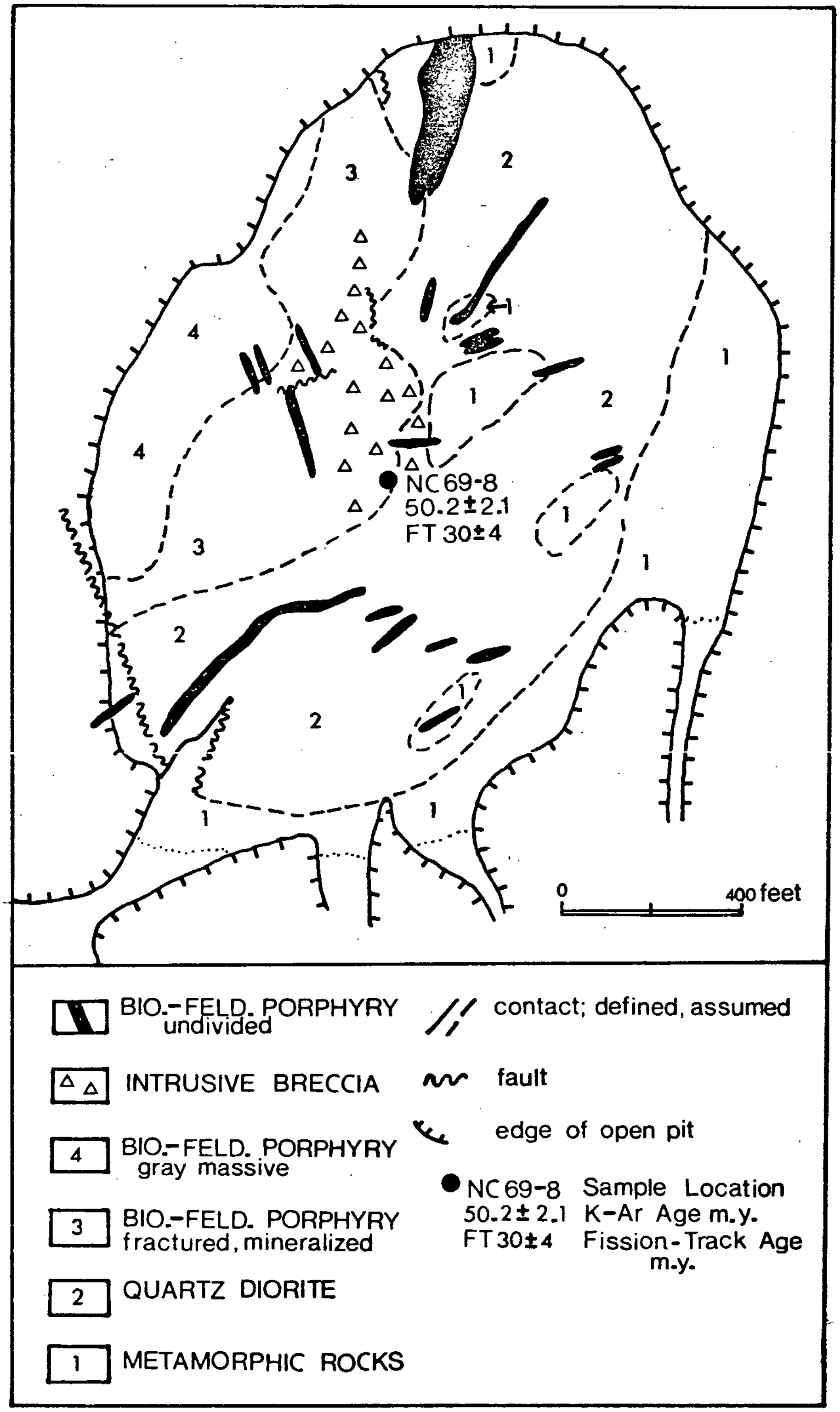

Figure 4-6. Geochronology and general geology of the Granisle Mine pit (geology from Carter, 1972b).

three samples of biotite-feldspar porphyry and one sample (NC-69-8) of a quartz-chalcopyrite-bornite-apatite vein from the Granisle Mine (Carter, 1972b). Biotite from sample NC-69-8 has a K-Ar age of 50.2 ± 2.1 m.y. (N.C. Carter personal communication, 1972).

4.5.3 Fission-Track Dating

Part of sample NC-69-8 was obtained from N.C. Carter to obtain apatite for a fission-track age determination. Apatite grain mounts used to determine the fission-track age revealed two generations of apatite; 1) minor very clear and relatively unaltered apatite (selectively counted), and 2) highly altered grains containing fluid, chalcopyrite and altered silicate inclusions. Only a few useable grains could be obtained by scanning the grain mounts at low power. A fission-track age of 29.6 ± 4.1 m.y. obtained for this sample is discordant with the 51.2 ± 2 m.y. biotite K-Ar age, but the apatite fission-track age does reflect the young Tertiary age.

4.5.4 Discussion

The 50.2 ± 2.1 m.y. biotite K-Ar age of sample NC-69-8 (Figure 4-6) is supported by mean K-Ar ages of 51.2 ± 2 m.y. for four samples from the Granisle Mine and 51.2 ± 2 m.y. for ten K-Ar age for porphyries in the Babine Lake area (Carter, 1972b). The 30 ± 4 m.y. apatite fission-track age is young and could be a reset age, but alteration of apatite grains made track distinction difficult and the error in this determination may be larger than the counting error.

4.6 COPPER MOUNTAIN AREA, BRITISH COLUMBIA

4.6.1 Introduction

The Copper Mountain and Ingerbelle mineral deposits, which are located on opposite sides of the Similkameen River, about 10 miles south of Princeton, British Columbia, occur in syenitic stocks and volcanic rocks of the Upper Triassic and Lower Jurassic Nicola Group. These 'syenitic' deposits have been classified on the basis of structure as complex porphyry deposits (Sutherland Brown, 1969a) and on the basis of the high-level of emplacement of an associated and genetically related variable shaped pluton as volcanic porphyry deposits (Sutherland Brown, 1972). Copper deposits of the 'syenitic' volcanic porphyry class appear to be restricted to the intermontane tectonic belt of the Canadian Cordillera.

Comprehensive geologic reports on the geology of the Copper Mountain area by Dolmage (1934), Rice (1947), Fahrni (1951, 1962, 1966), Montgomery (1967) and Preto (1972a and b) and K-Ar age dating studies by Sinclair and White (1967) and Preto et al. (1971) support the geologic interpretation presented in Figure 4-7.

Table 4-4 is a listing of the apatite fission-track ages obtained for samples previously dated by the biotite K-Ar method.

4.6.2 General Geology

Figure 4-7 shows the general geology of the Copper Mountain area and the location of the Ingerbelle and Copper Mountain mineral deposits. The oldest rocks in the area are part of the Upper Triassic Wolf Creek Formation of the Nicola Group (Rice, 1947). In the Copper Mountain area the Wolf Creek Formation is predominately andesite, tuff and volcanic clastic sediments

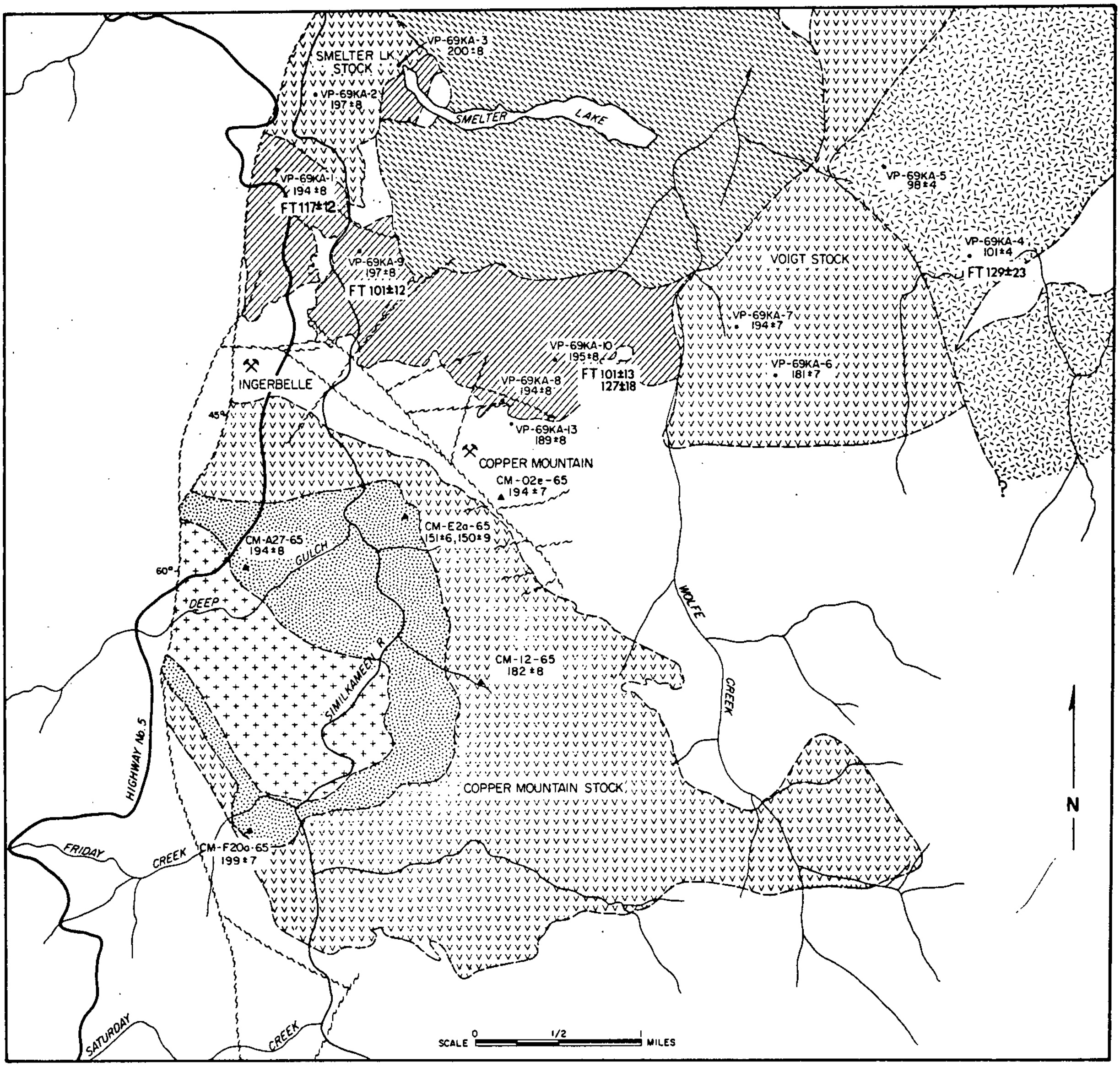

FIGURE 2-7 GENERAL GEOLOGY OF THE COPPER MOUNTAIN AREA BRITISH COLUMBIA

- PRINCETON GROUP
- VERDE CREEK QTZ. MONZ.
- LOST HORSE INTRUSION
- PERTHOSITE PEGMATITE
- MONZONITE
- DIORITE
- NICOLA GROUP
- VP-69AK-1 194±8 — SAMPLE LOCATION AND AGE IN M.Y. (Preto et al., 1971)
- CM-12-65 182±8 — SAMPLE LOCATION AND AGE IN M.Y. (Sinclair and White, 1968)
- FT 101±12 — FISSION-TRACK AGE M.Y. (this report)

that generally display very mild metamorphism and deformation, except in the immediate vicinity of intrusive bodies (Preto, 1972b). A number of quartz-poor plutons, collectively known as the Copper Mountain intrusions (Montgomery, 1967) are spatially and genetically related to the mineral deposits. The largest, the Copper Mountain stock, is a concentrically differentiated intrusion, elliptical in plan and about 6.5 square miles in area. It ranges in composition from diorite at its outer edge through monzonite to syenite and perthosite pegmatite at the core (Montgomery, 1967). Preto et al. (1971) divide the Copper Mountain intrusions into the zoned Copper Mountain stock, the satellite Smelter Lakes and Voigt stocks, and the Lost Horse intrusions (Figure 4-7). Northeast of Copper Mountain, diorite of the Voigt stock and volcanic rocks of the Nicola Group are cut by a body of younger quartz monzonite that was named the Verde Creek granite by Dolmage (1934) and believed by Rice (1947) to be correlative with the Otter intrusions of Upper Cretaceous or younger age. K-Ar age dating by Preto et al. (1971) supports the Cretaceous age assigned to the Verde Creek body.

In the vicinity of the Copper Mountain and Ingerbelle mineral deposits alkali metasomatism has produced a distinctive mineral assemblage characteristic of copper deposits of the Nicola Belt. Alteration is most intense in the Lost Horse intrusions and bears a close spatial relationship to faults and fractures (Preto, 1972a). Successive stages of alteration recognized by Preto (1972a) are:

1) Development of biotite that has been partly destroyed by later alteration.

2) Development of albitic plagioclase and epidote that was accompanied by removal of biotite and of disseminated magnetite, and bleaching of pyroxene. Secondary sphene, apatite and pyroxene are locally developed.

3) Development of pink potash and plagioclase feldspar along fractures that was accompanied by sulfide-bearing pegmatite veins characterized by selvages of coarse biotite along the edges and bornite, chalcopyrite, potash feldspar, and calcite at the center.

4) Development of late scapolite veins that are most prominent in the Ingerbelle area.

Because biotite and apatite used for some of the age dating was developed during the alteration stages, the interpretation of radiometric ages would be tenuous without the detailed description of alteration provided by Preto (1972a and b).

4.6.3 Fission-Track Dating

Ten samples (VP69 (KA1 to KA10)) from the Copper Mountain area that had previously been dated by the biotite K-Ar method (Preto et al. 1971) were obtained from the British Columbia Department of Mines. Apatite concentrates were obtained from eight of the ten samples, but intense alteration of apatite grains eliminated the possibility of using four of the eight apatite concentrates for fission-track dating. Sample KA4 from the Verde Creek quartz monzonite in the Copper Mountain area gave discordant 101 $\pm$ 4 m.y. biotite K-Ar and 129 $\pm$ 23 m.y. apatite fission-track apparent ages. The minor discordance is attributed to the altered nature of the apatite grains.

Samples KA1, KA9 and KA10 from the Copper Mountain intrusions yield a mean apatite fission-track age of 111 ± 7 m.y. and a mean biotite K-Ar age of 195 ± 2 m.y. Biotite K-Ar ages for samples KA1, KA9 and KA10 are in close agreement with mean biotite K-Ar age of 193 ± 8 m.y. reported by Preto et al. (1971) for eleven samples from Copper Mountain. The Copper Mountain intrusions are believed to be co-magmatic with the Upper Triassic to Lower Jurassic Nicola volcanics, and since extensive K-Ar dating supports an Upper Triassic or earliest Lower Jurassic age for the Copper Mountain intrusions (Preto et al. 1971; Sinclair and White 1968), the Cretaceous apatite fission-track ages for the Copper Mountain intrusions probably represent reset ages or thermally lowered ages. A widespread Cretaceous thermal event in the Copper Mountain area is suggested by:

1) the average age of 99.5 ± 4 m.y. determined by Preto et al. (1971) for the Verde Creek quartz monzonite.
2) a 104 m.y. age suggested for the major phases of the Eagle granodiorite lying to the west of Copper Mountain (Roddick and Farrar, 1972), and
3) an Early to Middle Cretaceous thermal event dated about 100 m.y. in northcentral Washington (Hibbard, 1971).

The consistent low ages obtained for apatite from the Copper Mountain intrusions suggest a thermal event that was strong enough to reset the apatite fission-track clocks but not the biotite K-Ar clocks. A temperature between about 75°C (Naeser and Faul, 1969; Wagner 1968) and 150°C (Damon, 1968) associated with a Cretaceous thermal event would account for the difference in apparent fission-track and biotite K-Ar ages.

4.6.4 Summary

A 129 ± 23 m.y. apatite fission-track age for the Verde Creek quartz monzonite supports the Cretaceous age for this unit. A mean apatite fission-track age of 111 ± 7 m.y. for samples KA1, KA9 and KA10 from the Copper Mountain intrusions reflect a heating event that is related to Early to Middle Cretaceous granitic intrusion.

Table 4-4. Fission-track and K-Ar ages obtained for granitic rocks in the Copper Mountain area, British Columbia. (K-Ar ages are from Preto et al., 1971)

Sample Number	Unit	Mineral dated	Fission-track age (m.y.)*	K-Ar age (m.y.)
KA1	Lost Horse intrusion	apatite	117 ± 12	
		biotite		194 ± 8
KA4	Verde Creek qtz. monz.	apatite	129 ± 23	
		biotite		101 ± 4
KA9	Lost Horse intrusion (dike)	apatite	101 ± 12	
		biotite		197 ± 8
KA10	Lost Horse intrusion	apatite	101 ± 13	
		apatite	127 ± 18	
		biotite		195 ± 8

* Fission-track analyses by P.A. Christopher. Constants used in model age calculations: λ_F for U^{238} = $6.85 \times 10^{-17} yr^{-1}$; λ_D for U^{238} = $1.54 \times 10^{-10} yr^{-1}$; σ for U^{235} = $582 \times 10^{-24} cm^2$.

5. REVIEW OF METALLOGENY AND METALLOGENIC EPOCHS FOR PORPHYRY MINERAL DEPOSITS OF THE CANADIAN CORDILLERA

5.1 Introduction

In this chapter the K-Ar ages obtained for this study and published ages are used to place porphyry mineral deposits of the Canadian Cordillera in a tectonic-stratigraphic-lithologic framework; the concept of metallogenic epochs is evaluated for porphyry and related mineral deposits; and the concept of metallogenic epochs for porphyry deposits is examined in terms of global tectonics.

5.2 Metallogeny and Metallogenic Epochs

Metallogeny is concerned with the genesis of mineral deposits and with their distribution in space and time. Metallogenic provinces and metallogenic epochs reflect an uneven distribution of various types of mineral deposits in space and time.

The first statement of the concept of metallogenic provinces and metallogenic epochs was presented by De Launay (1913). As the result of his regional studies of mineral deposits in France, De Launay suggested that each metallogenic province belongs to a definite regional type depending on the tectonics and that the nature of each province may be forecast, to a certain extent, by the knowledge of the latter. This is a very comprehensive and concise statement of the problem encountered by the geologist attempting to outline a genetic model for a metallogenic province.

Lindgren (1933) discussed the factor of time as it concerns the mineral deposits of a metallogenic province, and Petrascheck (1965) credits Lindgren with the introduction of the concept of a metallogenic epoch. Lindgren's examples suggest that metallogenic epochs coincide with the major orogenic epochs in the earth's history. Turneaure (1955) used the term metallogenic epoch to designate periods during which mineralization was most pronounced. Petroscheck (1965) restricted metallogenic epochs to tectonic metallogenic intervals within a major tectonic unit (e.g. orogenic belt, shield area, or craton).

If the concept of a metallogenic epoch is to be of use in classification and exploration of mineral prospects, a metallogenic epoch must be applied to a stage or interval within a tectonic cycle. The idea of relating mineral deposits to stages of development of orogenic belts was developed in the U.S.S.R. by Bilibin (1955). Bilibin's initial work was concerned with endogenous (hypogene) mineral deposits. Semenov and Serpuklov (1957) added a study of exogenous (sedimentary and supergene) deposits to the regional metallogenic analysis.

In Canada, the application of a tectonic approach to the study and classification of ore deposits is more recent. C.J. Sullivan's (1948) paper entitled "Ore and Granitization" was an early step toward a tectonic cycle approach. Sullivan emphasized the composition of the stratigraphic column through which intrusions make their way upward. Sullivan's (1957) classification of metalliferous provinces and deposits stresses field association and a "source bed" approach is used in his classification.

McCartney and Potter (1962) and McCartney (1965) reviewed metallogeny of the Canadian Appalachians using Russian metallogenic concepts. In these reviews the emphasis is on type of magmatic activity and related mineral deposits typical of successive stages of folded belt development. Sutherland Brown et al. (1971) related the general distribution of mineral deposits in the Canadian Cordillera to tectonic evolution.

Porphyry mineral deposits of the Canadian Cordillera fit into a generalized tectonic scheme (Figures 5-1a, b and c) that shows the distribution of porphyry mineral deposits in time and space within the Canadian Cordillera. A.Y. Bilibin (1955) and A.I. Semenov and V.I. Serpuklov (1957) applied a similar approach to mineral deposits in folded belts of the U.S.S.R., and W.D. McCartney and R.R. Potter (1962) applied the tectonic concepts developed in the U.S.S.R. to mineral deposits of the Canadian Appalachians. The classic geosyncline model (Stille, 1936 and Kay, 1951) used by these workers has been replaced by a plate-tectonic approach. The general idea of cyclic development of a mobile belt holds, but cyclic development should only apply to well-defined segments of recrystallized sial (Monger et al., 1972), segments with different metallogenic and tectonic development may now be contiguous belts. An hypothesis that can be applied to the metallogeny or tectonics of one part of a tectonic belt may not be valid once a major fault is crossed or an apparent unconformity is encountered in the stratigraphic section.

5.3 Tectonic Setting

Sutherland Brown et al. (1971), Souther (1970), Wheeler (1970), Hodder and Hollister (1972) and Monger et al. (1972) have described the tectonics and (or) mineral deposits of the Canadian Cordillera in terms of five distinct geological and physiographical belts. These are (from east

Figure 5-1a. Tectonic setting of porphyry mineral deposits in the Canadian Cordillera (49-52°N).

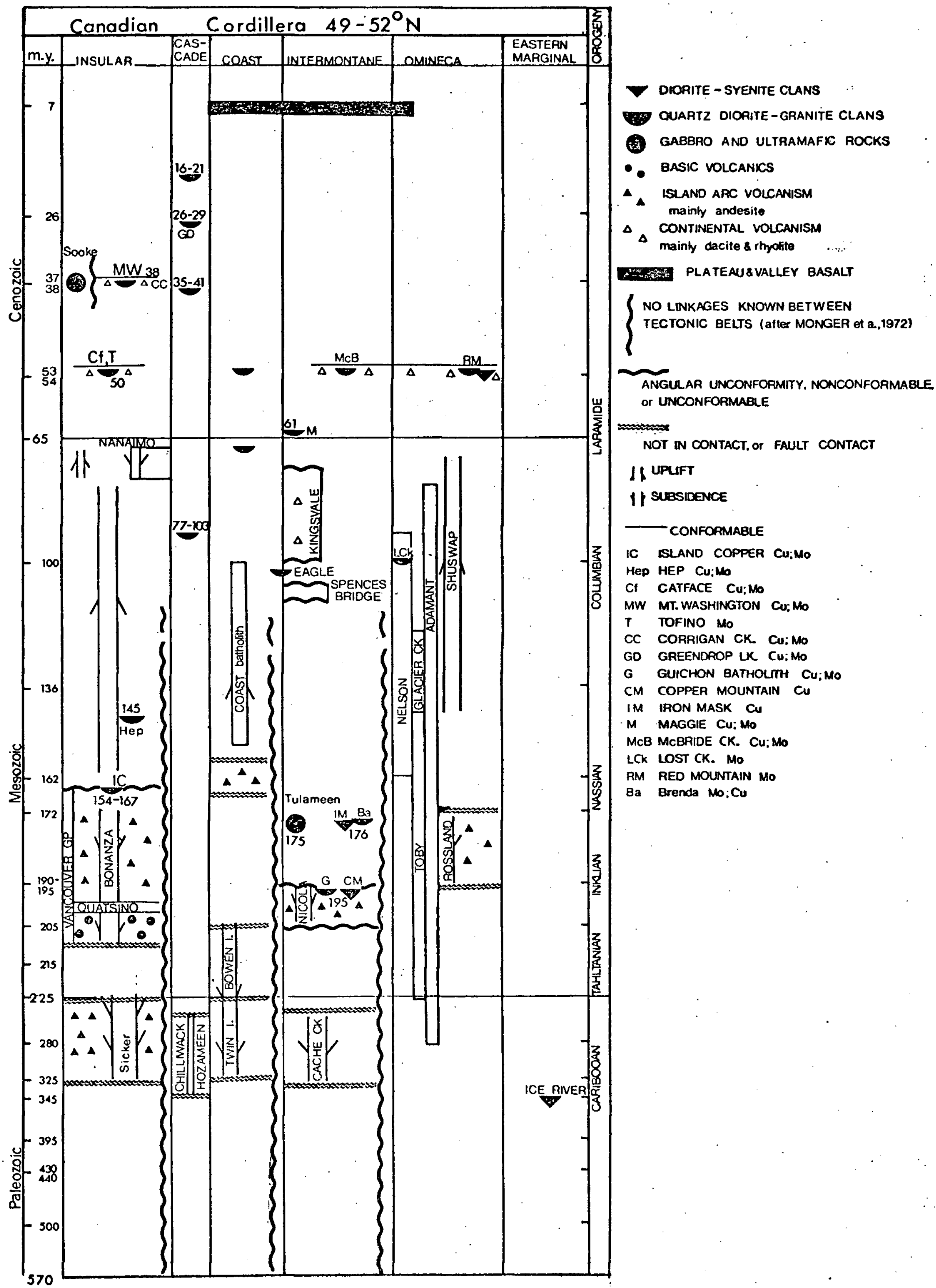

Figure 5-1b. Tectonic setting of porphyry mineral deposits in the Canadian Cordillera (52-56°N).

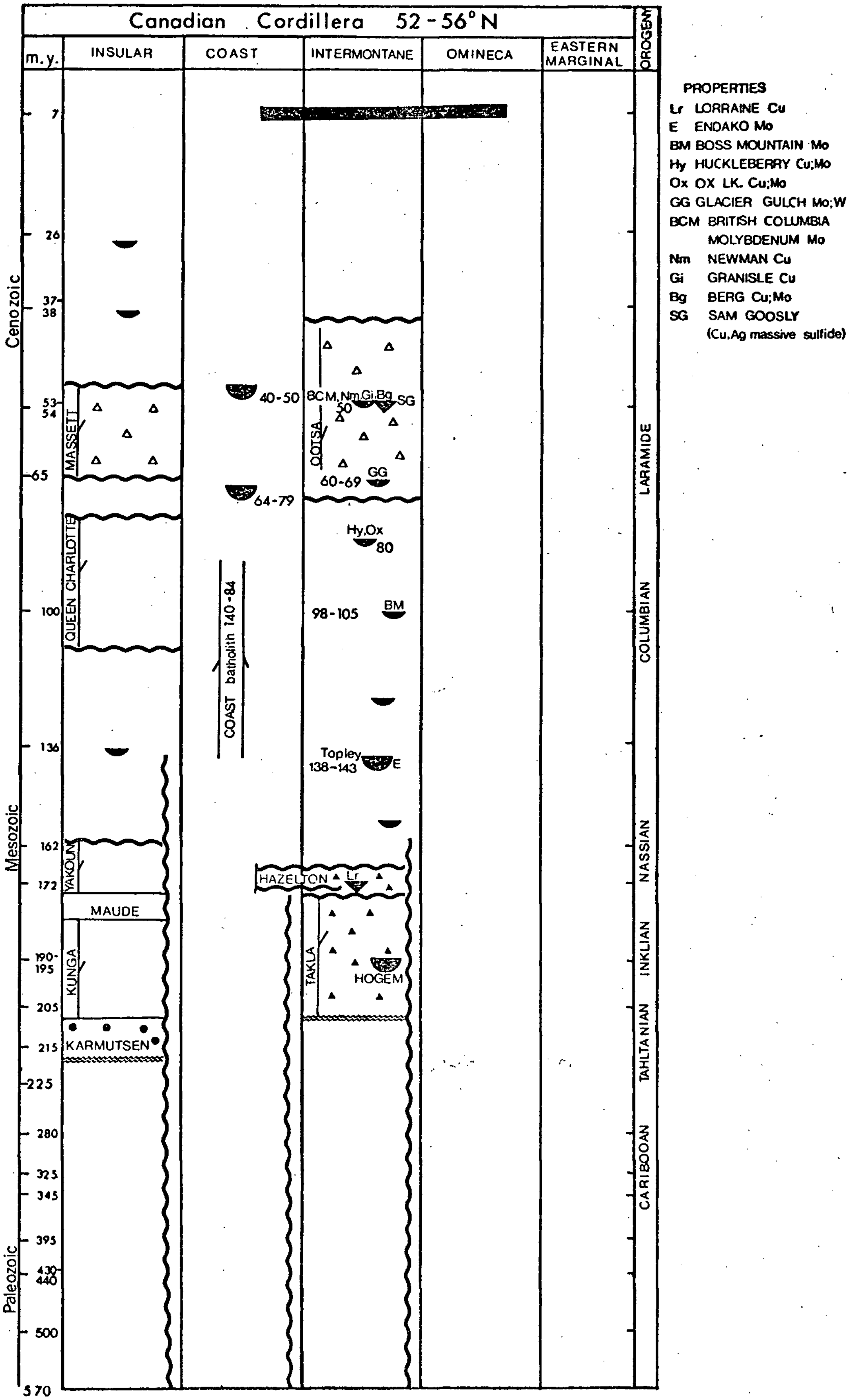

Figure 5-1c. Tectonic setting of porphyry mineral deposits in the Canadian Cordillera (56-64°N).

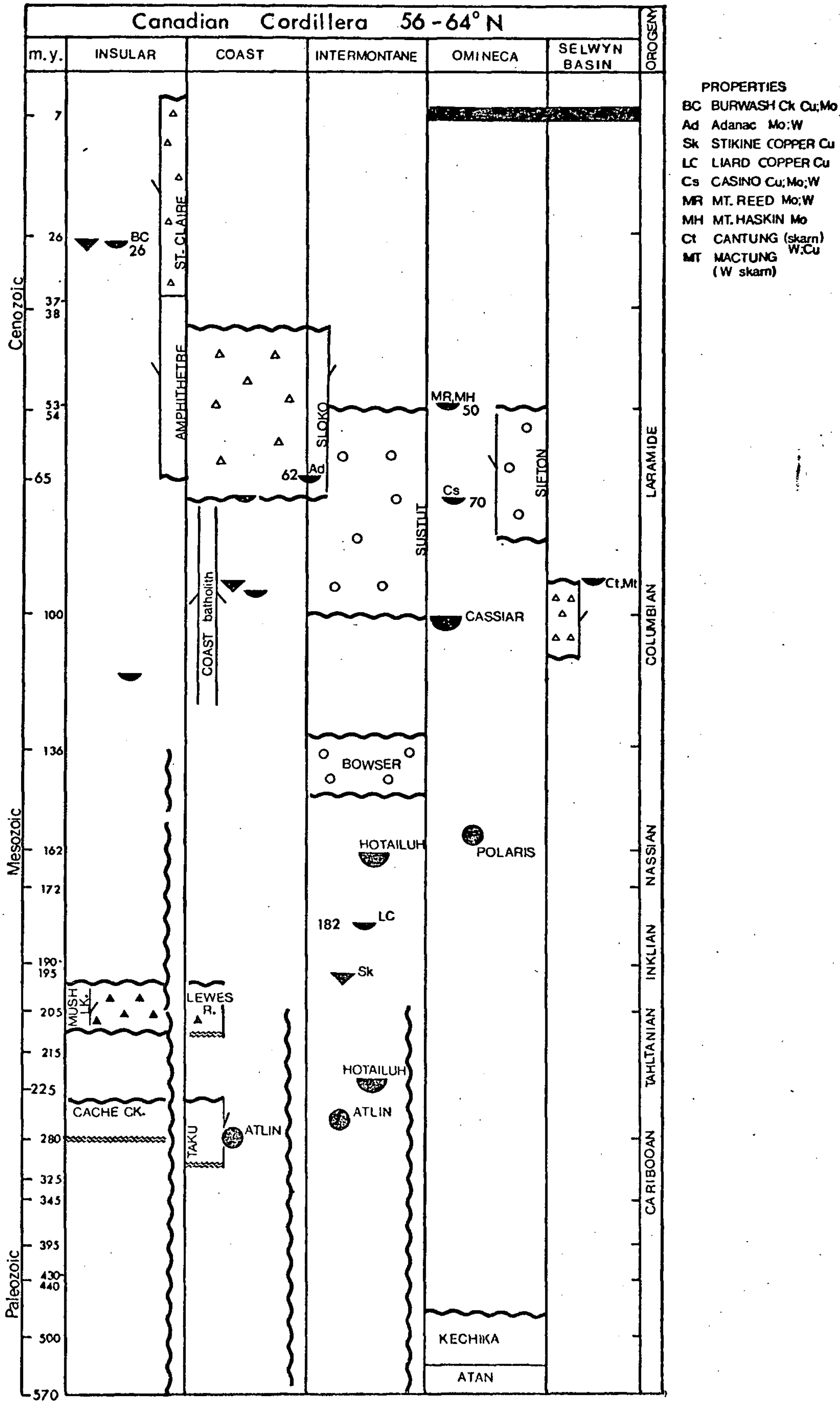

to west):

(1) Eastern Marginal Belt,

(2) Omineca Belt,

(3) Intermontane Belt,

(4) Coast Crystalline Belt, and

(5) Insular Belt.

The terminology and belt configuration (Figure 5-2) used in this discussion follows Sutherland Brown et al. (1971). Because mineral deposits appear to be characteristic of individual belts, the configuration of belts shown in Figure 5-2 is applicable to a discussion of the distribution of endogenic mineral deposits in space and time.

Monger et al. (1972) suggested that from the record in the Canadian Cordillera the present configuration of five geologic belts was only obtained by late Mesozoic time. Clastic wedges shed from the Omineca Belt during the Cariboοan Orogeny (Antler Orogeny in the western United States) indicate that the Omineca Belt existed as a positive feature by late Devonian time. All the present tectonic elements were in existence by late Triassic time and common stratigraphic units linked the northern parts of the Omineca, Intermontane and Coast Crystalline belts by Upper Triassic time (Monger et al., 1972).

In late Cretaceous and early Tertiary time the Canadian Cordillera represented a mobile belt similar to the present-day Andes (Monger et al., 1972) with great volumes of subaerial volcanic rocks. These volcanics represent the cover into which many small, calc-alkaline, epizonal,

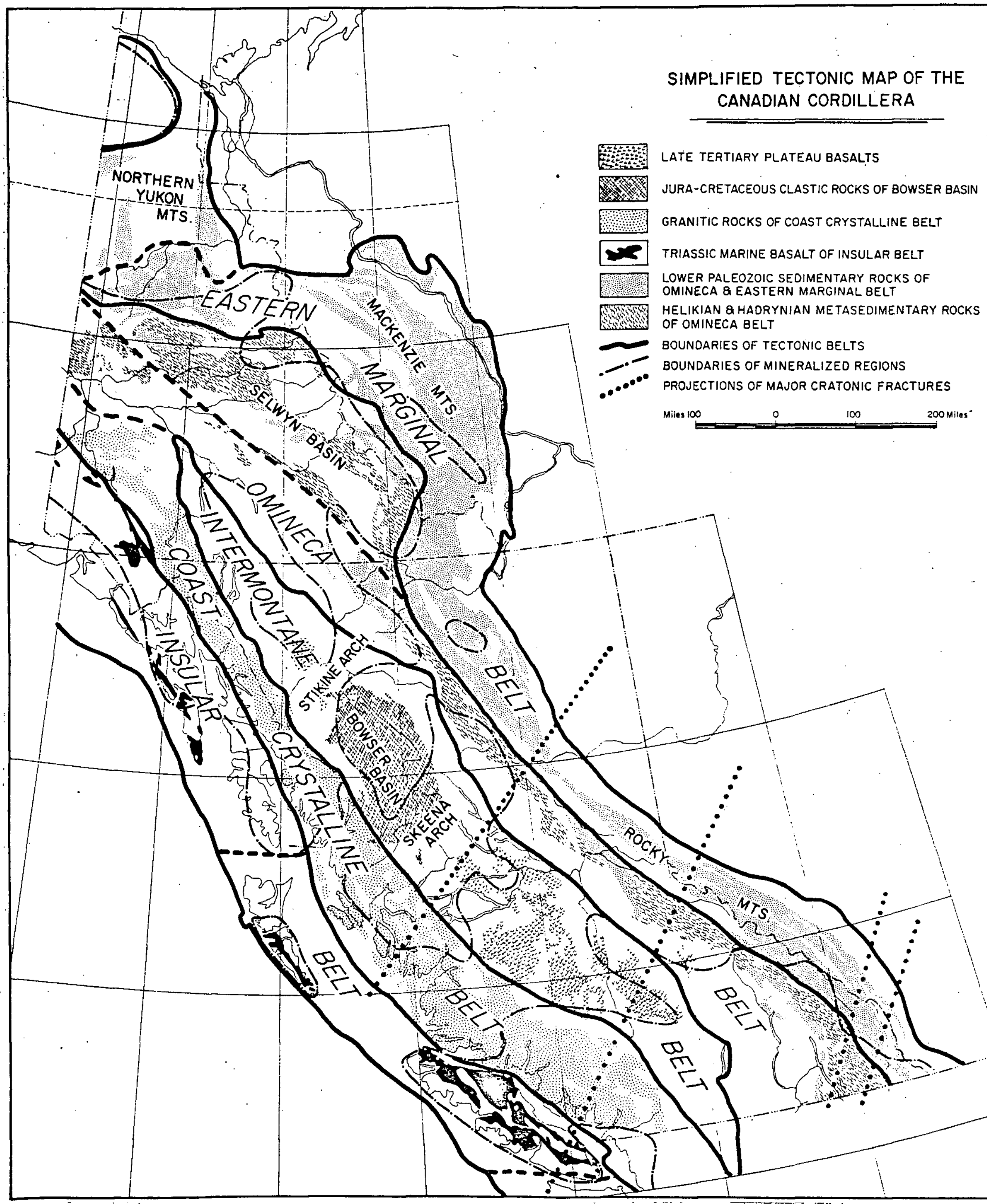

Figure 5-2. Tectonic Map (from Sutherland Brown et al., 1971).

subvolcanic stocks and some alkaline epizonal stocks were emplaced. Following the mid-Eocene volcanic events, most of the four eastern belts were inverted from a mobile belt under compressional stress to a stable continent edge. Souther (1970) suggested that onset of relaxation by late Eocene time was accompanied by a complete change in the structural style, volcanism and plutonism indicated by:

1) structural trend switching from predominately west-northwesterly to northerly,
2) acid volcanism replacing andesitic island-arc volcanism,
3) block faulting replacing elongate grabens and,
4) high-level intrusions of granitic plutons and dikes.

Atwater (1970) suggested that intrusion and eruption of calc-alkaline magmas of predominately intermediate and silicic compositions should have existed above formerly active Benioff zones and should have ceased when subduction ceased. The 25-30 m.y. paucity of volcanism between Late Eocene and Miocene time suggests a major change in the plate interactions.

5.4 Age Dating and Metallogenic Epochs

The importance of isotopic age dating in establishing metallogenic epochs and concepts of metallogeny has been stressed by White (1966), White et al. (1968), and Livingston et al. (1968). Several authors (White et al., 1968; Livingston et al., 1968; Moore et al., 1968; Fyles et al., 1973) have demonstrated the close association of intrusion and mineral deposition in Cordilleran porphyry mineral deposits by showing that the ages of the mineral deposit and the host or associated intrusion are within the limits of detection of the K-Ar method. The sub-volcanic setting for porphyry mineral deposits has been suggested by White (1966), Carter (1970 and 1972b), Sutherland Brown et al. (1971), Northcote and Muller (1972) and others. Therefore, by obtaining the age of the porphyritic mineral deposit, the deposit can be placed in the proper lithologic-tectonic-stratigraphic environment.

The K-Ar dating method has been extensively used for determining the apparent age of intrusive rock in the Canadian Cordillera. Since the early 1960s several hundred K-Ar determinations have been published. Published age determinations that form a basis for this review are listed in Appendix D. Age patterns for intrusive rocks are examined by plotting histograms (Figures 5-3 and 5-4) of K-Ar ages published after 1965 and ages obtained by Mathews (1964) that are in close agreement with fossil evidence. Many ages reported before 1965 have been found to be unreliable and therefore, ages reported before 1965 are not used in histogram plots.

Variation in apparent age of plutonic rocks is examined by plotting histograms for segments parallel to the north-westerly trend of the Canadian Cordillera (tectonic belts) and normal to the trend of the Canadian Cordillera (arbitrary segmenting by latitude). Figure 5-3 shows the variation of K-Ar ages for tectonic belts and Figure 5-4 shows variation of K-Ar ages for southern, central and northern segments of the Canadian Cordillera. The total plot of K-Ar ages has concentrations at about 26 m.y., 50 m.y., 78 m.y., 98 m.y., 140 m.y. and 198 m.y. but only the 50 m.y. peak consistently appears in the various tectonic segments. Age plots appear to reflect both a geographic bias and a mineral deposit bias. The Late Triassic (Guichon Batholith and Copper Mountain intrusions), Late Jurassic

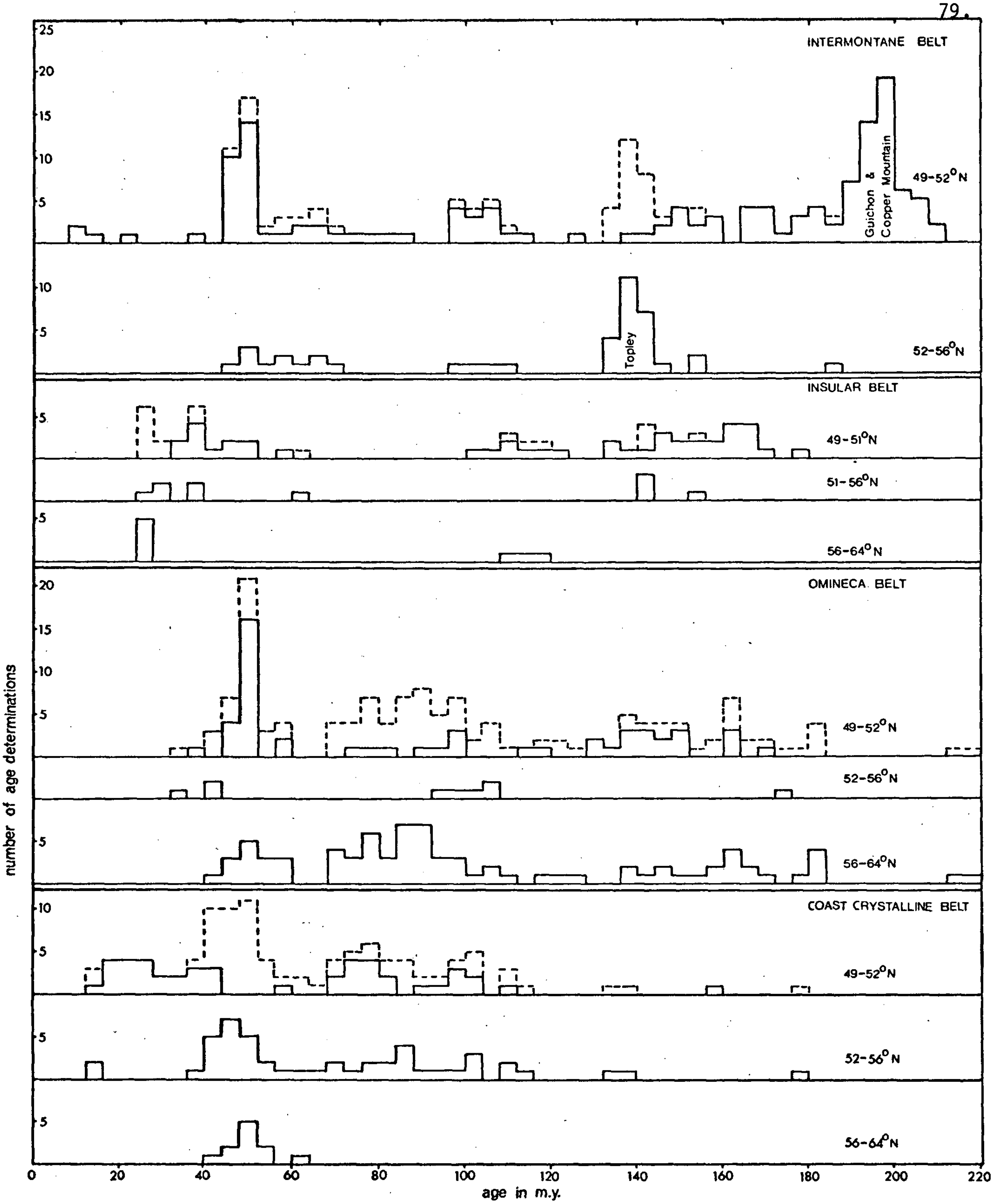

Figure 5-3. K-Ar age determinations for igneous rocks in the Canadian Cordillera. Dashed line represents total for tectonic belt.

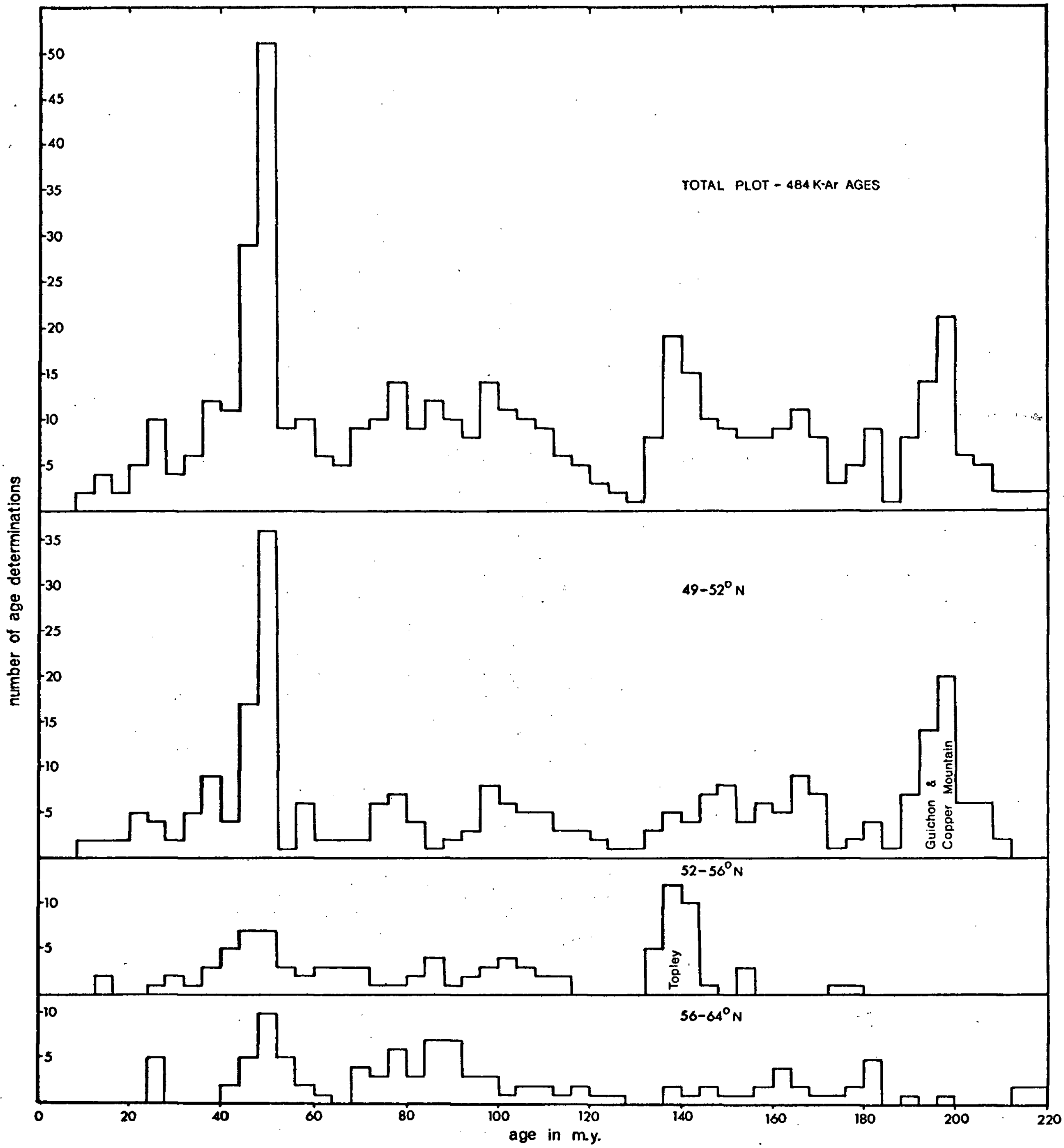

Figure 5-4. K-Ar age determinations for igneous rocks in segments of the Canadian Cordillera between 49-52°N, 52-56°N and 56-64°N.

(Topley Intrusions) and in part the Eocene peaks reflect vigorous collecting of samples that are from porphyry mineral deposits and the Isotopic Age Map of Canada (Wanless, 1969) shows concentrations of samples in south-central British Columbia, the Skeena Arch area and the Cassiar Mountains.

Gilluly (1973) suggested that, "taking the Cordillera as a whole, magmatism was roughly constant except for the apparent low about 115 to 125 m.y. ago". This low in number of K-Ar ages for igneous rocks is especially apparent in the Canadian Cordillera (Figure 5-4) and may represent a time of major change in either direction or rate of plate motion. Evolution of the continental margin from an Indonesian type island arc to an Andean type margin (Wheeler et al., 1972) occurred during early Cretaceous time and may be related to rebound of light sialic material consumed during early Mesozoic subduction. Gilluly's (1973) suggestion that episodic magmatism is a local phenomenon and that magmatism was roughly constant in the Cordillera, appears to hold for early Mesozoic time in the Canadian Cordillera but his suggestion is not supported by the low in early Cretaceous K-Ar ages or by the widespread pulse of Eocene igneous activity. The apparent early Cretaceous change in the pattern of K-Ar ages for igneous rocks may represent either a reduction in the effect of burial on the apparent K-Ar age of igneous rock emplacement or a more uniform history for the various tectonic belts that were completely linked by Cretaceous time (Monger et al., 1972).

Metallogenic epochs for porphyry mineral deposits are also examined by plotting a histogram (Figure 5-5). For porphyry deposits, the number of significant mineral deposits is plotted against the K-Ar age. Porphyry

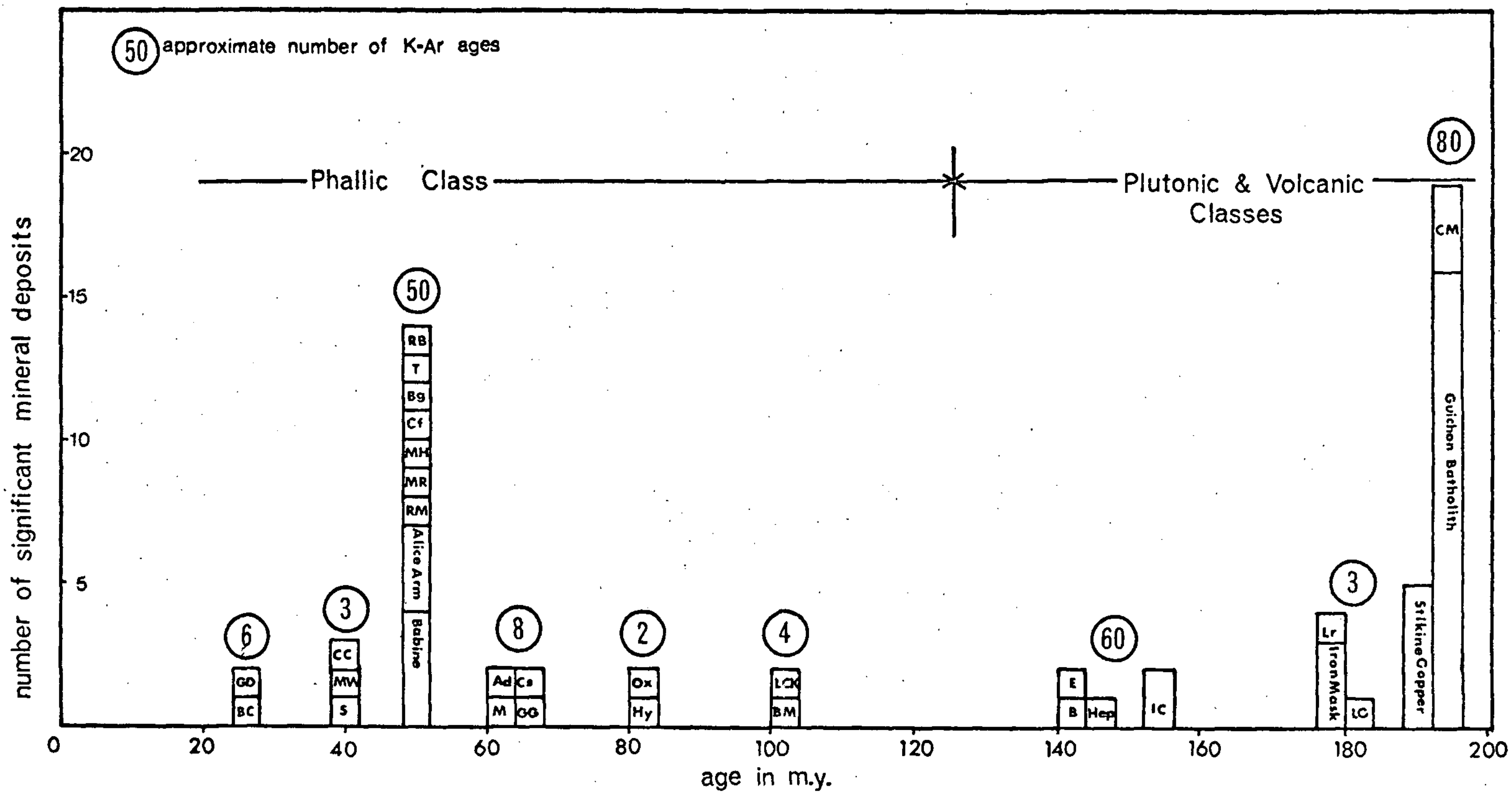

Figure 5-5. K-Ar age of porphyry mineral deposits in the Canadian Cordillera. GD - Greendrop Lk.; BC - Burwash Ck.; CC - Corrigan Ck.; MW - Mt. Washington; S - Serb; RB - Red Bird; T - Tofino Mo.; Bg - Berg; Cf - Catface; MH - Mt. Haskin; MR - Mt. Reed; Ad - Adanac; M - Maggie; Cs - Casino; GG - Glacier Gulch; LCK - Lost Ck.; BM - Boss Mtn.; E - Endako; B - Brenda; IC - Island Copper; Lr - Lorraine; LC - Liard Copper; CM - Copper Mountain.

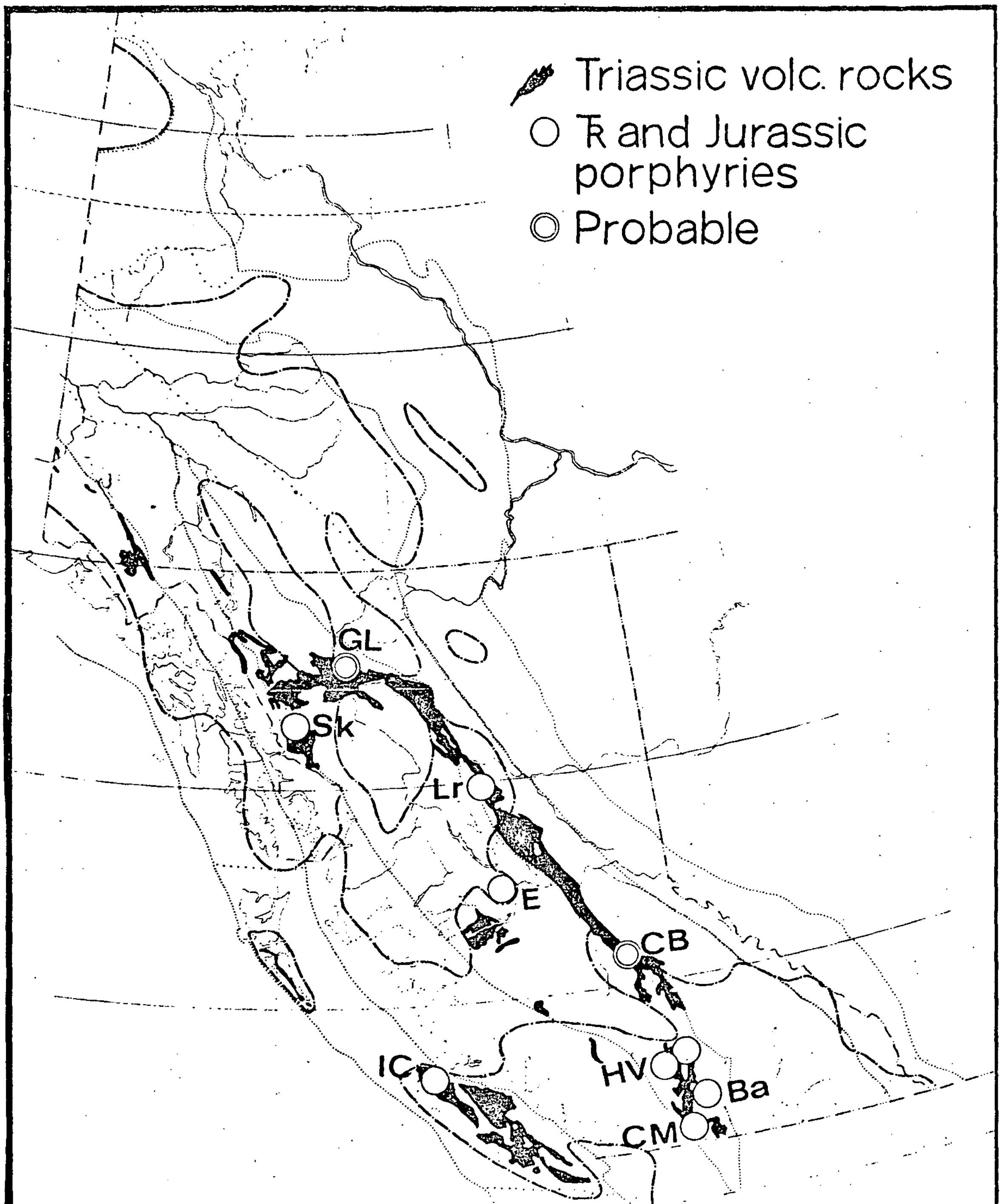

Figure 5-6. Triassic lavas and the Triassic and Jurassic porphyry deposits (from Sutherland Brown et al., 1971). IC - Island Copper; CM - Copper Mountain and Ingerbell; Ba - Brenda; HV - Highland Valley; CB - Cariboo Bell; E - Endako; Lr - Lorraine; Sk - Stikine Copper; GL - Gnat Lake.

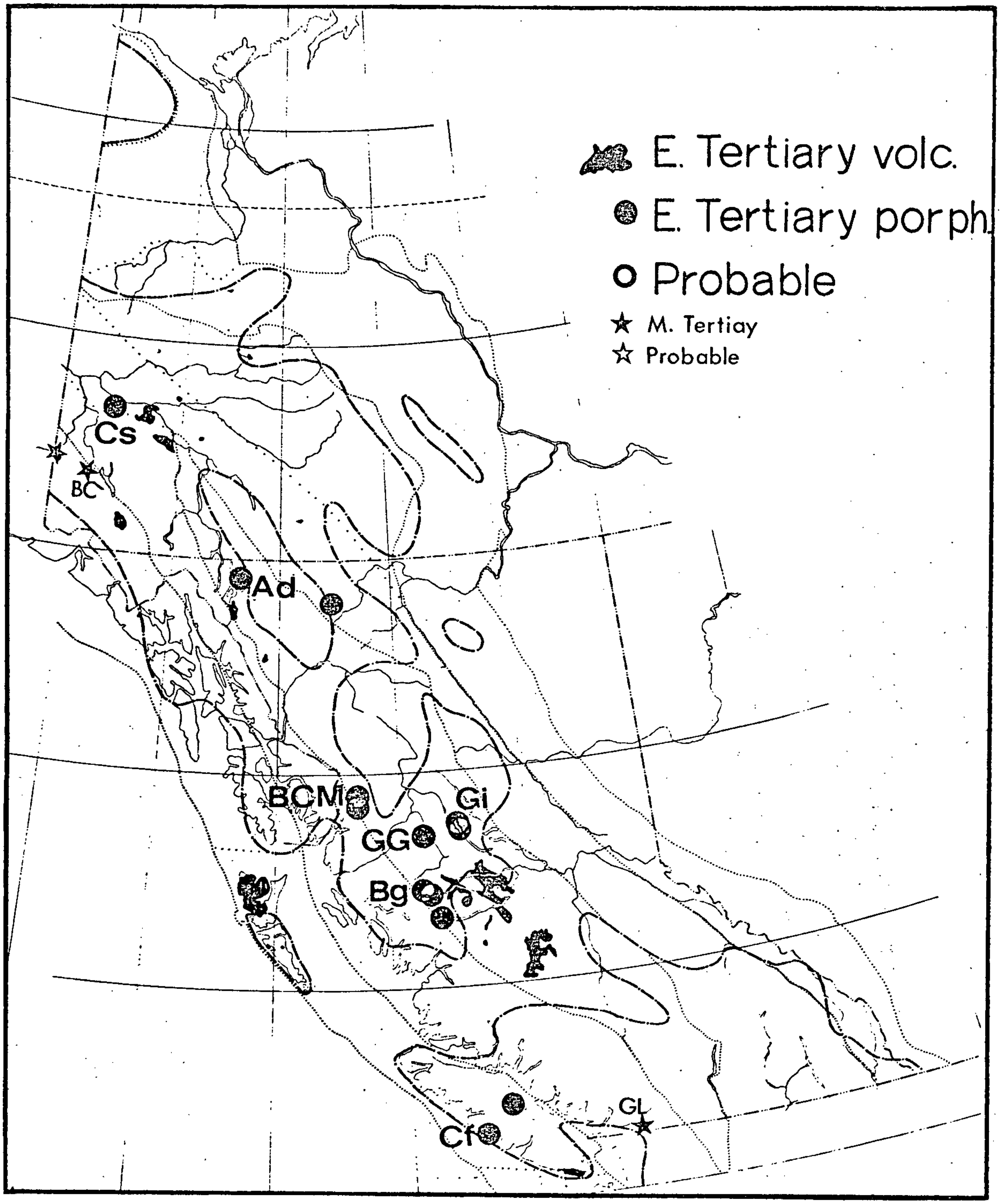

Figure 5-7. Early Tertiary volcanic rocks and porphyry deposits (modified from Sutherland Brown et al. 1971). Cs - Casino; BC - Burwash Creek; Ad - Adanac; BCM - British Columbia Molybdenum; Gi - Granisle; GG - Glacier Gulch; Bg - Berg; Cf - Catface; GD - Greendrop Lake.

mineral deposits fit into several age groupings that show consistent metal content and geologic setting. K-Ar dating of porphyry mineral deposits indicates metallogenic epochs at about 195 m.y. and 150 ± 10 m.y. for deposits that fit in Sutherland Brown's plutonic and volcanic classes; and at about 100 m.y., 80 m.y., 65 m.y., 50 m.y., 35-40 m.y. and 26 m.y. for deposits that fit into Sutherland Brown's phallic class.

Porphyry mineral deposits are distributed throughout the four western tectonic belts. Porphyry copper deposits are associated with Triassic to Miocene intrusions and volcanic rocks (Figures 5-6 and 5-7) of the Insular and Intermontane belts and porphyry molybdenum and tungsten deposits are associated with Jurassic to Eocene intrusions into metasedimentary and sedimentary rocks of the Coast Crystalline Belt, Intermontane Belt and Omineca Belt. The 50 m.y. metallogenic epoch is the only mineralizing event that has been documented and is significant in the four western tectonic belts.

Porphyry deposits of the plutonic and volcanic classes have received the most attention from exploration and research projects because they are the major producers and contain the major proven reserves of copper and molybdenum in the Canadian Cordillera.

5.5. PLATE TECTONICS AND METALLOGENY OF PORPHYRY MINERAL DEPOSITS

The relationship of porphyry mineral deposits to paleo-Benioff zones has been discussed on a global basis by Sillitoe (1972 a and b), Guild (1971 and 1972), and Mitchell and Garson (1972). These authors generally conclude that porphyry copper deposits are derived from materials regenerated in subduction zones and emplaced at high levels in the crust with stocks of calc-alkaline affinity. An eastern migration of intrusive centers has been suggested for western South America (Farrar et al., 1970; Ruiz et al., 1965) and Sillitoe (1972) suggests that the age of porphyry deposits show a similar age distribution in the Cordillera of the United States and Mexico. Age patterns for porphyry mineral deposits in the Canadian Cordillera do not show a simple trend. Deposits range in age from Jurassic (Island Copper) to Miocene (Burwash Creek) in the Insular belt and from Triassic (Copper Mountain, Bethlehem, Lornex, Stikine Copper etc.) to Eocene (B.C. Molybdenum, Granisle, Bell etc.) in the Intermontane Belt.

The age pattern of mineral deposits does support a basic difference between the pattern of development of porphyry deposits in the Intermontane and Insular belts. Triassic 'syenitic' volcanic porphyry deposits are restricted to the Intermontane belt and porphyry deposits of the volcanic class are associated with a middle Jurassic island arc assemblage (Bonanza Group) on Vancouver Island. Post-Eocene porphyry deposits are restricted to the Insular tectonic belt and Cascade Mountains and in particular to areas that appear to be affected by post-Eocene subduction. Atwater (1970) and Grow and Atwater (1970) suggest post-Eocene underthrusting of the Farallon Plate and Kula Plate below Vancouver Island and the Aleutian Arc respectively. The timing and direction of underthrusting of these plates is supported by the young age of the Mt. Washington and Corrigan Creek porphyry deposits on Vancouver Island (Carson, 1969), the Greendrop Lake property in the Cascades, and the Burwash Creek porphyry deposit southwest of the Shakwak Trench in the Yukon Territory. Widespread Eocene igneous activity in the Canadian Cordillera suggests that subduction was occuring along the western margin of the continent until about 45 m.y. Post-Eocene transform motion from north of Vancouver Island to the Aleutian Trench would explain the distribution of igneous activity and the presence of younger porphyry mineral deposits on Vancouver Island, in the Cascade Mountains and in the St. Elias Fold Belt.

6. CONCLUSIONS

The following conclusions are based on fission-track and K-Ar dating of intrusive rocks from the Syenite Range and Burwash Landing area in the Yukon Territory and from the Cassiar area, Adanac property, Granisle Mine and Copper Mountain area in British Columbia; and on a review of published K-Ar ages for igneous rocks in the Canadian Cordillera.

1. A 26 ± 0.3 m.y. mean K-Ar age was determined for four biotite concentrates from quartz latite porphyry near Burwash Creek, Yukon Territory. This apparent age for mineralized porphyry represents the youngest documented porphyry prospect in the Canadian Cordillera.
2. The 115 ± 4 m.y. and 117 ± 4 m.y. hornblende K-Ar ages determined for Kluane Range intrusions on the Cork (Burwash Creek) property agree with the Cretaceous age assigned to this unit by Muller (1967).
3. The 51.9 ± 2.0 m.y. and 54.5 ± 2.0 m.y. biotite K-Ar ages determined for the Ruby Range batholith east of Burwash Landing agree with a previous 58 m.y. K-Ar age (Muller in Lowdon, 1960) for a marginal phase of the batholith. Muller (in Lowdon, 1960, p. 9) described the 58 m.y. age as unexpected, but concordant biotite K-Ar and apatite fission-track ages of 54.5 ± 2.0 m.y. and 48.9 ± 6.6 m.y. respectively for granodiorite sample PC8 provides convincing support for the early Tertiary apparent age for at least

part of the Ruby Range batholith.

4. Granite porphyry on the Mt. Haskin Mo and Mt. Reed Mo-W properties east of Cassiar, British Columbia has four biotite K-Ar ages ranging from 48.7 to 50.5 m.y. and a mean biotite K-Ar age of 49.8 $\pm$ 0.7 m.y. Apatite fission-track ages of 48 $\pm$ 6 m.y. and 60 $\pm$ 8 m.y. for granite porphyry sample PC9 from the Mt. Haskin property and an apatite fission-track age of 54 $\pm$ 7 m.y. for granite porphyry sample PC12 from the Mt. Reed property provide an internal check on the K-Ar age of these bodies.

5. Mineralized and barren quartz latite porphyry near Burwash Creek and mineralized and barren granite porphyry from the Mt. Reed and Mt. Haskin properties yield ages that are identical within the limits of precision of the K-Ar method. This agrees with the findings of White et. al. (1968) that for many British Columbia porphyry deposits, mineralization is an integral feature of a magmatic event. On radiometric evidence these porphyry deposits fit into the paramagmatic class of mineral deposits suggested by White.

6. Biotite K-Ar ages of 71.7 $\pm$ 2.6 m.y. and 68.3 $\pm$ 2.7 m.y. obtained from a young phase of the Cassiar intrusions, place an upper limit on the age of the molybdenum mineralization on the Cassiar Molybdenum property.

7. A 62.0 ± 2.2 m.y. age, determined for a biotite concentrate from the coarse alaskite phase of the Mt. Leonard Boss, dates the molybdenum mineralization on the Adanac property.
8. Late Cretaceous and Early Tertiary ages obtained for the Adanac Mo property, Cassiar Molybdenum property, Mt. Haskin Mo property, and Mt. Reed Mo-W property and Early Tertiary ages reported for quartz monzonite and pegmatite associated with the Blue Light tungsten property (Wanless et al., 1970) indicate that the Early Tertiary metallogenic epoch, documented in central British Columbia and southeastern Alaska, can be extended through northern British Columbia.
9. Apatite fission-track ages from the Burwash Landing area, Cassiar area and Syenite Range are consistent and in general concordant with K-Ar ages determined on co-genetic biotite. These results suggest that the apatite fission-track method is a suitable method for dating late Mesozoic and Cenozoic igneous and metamorphic events in the Burwash Landing area, Cassiar area and Syenite Range.
10. One sample from a mineralized potassic-zone vein at the Granisle Mine has respectively 30 ± 4 m.y. and 50.2 ± 2.1 m.y. apatite fission-track and biotite K-Ar ages. Discordant results is attributed to the altered nature of the apatite.

11. Apatite fission-track ages from the Copper Mountain intrusions are consistently younger than K-Ar ages on co-genetic biotite. The fission-track ages are interpreted to reflect a heating event that is related to Early to Middle Cretaceous granitic intrusions. Because biotite K-Ar ages are affected only by contact events, and apatite fission-track ages appear to be regionally reset, temperatures below approximately 150°C are suggested for a thermal event of Cretaceous age.
12. Without additional geologic and geochronologic evidence, apatite fission-track ages from the Copper Mountain area and the Granisle Mine give misleading results with resulting misinterpretation of the thermal history. Therefore, in cases where alteration or thermal events are involved, apatite fission-track ages should be checked by using another more refractory mineral for fission-track dating or another radiometric clock.
13. Porphyry mineral deposits in the Canadian Cordillera fit into several classes that show consistent metal content, geologic setting, and age. K-Ar apparent ages support metallogenic epochs for porphyry mineral deposits at approximately 190 m.y. and 150 $\pm$ 10 m.y. for deposits that fit into Sutherland Brown's plutonic and volcanic classes; and at approximately 100 m.y., 80 m.y., 65 m.y., 50 m.y., 35-40 m.y. and 26 m.y. for deposits that fit into Sutherland

Brown's phallic class.

14. The age and distribution of the various classes of porphyry mineral deposits in the Canadian Cordillera are compatible with Monger et al. (1972) plate-tectonic model for the evolution of the Canadian Cordillera, but do not suggest a simple pattern of eastern migration of intrusive centers that has been suggested for western South America (Farrar et al., 1970; Ruiz et al., 1965) and for porphyry mineral deposits of the Cordillera of the United States and Mexico (Sillitoe, 1972b).

REFERENCES

Aitken, J.D., 1959. Atlin map-area, British Columbia. Geol. Surv. Can. Mem. 307.

Atwater, T., 1970. Implications of plate tectonics for the Cenozoic tectonic evolution of western North America. Geol. Soc. America Bull., 81, No. 12, pp. 3513-3536.

Baadsgaard, H., Folinsbee, R.E., and Lipson, J., 1961a. Potassium-argon dates of biotites from Cordilleran granites. Geol. Soc. America Bull., 72, pp. 689-702.

______________________________, 1961b. Caledonian or Acadian granites of northern Yukon Territory. in Geology of the Arctic, Vol. 1, G.O. Raasch, Ed., pp. 458-465.

Bilibin, Yu. A., 1955. Metallogenic provinces and metallogenic epochs - translated from Russian to English by E. Alexandrov, 1968. Geol. Bull. 1, Queens College New York, 35 p.

Blanchflower, J.D., 1971. Isotopic dating of copper mineralization at Alwin and Valley properties, Highland Valley, southcentral British Columbia. Unpublished B.Sc. Thesis, Dept. of Geology, U.B.C., 83 p.

Bostock, H.S., 1964. Geology, McQuesten, Yukon Territory. Geol. Surv. Can., Map 1143A.

__________, 1968. McQuesten, Yukon Territory. Geol. Surv. Can., Paper 48-25.

Brill, R.M., Fleischer, R.L., Price, P.B., and Walker, R.M., 1964. The fission-track dating of man-made glasses: Preliminary Results. Jour. Glass Studies, 6, pp. 151-155.

Campbell, D.D., 1968. Cassiar Molybdenum Property, Cassiar, B.C. Unpublished assessment Report No. 1700, on file with Min. Branch B.C. Dept. Mines and Pet. Res.

Carson, D.J.T., 1969. Tertiary mineral deposits of Vancouver Island. Can. Inst. Min. Met. Bull., 62, May, pp. 511-520.

__________, Muller, J.E., Wanless, R.K., and Stevens, R.D., 1971. Age of the contact metasomatic copper and iron deposits, Vancouver and Texada Islands, British Columbia. Geol. Surv. Can., Paper 71-36.

Carter, N.C., 1970. Copper and molybdenum porphyry deposits in central British Columbia. Cdn. Min. Jour., 91, No. 4, pp. 74-76.

___________, 1972a. Faults, lineaments, and porphyry copper deposits, Babine Lake Area, B.C. (Abstr.) G.A.C. symposium on faults, fractures, lineaments, and related mineralization in the Canadian Cordillera.

___________, 1972b. Granisle. In Excursion A09-C09, Copper and Molybdenum Deposits of the Western Cordillera (C.S. Ney and A. Sutherland Brown (Eds.)), pp. 27-36.

Christopher, P.A., 1968. Fission-track ages of younger intrusions in southern Maine. Unpublished M.A. Thesis, Geology Dept., Dartmouth College, 45 p.

_______________, 1969. Fission-track ages of younger intrusions in southern Maine, Geol. Soc. America Bull. 80, pp. 1809-1814.

_______________, 1972. Metallogenic epochs for "porphyry type" mineral deposits in the Canadian Cordillera (Abstr.). In proceedings of the 9th. Annual Western Inter-University Geological Conference, Vancouver, B.C. p. 15.

_______________, 1973. Application of apatite fission-track dating to the study of porphyry mineral deposits. Can. J. Earth Sci., 10, May, in press.

_______________, White, W.H., and Harakal, J.E., 1972a. K-Ar dating of the 'Cork' (Burwash Creek) Cu-Mo prospect, Burwash Landing area, Yukon Territory. Can. J. Earth Sci., 9, pp. 918-921.

____, 1972b. Age of molybdenum and tungsten mineralization in northern British Columbia. Can. J. Earth Sci., 9, pp. 1727-1734.

Church, B.N., 1970. The geology of the White Lake Basin, in Geology, Exploration and Mining in B.C., B.C. Dept. of Mines & Pet. Res., pp. 396-402.

Dalrymple, G.B., and Lanphere, M.A., 1969. Potassium-argon dating. W.H. Freeman & Co., San Francisco, 258 p.

Damon, P.E., 1968. Potassium-argon dating of igneous and metamorphic rocks with application to Basin Ranges of Arizona and Sonora. In Radiometric dating for geologists (E.I. Hamilton and R.M. Farquhar (Eds.)), Interscience Publishers, New York, pp. 1-71.

DeLaunay, L., 1913. Gites Mineraux. Paris.

Dolmage, V., 1934. Geology and ore deposits of Copper Mountain, British Columbia. Geol. Surv. Can., Mem. 171.

Engels, J.C., and Crowder, D.F., 1971. Late Cretaceous fission-track and potassium-argon ages of the Mount Stuart Granodiorite and Becker Peak Stock, North Cascades, Washington. U.S. Geol. Surv. Prof. Paper 750-D, pp. D39-D43.

Fahrni, K.C., 1951. Geology of Copper Mountain. Can. Inst. Min. Met. Bull., 44, No. 469, pp. 317-324.

__________, 1962. Post production geology at Copper Mountain. Western Miner and Oil Review, 35, No. 2, pp. 53-54.

__________, 1966. Geological relations at Copper Mountain, Phoenix and Granisle Mines. In Tectonic History and Mineral Deposits of the Western Cordillera, Can. Inst. Min. Met., Spec. Vol. No. 8, pp. 315-320.

Farrar, E., Clark, A.H., Haynes, S.J., Quirt, G.S., Conn, H., and Zentilli, M., 1970. K-Ar evidence for the post-Paleozoic migration of granitic intrusion foci in the Andes of Northern Chile. Earth Planet. Sci. Letters, 10, pp. 60-66.

Faul, H., 1966. Ages of Rocks, Planets, and Stars. New York: McGraw-Hill Book Co., 109 p.

Fleischer, R.L., and Price, P.B., 1964a. Glass dating by fission fragment tracks. Jour. Geophys. Res., 69, pp. 331-339.

__________________________, 1964b. Fission track evidence for the simultaneous origin of tectites and other natural glasses. Geochim. Cosmochim. Acta, 28, pp. 755-760.

__________________________, 1964c. Decay constant for spontaneous fission of U238. Physical Review, 133, pp. 63-64.

__________________________, 1964d. Techniques for geological dating of minerals by chemical etching of fission fragment tracks. Geochim. Cosmochim. Acta, 28, pp. 1705-1714.

__________________________, and Walker, R.M., 1964. Neutron flux measurement by fission-tracks in solids. General Electric Research Laboratory Report No. 64-R.L.-383M, Schenectady, N.Y. 5 p.

____________________________________, 1965a. Tracks of charged particles in solids. Science, 149, pp. 383-393.

____________________________________, 1965b. Effects of temperature, pressure, and ionization on the formation and stability of fission tracks in minerals and glasses. Jour. Geophys. Res., 70, pp. 1497-1502.

Forbes, R.B., and Engels, J.C., 1970. K^{40}/Ar^{40} age relations of the Coast Range Batholith and related rocks of the Juneau Ice Field Area, Alaska. Geol. Soc. America Bull., 81, pp. 579-584.

Fyles, J.T., Harakal, J.E., and White, W.H., 1973. The age of sulfide mineralization at Rossland, British Columbia. Econ. Geol., 68, pp. 23-33.

Gabrielse, H., 1963. McDame map-area, Cassiar District, British Columbia. Geol. Surv. Can. Mem. 319

__________, 1967. Tectonic evolution of the northern Canadian Cordillera. Can. J. Earth Sci., 4, pp. 271-298.

Galliker, D., Hugentobler, E., and Hahn, B., 1970. Spontane Kerrspaltung von ^{238}U und ^{241}Am. Helv. Phys. Acta, 43, pp. 593-606.

Giletti, B.J., 1971. Discordant isotopic ages and excess argon in biotites. Earth Planet. Sci. Letters, 10, pp. 157-164.

Gilluly, J., 1973. Steady plate motion and episodic orogeny and magmatism. Geol. Soc. America Bull., 84, pp. 499-514.

Green, L.H., 1971. Geology of Mayo Lake, Scougale Creek and McQuesten Lake map-areas, Yukon Territory. Geol. Surv. Can., Mem. 357.

__________, 1972. Geology of Nash Creek, Larsen Creek and Dawson map-areas, Yukon Territory. Geol. Surv. Can. Mem. 364.

Grow, J.A., and Atwater, T., 1970. Mid-Tertiary tectonic transition in the Aleutian Arc. Geol. Soc. America Bull., 81, No. 12, pp. 3715-3722.

Guild, P.W., 1971. Metallogeny: a key to exploration. Mining Engineering, January, pp. 69-72.

__________, 1972. Metallogeny and the new global tectonics. 24th Int. Geol. Congress, Montreal, Canada, section 4, pp. 17-24.

Hamilton, E.I., 1965. Applied Geochronology. Academic Press, London and New York, 267 p.

Hart, R.S., and Dodd, R.T., 1962. Excess radiogenic argon in pyroxenes. Jour. Geophys. Res., 67, p. 2998.

Hayatsu, A., and Carmichael, 1970. K-Ar isochron method and initial argon ratios. Earth Planet. Sci. Letters, 8, pp. 71-76.

Hibbard, M.J., 1971. Evolution of a plutonic complex; Okanagan Range, Washington. Geol. Soc. Amer. Bull., 82, No. 11, pp. 3013-3048.

Hills, L.V., and Baadsgaard, H., 1967. K-Ar dating of some Lower Tertiary strata in B.C. Bull. Can. Pet. Geol., 15, No. 2, pp. 138-149.

Hodder, R.W., and Hollister, V.F., 1972. Structural features of porphyry copper deposits and the tectonic evolution of continents. Can. Inst. Min. Met. Bull., 65, February, pp. 41-44.

Kay, M., 1951. North American geosynclines. Geol. Soc. America Mem. 48, 143 p.

Kleeman, J.D., and Lovering, J.F., 1971. A determination of the decay constant for spontaneous fission of natural uranium using fission-track accumulation. Geochimica. Cosmochimica Acta, 35, pp. 637-640.

Koo, J.H., 1968. Geology and mineralization in the Lorraine property area, Ominica Mining Division, British Columbia. Unpublished M.Sc. Thesis, Dept. of Geology, U.B.C.

Lahoud, J.A., Miller, D.S., and Friedman, G.M., 1966. Relationship between depositional environment and uranium concentrations of Molluskan shells. Jour. Sed. Pet., 36, pp. 541-547.

Laughlin, A.W., 1969. Excess radiogenic argon in pegmatite minerals. Trans. Amer. Geophys. Union, 74, pp. 6684-6690.

Lindgren, W., 1933. Mineral Deposits. 4th Ed., New York, 930 p.

Livingston, D.E., Damon, P.E., Mauger, R.L., Bennett, R., and Laughlin, A.W., 1967. Ar^{40} in cogenetic feldspar-mica mineral assemblages. Jour. Geophys. Res., 72, pp. 1361-1375.

Livingston, D.E, Mauger, R.L., and Damon, P.E., 1968. Geochronology of the emplacement, enrichment and preservation of the Arizona porphyry copper deposits. Econ. Geol., 63, No. 1, pp. 30-36.

Lowdon, J.A., 1960. Age determinations by the Geological Survey of Canada, Rep. 1 - Isotopic ages. Geol. Surv. Can., Paper 60-17.

__________, 1961. Age determinations by the Geological Survey of Canada, Rep. 2 - Isotopic ages. Geol. Surv. Can., Paper 61-17.

__________, 1973. Age determinations by the Geological Survey of Canada, Rep. 4 - Isotopic ages. Geol. Surv. Can., Paper 63-17.

Lowdon, J.A., Stockwell, Tipper, C.H., and Wanless, R.K., 1963. Age determinations and geological studies (including isotopic ages - Rep. 3). Geol. Surv. Can., Paper 62-17.

Lowell, J.D., and Guilbert, J.M., 1970. Lateral and vertical alteration-mineralization zoning in porphyry ore deposits. Econ. Geol. 65, No. 4, pp. 373-408.

McCartney, W.D., 1965. Metallogeny of post-Precambrian geosynclines. Geol. Surv. Can., Paper 65-6, pp. 19-23.

McCartney, W.D., and Potter, R.R., 1962. Mineralization as related to structural deformation, igneous activity and sedimentation in folded geosynclines. Can. Min. Jour., April, pp. 83-87.

McDougall, I., and Stipp, J.J., 1969. Potassium-argon isochrons (Abstr.). Trans. Amer. Geophys. Union, 50, No. 4, p. 330.

MacDougall, D., 1971. Deep sea drilling - Age and composition of an Atlantic basaltic intrusion. Science, 171, No. 3977, pp. 1244-1245.

McMillian, W.J., 1970. Maggie Mine. in Geology, Exploration and Mining in B.C., B.C. Dept. of Mines & Pet. Res., pp. 324-325.

McTaggart, K.C., and Thompson, R.M., 1967. Geology of part of the northern Cascades in southern British Columbia. Can. J. Earth Sci., 4, pp. 1191-1228.

Macintyre, R.M., York, D., and Gittens, J., 1969. The K-Ar characteristics of nepheline. Earth Planet. Sci. Letters, 7, pp. 125-131.

Mathews, W.H., 1964. Potassium-argon age determinations of Cenozoic volcanic rocks from British Columbia. Geol. Soc. America Bull. 75, pp. 465-468.

__________, 1968. Guidebook for geological field trips in southwestern British Columbia. Dept. of Geology, U.B.C., Report No. 6.

Mitchell, A.H.G., and Garson, M.S., 1972. Relationship of porphyry copper and circum-Pacific tin deposits to paleo-Benioff zones. Trans. IMM, 181, Bull. 783, pp. B-10-B-25.

Monger, J.W.H., Souther, J.G., and Gabrielse, H., 1972. Evolution of the Canadian Cordillera: a plate-tectonic model. Amer. J. Sci., 272, pp. 577-602.

Montgomery, J.H., 1967. Petrology, structure and origin of the Copper Mountain intrusions near Princeton, British Columbia. Unpublished Ph.D. Thesis, Dept. of Geology, U.B.C.

Moore, W.J., Lanphere, M.A., and Obradovich, J.D., 1968. Chronology of intrusion, volcanism, and ore deposition at Bingham, Utah. Econ. Geol., 63, pp. 612-621.

Muller, J.E., 1967. Kluane Lake map-area, Yukon Territory, Geol. Surv. Can., Mem. 340.

Muller, J.E., and Carson, D.J.T., 1969. Geology and mineral possibilities of Vancouver Island. Can. Min. Jour., 90, No. 5, pp. 66-70.

Mulligan, R., 1969. Metallogeny of the region adjacent to the northern part of the Cassiar Batholith, Yukon Territory and British Columbia. Geol. Surv. Can., Paper 68-70.

Naeser, C.W., 1967a. Fission-track age relationships in a contact zone, Eldora, Colorado. Unpublished Ph.D. Thesis, Dept. of Geology, Southern Methodist University.

__________, 1967b. The use of apatite and sphene for fission-track age determinations. Geol. Soc. America Bull., 78, pp. 1523-1526.

__________, 1969. Etching fission-tracks in zircons. Science, 165, No. 3891, p. 388.

Naeser, C.W., and Faul, H., 1969. Fission-track annealing in apatite and sphene. Jour. Geophys. Res., 74, pp. 705-710.

Naeser, C.W., and Dodge, F.C.W., 1969. Fission-track ages of accessory minerals from granitic rocks of the central Sierra Nevada Batholith, California. Geol. Soc. America Bull., 80, No. 11, pp. 2201-2211.

Naeser, C.W., and McKee, E.H., 1970. Fission-track and K-Ar ages of Tertiary ash-flow tuffs, north-central Nevado. Geol. Soc. America Bull., 81, pp. 3375-3383.

Naeser, C.W., Engels, J.C., and Dodge, F.C.W., 1970. Fission-track annealing and age determination of epidote minerals. Jour. Geophys. Res., 75, No. 8, pp. 1579-1584.

Nguyen, K.K., Sinclair, A.J., and Libby, W.G., 1968. Age of the northern part of the Nelson batholith. Can. J. Earth Sci., 5, pp. 955-957.

Nier, A.O., 1950. A redetermination of the relative abundances of the isotopes of carbon, nitrogen, oxygen, argon, and potassium. Phys. Rev., 77, p. 789.

Northcote, K.E., 1969. Geology and geochronology of the Guichon Creek batholith. B.C. Dept. Mines & Pet. Res., Bull. No. 56.

Northcote, K.E., and Muller, J.E., 1972. Volcanism, plutonism and mineralization: Vancouver Island. Can. Inst. Min. Met. Bull. 65, No. 726, pp. 49-57.

Oriel, W.M., 1972. Detailed bedrock geology of the Brenda Copper-Molybdenum Mine, Peachland, British Columbia. Unpublished M.Sc. Thesis, Dept. of Geology, U.B.C.

Petrascheck, W.E., 1965. Typical features of metallogenic provinces. Econ. Geol., 60, pp. 1620-1634.

Phillips, M.P., and Godwin, C.I., 1970. Geology and rotary drilling at the Casino Silver Mines property. Western Miner, 43, pp. 43-49.

Preto, V.A.G., White, W.H., and Harakal, J.E., 1971. Further potassium-argon age dating at Copper Mountain, B.C. Can. Inst. Min. Met. Bull., 64, No. 708, pp. 58-61.

Preto, V.A.G., 1972a. Copper Mountain (and Ingerbelle). In Excursion A09-C09, Copper and Molybdenum Deposits of the western Cordillera (C.S. Ney and A. Sutherland Brown (Eds.)), pp. 69-76.

__________, 1972b. Geology of Copper Mountain. B.C. Dept. of Mines & Pet. Res., Bull. 59.

Price, P.B., and Walker, R.M., 1962. Chemical etching of charged-particle tracks in solids. Jour. Appl. Phys., 78, pp. 3407-3412.

__________, 1963. Fossil tracks of charged particles in mica and the age of minerals. Jour. Geophys. Res., 68, pp. 4847-4862.

Rapson, J.E., 1963. Age and aspects of metamorphism associated with the Ice River Complex, B.C. Bull. Can. Pet. Geol., 11, No. 2, pp. 116-124.

Reed, B.L., and Lanphere, M.A., 1969. Age and chemistry of Mesozoic and Tertiary plutonic rocks in south-central Alaska. Geol. Soc. America Bull., 80, pp. 23-43.

Reimer, G.M., Storzer, D., and Wagner, G.A., 1970. Geometry factor in fission-track counting. Earth Planet. Sci. Letters, 9, pp. 401-404.

Rice, H.M.A., 1960. Geology and mineral deposits of the Princeton map-area, British Columbia. Geol. Surv. Can. Mem. 243, 136 p.

Richards, T., 1971. Plutonic rocks between Hope, B.C., and the 49th Parallel, Unpublished Ph.D. Thesis, Dept. of Geology, U.B.C.

Richards, T., and White, W.H., 1970. K-Ar ages of plutonic rocks between Hope, British Columbia, and the 49th parallel. Can. J. Earth Sci., 7, No. 5, pp. 1203-1207.

Roberts, J.H. Gold, R., and Armani, R.J., 1968. Spontaneous-fission decay constant of uranium-238. Phys. Rev., 174, pp. 1482-1484.

Roddick, J.C., 1970. The geochronology of the Tulameen and Hedley Complexes, British Columbia. Unpublished M.Sc. Thesis, Dept. of Geology, Queen's Univ., Kingston, Ontario.

Roddick, J.C., and Farrar, E., 1971. High initial argon ratios in hornblendes. Earth Planet. Sci. Letters, 12, pp. 208-214.

__________, 1972. Potassium-argon ages of the Eagle Granodiorite, southern British Columbia. Can. J. Earth Sci., 9, pp. 596-599.

Rose, A.W., 1970. Zonal relations of wallrock alteration and sulfide distribution at porphyry copper deposits. Econ. Geol., 65, pp. 920-936.

Rosenblum, S., 1958. Magnetic susceptibility of minerals in the Franz isodynamic magnetic separator. Am. Min., 43, p. 171.

Ruiz, F.C., Aguirre, L., Corvalan, J., Klohn, E., and Levi, B., 1965. Geologia y yacimientos metaliferos de Chile. Santiago, Chile, Inst. Invest. Geologicas, 385 p.

Semenov, A.I., and Serpuklov, V.I., 1957. General principle of regional metallogenetic analysis and methods of compiling metallogenetic maps of folded regions. Dept. of Geology and Conservation of Resources; U.S.S.R. Issue 22, Central Series, printed in Moscow, pp. 5-20.

Senftle, F.E., Stieff, L., Cuttitta, F., and Kuroda, P.K., 1957. Comparison of the isotopic abundance of U235 and U238 and the radium activity ratios in Colorado Plateau uranium ores. Geochim. et Cosmochim. Acta, 11, pp. 189-193.

Silk, E.C.H., and Barnes, R.S., 1959. Examination of fission fragment tracks with an electron microscope. Phil. Mag., 4, pp. 970-972.

Sillitoe, R.H., 1972a. A plate tectonic model for the origin of porphyry copper deposits. Econ. Geol. 67, pp. 184-197.

____________, 1972b. Relation of metal provinces in western America and the subduction of oceanic lithosphere. Geol. Soc. America Bull., 83, pp. 813-818.

Sinclair, A.J., and White, W.H., 1968. Age of mineralization and post-ore hydrothermal alteration at Copper Mountain, B.C. Can. Min. Met. Bull., 61, No. 673, pp. 633-636.

Souther, J.G., 1970. Volcanism and its relationship to recent crustal movements in the Canadian Cordillera. In Symposium on recent crustal movements, Ottawa, Canada, 1969, Papers; Can. J. Earth Sci., 7, No. 2, pp. 553-568.

Spadavecchia, A., and Hahn, B., 1967. Die Rotationskammer und einige Anwendungen. Helvetica Physica Acta, 40, pp. 1063-1079.

Stille, Hans, 1936. Present tectonic state of the earth. Am. Assoc. Petrol. Geol. Bull., 20, pp. 849-880.

Sullivan, J.C., 1948. Ore and granitization. Econ. Geol., 43, pp. 471-498.

____________, 1957. The classification of metalliferous provinces and deposits. Trans. Can. Inst. Min. Met., 60, pp. 333-335.

Sutherland Brown, A., 1969a. Mineralization in British Columbia and the copper and molybdenum deposits. Can. Min. Met. Bull., 62, No. 681, pp. 26-40.

__________________, 1969b. Geology of the Adera Claims. B.C. Min. of Mines and Pet. Res., Ann. Rept., pp. 29-35.

__________________, 1972. Morphology and classification of porphyry deposits of the Canadian Cordillera. (Abstr.) In proceedings of the 9th annual Western Inter-University Geological Conference, Vancouver, B.C. Oct. 27 and 28.

Sutherland Brown, A., Cathro, R.J., Panteleyev, A., and Ney, C.S., 1971. Metallogeny of the Canadian Cordillera. Can. Inst. Min. Met. Bull., 64, pp. 37-61.

Turneaure, F.S., 1955. Metallogenic provinces and epochs. Econ. Geol. 50th Anniversary Volume, pp. 38-98.

Wagner, G.A., 1968. Fission-track dating of apatites. Earth Planet, Sci. Letters, 4, pp. 411-415.

Wagner, G.A., and Reimer, G.M., 1972. Fission-track tectonics: the tectonic interpretation of fission-track apatite ages. Earth Planet. Sci. Letters, 14, pp. 263-268.

Wanless, R.K., 1969. Isotopic age map of Canada. Geol. Surv. Can. map 1256A.

Wanless, R.K., Stevens, R.D., and Loveridge, W.D., 1969. Excess radiogenic argon in biotites. Earth Planet. Sci. Letters, 7, pp. 167-168.

Wanless, R.K., Stevens, R.D., Lachance, G.R., and Rimsaite, R.Y.H., 1965. Age determinations and geological studies. Part 1 - Isotopic Ages, Report 5. Geol. Surv. Can. Paper 64-17.

____, and __________________, 1966. Age determinations and geological studies, K-Ar isotopic ages, Report 6. Geol. Surv. Can. Paper 65-17.

____, and Edmonds, C.M., 1967. Age determinations and geological studies, K-Ar isotopic ages, Report 7. Geol. Surv. Can. Paper 66-17.

____, 1968. Age determinations and geological studies, K-Ar isotopic ages, Report 8, Geol. Surv. Can. Paper 67-2, Part A.

____, and Delabio, R.N., 1970. Age determinations and geological studies, K-Ar isotopic ages, Report 9. Geol. Surv. Can. Paper 69-2A.

____, 1972. Age determinations and geological studies, K-Ar isotopic ages, Report 10. Geol. Surv. Can. Paper 71-2.

Wheeler, J.O., 1970. Summary and discussion. In Structure of the Southern Canadian Cordillera. Geol. Assoc. Can., Special Paper No. 6, pp. 155-166.

Wheeler, J.O., Aitken, J.D., Berry, M.J., Gabrielse, H., Hutchinson, W.W., Jacoby, W.R., Monger, J.W.H., Niblett, E.R., Norris, D.K., Price, R.A., and Stacey, R.A., 1972. The Cordilleran Structural Province. In Variations in Tectonic Styles in Canada (R.A. Price and R.J.W. Douglas (Eds.)), Geol. Assoc. Can., Special Paper 2., pp. 1-82.

White, W.H., 1966. Summary of tectonic history of B.C. In Tectonic history and mineral deposits of the western Cordillera. C.I.M.M. Spec. Volume No. 8, pp. 185-189.

White, W.H., Erickson, G.P., Northcote, K.E., and Harakal, J.E., 1967. Isotopic dating of the Guichon batholith, B.C. Can. J. Earth Sci., 4, pp. 677-690.

White, W.H., Harakal, J.E., and Carter, N.C., 1968. Potassium-argon ages of some ore deposits in British Columbia. Can. Inst. Min. Met. Bull., 61, pp. 1326-1334.

White, W.H., Sinclair, A.J., Harakal, J.E., and Dawson, K.M., 1970. Potassium-argon ages of Topley Intrusions near Endako, British Columbia. Can. J. Earth Sci., 7, No. 4, pp. 1172-1178.

Wilkening, L., Lal, D., and Reid, A.M., 1971. The evolution of the Kapoeta Howardite based on fossil track studies. Earth Planet. Sci. Letters, 10, pp. 334-340.

York, D., 1966. Least squares fitting of a straight line. Can. J. Phys., 44, p. 1079.

________, 1970. Recent developments in potassium-argon dating. Comments Earth Sci. - Geophysics, 1, No. 2, pp. 47-54.

York, D., Macintyre, R.M., and Gittins, 1969. Excess radiogenic Ar^{40} in cancrinite and sodalite. Earth Planet. Sci. Letters, 7, pp. 25-28.

York, D., and Farquhar, R.M., 1972. The earth's age and geochronology. Pergamon Press, Toronto, 178 p.

APPENDIX A - DESCRIPTION OF SAMPLES USED FOR K-AR AND FISSION TRACK AGE DETERMINATIONS

Burwash Creek, Yukon Territory (Fig. 4-2 & 4-3)

PC1 Quartz Latite Porphyry

Sample is from recent road cut in barren, quartz-feldspar-biotite porphyry located three miles each of the Cork property. The rock contains 40% phenocrysts that are 65% plagioclase feldspar (zoned An_{30}-An_{38}), 20% quartz, 6% biotite, 3% amphibole and 5% carbonate in a microgranular matrix of plagioclase, quartz and k-feldspar. Accessories are apatite, zircon and limonite after magnetite.

Alteration

Biotite is generally fresh but some grains show weak chlorite alteration along edges and limonite replacing magnetite inclusions. Amphibole is pseudomorphicly replaced by tremolite and iron oxide. Carbonate replaces cores of plagioclase phenocrysts and occurs along microfractures.

PC2 Quartz Late Porphyry

Sample is from recent cut about 500' east of PC1. The sample is similar in texture and mineralogy to PC1, but altered plagioclase phenocrysts have chlorite cores rimmed by carbonate and amphibole is replaced by carbonate, tremolite and iron oxides.

PC3 Quartz Latite Porphyry

Sample is from a recent cut near the West Fork of Johnson's Creek in the mineralized zone on the Cork property. Hand specimen contains molybdenite, pyrite and chalcopyrite in quartz veinlets and along "dry" fractures. The rock contains 20% phenocrysts that are 85% plagioclase (about An_{25}), 11% quartz "eyes", 3% biotite, and 1% amphibole in a microgranular matrix of plagioclase, k-feldspar, quartz and biotite. Accessories are iron-oxide, sphene, epidote and apatite.

Alteration

Biotite is altered to chlorite in the matrix but the biotite phenocrysts show only weak chlorite alteration along cleavage planes. Amphibole is altered to carbonate and chlorite.

PC4 Quartz Latite Porphyry

Sample is from barren quartz-feldspar-biotite porphyry from recent cut on the Cork property. The sample is similar in mineralogy and texture to PC1 and PC2 with 1% biotite as phenocrysts altering to chlorite along cleavage planes.

PC5 Gabbro

Sample is from barren gabbro along Johnson's Creek. Hypidiomorphic granular textured rock containing plagioclase (60% An_{60}), hornblende (18%), orthopyroxene (3% hypersthene), clinopyroxene (13% augitic), magnetite (5%) and apatite (tr).

PC6 Gabbro

Sample is from the Cork property 500' south of PC5. Hypidiomorphic granular textured rock containing plagioclase (60%-An_{60}), hornblende (20%), pyroxene (8% mainly augitic), magnetite (5%), and apatite (tr). Chlorite and carbonate (1%) occurs as alteration along fractures.

Ruby Range Batholith, Yukon Territory (Fig. 4-2)

PC7 Biotite Granodiorite

Medium grained, hypidiomorphic granular textured rock contains 36%

plagioclase (An_{20}), 38% orthoclase, 19% quartz, 6% biotite and accessory apatite and sphene. Biotite shows minor alteration to chlorite along cleavage planes and edges.

PC8 Biotite - Hornblende Granodiorite

Medium grained, hypidiomorphic granular textured rock contains 58% plagioclase (An_{38}), 10% orthoclase, 18% quartz, 8% biotite, 4% hornblende, 2% sphene and accessory apatite and magnetite. Biotite shows minor alteration to chlorite along cleavage planes and edges and plagioclase cores show minor alteration to sericite.

Mount Haskin, British Columbia (Fig. 4-4)

PC9 Granite Porphyry (ref. Gabrielse 1963, p. 94)

Mineralized sample is from outcrop along southern edge of small "stock" on Mt. Haskin Mo property. The rock contains 60% phenocrysts that are 45% orthoclase, 25% quartz, 22% plagioclase (zoned albite) and 3% biotite in a micro-crystalline groundmass of K-feldspar-plagioclase-quartz-biotite. Apatite, zircon and pyrite occur as accessory minerals, and the hand specimen is cut by 1/4" molybdenite bearing quartz vein. Biotite contains inclusions of apatite and zircon and is altered to chlorite.

PC10 Granite Porphyry

Sample of barren drill core (hole DM 68-16) is from northern edge of small "stock" on Mt. Haskin Mo property. The rock contains 35% phenocrysts that are 40% orthoclase, 40% quartz, 16% plagioclase (zoned oligoclase), and 4% biotite in a microcrystalline groundmass of K-feldspar-quartz-plagioclase. Garnet occurs as an accessory mineral. A quartz vein and quartz-carbonate-K-feldspar coatings along hairline fractures compose 20% of the thin section. Biotite phenocrysts are fresh, but a finer, felted secondary biotite, that is associated with fractures, is altered to chlorite.

Mt. Reed, British Columbia (Fig. 4-4)

PC11 Granite Porphyry

Sample is from a barren "stock" on the Mt. Reed Mo-W property. The rock contains 60% phenocrysts that are 70% orthoclase, 20% quartz and 10% albite in a phaneritic groundmass of K-feldspar-albite-quartz-biotite. Sphene, apatite and magnetite occur as accessory minerals. Biotite shows 5% alteration to chlorite along cleavage planes and edges.

PC12 Granite Porphyry

Sample is from the central mineralized part of the small "stock" on the Mt. Reed Mo-W property. The specimen contains 80% phenocrysts that are 50% orthoclase, 25% quartz, 20% albite and 5% biotite in a microcystalline groundmass of quartz-K-feldspar-plagioclase-biotite. Apatite, sphene, and magnetite occur as accessory minerals. Biotite shows minor chlorite alteration along edges.

Cassiar Area, British Columbia (Fig. 4-5)

(young phase of Cassiar Intrusions that cuts Cassiar Batholith)

PC13 Quartz Monzonite

Medium grained, hypidiomorphic granular rock contains 32% plagioclase (An_{30}, 30% K-feldspar-(microperthite), 30% quartz, and 8% biotite. Apatite, sphene and magnetite occur as accessory minerals. Biotite is 10% altered to green biotite and chlorite.

PC14 Quartz Monzonite

Medium grained, hypidiomorphic granular rock contains 35% quartz, 30% plagioclase (An_{30}), and 24% K-feldspar (microperthite). Sphene (1%), apatite (1/2%), zircon (tr) and magnetite (tr) occur as accessory minerals. Biotite is 10% altered to chlorite along cleavage planes and edges.

Adera Claims - Adanac Mo Property

Atlin Area, British Columbia (Fig. 4-5)

PC15 Coarse Alaskite (ref. Sutherland Brown 1969, pp. 29-35

Coarse grained, hypidiomorphic granular rock contains 30% K-feldspar (perthite), 38% quartz, 27% plagioclase (zoned oligoclase), 2% carbonate, 1% biotite and 1% allamite. Molybdenite, pyrite, zircon, sphene and apatite occur as accessory minerals. Biotite is 20% altered to chlorite.

Syenite Range, Yukon Territory (Fig. 4-1)

PC16 Quartz Monzonite

Coarse-grained, hypidiomorphic granular rock contains up to 3/4" crystals of K-feldspar (40%) in finer-grained, phaneritic quartz (15%), plagioclase (An_{28}-30%), hornblende (7%), biotite (5%), sphene (1%), apatite (1%) and accessory zircon, fluorite, magnetite and allanite.

Alteration

Biotite shows minor chlorite alteration and contains inclusions of apatite, sphene, quartz and other accessories. Hornblende shows stronger alteration to chlorite, carbonate, epidote and biotite.

PC17 <u>Quartz Monzonite</u>

Although this specimen was obtained from the margin of a small stock, mapped by Bostock (1948) as zoned from a granite core (PC16) to a syenite outer rim, the specimen is texturally and mineralogically similar to sample PC16. Samples PC16 and PC17 were collected by K. Dawson and C. Godwin.

Copper Mountain, B.C. (Fig. 4-7)

KA1 to KA11

Samples KA1 to KA11 inclusive were obtained from Dr. V. Preto. Specimens and K-Ar ages obtained on biotite concentrates are described by Preto et al. (1971).

Granisle, Central British Columbia (Fig. 4-6)

NC-69-8 <u>Sulfide Rich Vein</u>

This sample is from a biotite (25 to 50% altered to chl.)-quartz-feldspar-apatite-bornite-chalcopyrite vein that was exposed in the Granisle open-pit in 1969. N. Carter collected the sample and has obtained a K-Ar biotite age of 50.2 $\pm$ 2.1 m.y. for this sample (N. Carter personal communication).

Brenda Mines, Southern British Columbia

JH5-68 <u>Quartz Diorite</u> (ref. Oriel 1972)

This sample is from the speckled quartz diorite phase of the Brenda stock. Dr. W.H. White provided a 90% sphene concentrate from this sample. Concordant ages of 174 $\pm$ 7 m.y. on biotite and 177 $\pm$ 7 m.y. on hornblende have been obtained for this sample (J. Harakal personal communication).

APPENDIX B - POTASSIUM-ARGON METHOD

B.1 PROCEDURE

Biotite and hornblende potassium-argon ages were determined in laboratories of the Department of Geology, University of British Columbia, using procedures and equipment previously described (White et al. 1967, p. 683; Northcote 1969, pp. 61-65). In addition to the normal procedure, the sample and entire fusion system were baked at 130°C for 16 hours which effectively eliminates atmospheric argon contamination in the fusion system (Roddick and Farrar 1971).

Analytical data and K-Ar isotopic ages are given in Table 2-1.

B.2 PRECISION AND ACCURACY

The precision and accuracy of the potassium-argon age determinations must be continually monitored to determine reliability of potassium-argon model ages. Interlaboratory standard mineral and rock samples are analyzed in the U.B.C. potassium-argon laboratory to establish the accuracy of the equipment and replicate analyses of minerals are used to determine the precision of the equipment (see White et al. 1967, and Northcote, 1969). J. Harakal runs periodic checks on the Ar^{40}/Ar^{36} ratio of atmospheric argon and on the argon isotope ratios in the spike system as measured on the U.B.C. MS-10 mass spectrometer. For samples containing less than 50% atmospheric argon contamination, U.B.C. results are internally consistent within 1% and a limit of error in an age determination (accuracy) is within 3% of the calculated age (J. Harakal, personal comm. June 1972).

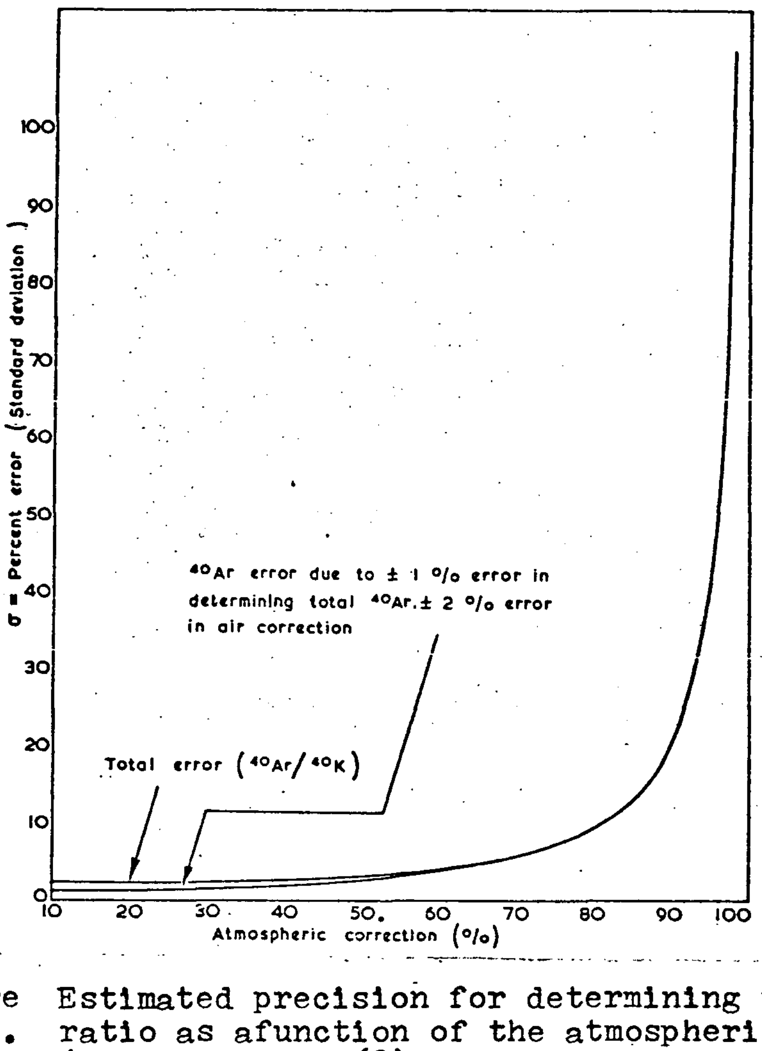

Figure (B-1). Estimated precision for determining the $^{40}Ar/^{40}K$ ratio as afunction of the atmospheric correction (from Damon, 1968).

B.3 ATMOSPHERIC CONTAMINATION

The atmospheric argon correction often introduces the largest error in the precision of the calculated age. The percentage standard deviation in a potassium-argon age as a function of the fraction of radiometric argon is shown in Figure B-1. This diagram demonstrates the effect of subtracting a large percentage of atmospheric argon from the total Ar^{40} measured. Error increases rapidly once atmospheric contamination reaches about 70% and therefore, the baking procedure described above should be used even if samples are not likely to be suitable for isochron determinations.

B.4 APPLICATION OF Ar^{40} (RAD.) VS %K ISOCHRONS TO PUBLISHED DATA

K-Ar data (Table B-2) from the Topley Intrusions and (Table B-1) from the Guichon Batholith was evaluated using Ar^{40} radiogenic vs %K diagrams. Plotting of Ar^{40}/Ar^{36} vs K^{40}/Ar^{36} diagrams is not attempted because the fusion system had not been baked prior to each analysis.

B.4.1 Guichon Batholith

Figure B-2a contains a plot of Ar^{40} rad. vs %K data for 18 biotite samples from the Guichon Batholith. A mean of the individual K-Ar ages of 199 $\pm$ 4 is in good agreement with the isochron age of 196 $\pm$ 5 m.y. and the intercept near zero suggests that the use of the present atmospheric Ar^{40}/Ar^{36} ratio in the correction for initial argon is reasonable. Figure B-2b is a plot of Ar^{40} rad. vs %K data for 6 biotite samples from the Witches Brook phase of the Guichon Batholith. The isochron age of 189 $\pm$ 9 m.y. for the Witches Brook phase is consistent with the composite isochron age and with the mean biotite K-Ar age of 199 $\pm$ 5 m.y. for the Witches Brook

TABLE B-1 Potassium-argon data for Guichon Creek Batholith (Northcote, 1969; White et al. 1967; Blanchflower, 1971).

Sample No. (Isochron No.)	Rock Unit	Mineral analyzed*	K±s(%)**	^{40}Ar**/Total ^{40}Ar	^{40}Ar*** (10^{-5} cc STP/gm)	Apparent Age**** (m.y.)
K64-102 (1)	Witches Brook	Biotite	4.91 ±0.03 4.91 ±0.03	0.87 0.91	4.055 4.077	198±8 199±8
K64-105-1 (2)	Witches Brook	Biotite	6.53 ±0.04	0.90	5.442	198±8
K63-171 (3)	Witches Brook	Biotite	6.59 ±0.06	0.75	5.263	192±8
K64-203 (4)	Witches Brook	Biotite	4.42 ±0.02 4.42 ±0.02	0.64 0.79	3.759 3.750	203±8 203±8
K64-17 (5)	Witches Brook	Biotite	3.59 ±0.02	0.74	3.093	206±8
K63-222 (6)	Witches Brook	Biotite	7.16 ±0.01	0.87	5.903	198±8
K63-223 (7)	Guichon	Biotite	5.77 ±0.02	0.87	4.689	195±8
GD12 (8)	Guichon	Biotite Hb.(alt.)	5.56 ±0.01 0.424±0.004	0.83 0.60	4.663 0.3629	201±8 205±8
K64-116a (9)	Chataway	Biotite	5.24 ±0.04	0.77	4.358	199±8
K63-220 (10)	Chataway-Leroy	Biotite	5.20 ±0.02 5.20 ±0.02	0.92 0.30	4.325 5.390	199±8 201±10
K63-37 (11)	Leroy	Biotite	6.42 ±0.03 6.42 ±0.03	0.78 0.85	5.385 3.795	201±8 202±8
K64-101 (12)	Leroy	Biotite	5.16 ±0.05	0.90	4.295	199±8
K63-13 (13)	Hybrid	Biotite	4.49 ±0.02 4.49 ±0.02	0.91 0.52	3.716 5.776	198±8 206±8
K64-156a (14)	Hybrid	Biotite	6.73 ±0.01	0.93	5.659	198±8
K64-98-1 (15)	Gump Lake	Biotite	5.95 ±0.01 5.95 ±0.01	0.37 0.91	4.817 4.919	194±10 198±8
K63-187 (16)	Bethsaida	Biotite	4.48 ±0.02 4.48 ±0.02	0.80 0.88	3.573 3.648	192±8 195±8
K63-231 (17)	Bethsaida	Biotite	5.86 ±0.07	0.86	5.044	205±8
K63-240 (18)	Breccia	Biotite	5.60 ±0.01	0.84	4.643	199±8
K63-115 (19)	Bethlehem	Biotite	5.90 ±0.07	0.90	4.307	195±8
GD-10 (20)	P3 Porphyry	Hb.(alt.)	0.292±0.002	0.53	0.2432	199±8
GD-102 (21)	P3 Porphyry	Hb.(alt.)	0.140±0.001 0.140±0.001	0.24 0.39	0.09845 0.09879	170±12 171±12
K64-186a (22)	Bethlehem	Biotite	1.87 ±0.01 1.87 ±0.01	0.83 0.27	1.644 1.634	210±12 212±12
GD-5 (23)	Dacite Porphyry	Biotite	5.56 ±0.03	0.50	4.717	203±8
GD-11a (24)	Bethlehem	Hb.(alt.)	0.161±0.00	0.44	0.1305	194±10
GD-4 (25)	Guichon	Hb.(alt.)	0.169±0.001	0.60	0.1474	208±8
K63-114 (26)	Volcanic dike	Biotite	6.99 ±0.02 6.99 ±0.02	0.88 0.83	1.389 1.433	49±3 51±3

* Hb.(alt.) = altered hornblende

** Potassium analyses by Wm. H. White, J. E. Harakal and others using KY and KY-3 flame photometers. s-standard deviation of quadruplicate analyses.

*** Argon analyses by J. E. Harakal and others using MS-10 mass spectrometer.

**** Constants used in model age calculations : $\lambda_e = 0.585 \times 10^{-10}y^{-1}$, $\lambda_\beta = 4.72 \times 10^{-10}y^{-1}$; $^{40}K/K = 1.181 \times 10^{-4}$.

TABLE B-2 Potassium-argon data for the Topley Intrusions (from White et al., 1970, and White et al., 1968).

Sample No. (Isochron No.)	Rock unit	Type	Mineral analyzed	K±s(%)*	^{40}Ar* / Total ^{40}Ar	^{40}Ar** (10^{-5} cc STP/gm)	Apparent Age*** (m.y.)
T66-15 (1)	Endako	Qtz. Monzonite	Biotite	5.67±0.07	0.82	3.328	143±6
T66-14 (2)	Endako	Qtz. Monzonite	Biotite	6.46±0.03	0.85	3.748	141±5
T65-3 (3)	Endako	Qtz. Monzonite	Biotite	5.81±0.04	0.70	3.318	140±6
T66-21 (4)	Nithi	Qtz. Monzonite	Biotite	5.13±0.04	0.89	2.974	141±6
T66-20 (5)	Nithi	Qtz. Monzonite	Biotite	5.80±0.03	0.78	3.281	138±5
T66-25 (6)	Glenannon	Qtz. Monzonite	Biotite	4.58±0.03	0.75	2.639	140±6
T67-29 (7)	Glenannon	Qtz. Monzonite	Biotite	4.39±0.02 4.39±0.02	0.65 0.87	2.419 2.423	134±5 135±5
T66-10 (8)	Tatin	Qtz. Monzonite	Biotite	5.69±0.04	0.73	3.327	142±6
T66-27 (9)	Tatin	Qtz. Monzonite	Biotite	6.59±0.02	0.65	3.687	136±5
T66-18 (10)	Casey	Qtz. Monzonite	Biotite	5.46±0.03	0.80	3.118	139±5
T66-26 (11)	Casey	Qtz. Monzonite	Biotite	6.34±0.06	0.68	3.558	137±6
T67-31 (12)	Francois	Granite	Biotite	6.06±0.03	0.80	3.408	137±5
T67-30 (13)	Francois	Qtz. Monzonite	Biotite	5.31±0.05	0.76	2.993	137±6
T66-16 (14)	Stellako	Qtz. Monzonite	Biotite	4.99±0.03	0.65	2.804	137±5
T65-2 (15)	Stellako	Qtz. Monzonite	Biotite	3.70±0.03	0.57	2.063	136±5
T66-11 (16)	Triangle	Qtz. Monzonite	Biotite	6.21±0.01 6.22±0.01	0.85 0.78	3.393 3.403	133±5 133±5
T65-4 (17)	Casey	Qtz. Monzonite	Biotite	7.054±0.026	0.85	4.099	141±5
T66-23 (18)	Casey	Qtz.-Biotite dike	Biotite	7.03±0.06	0.58	4.012	139±6
T65-6 (19)		Qtz. Monzonite	Biotite	6.903±0.025	0.88	3.961	140±5
T66-12 (20)		Qtz. Monzonite	Biotite	6.94±0.03	0.82	4.064	142±5
T66-13 (21)		Bio. with qtz.-moly vein	Biotite	6.53±0.02	0.74	3.808	142±5
T68-33 (22)	Simon Bay	Diorite	Hb.	1.21±0.01	0.62	0.7745	155±8
T68-33 (23)	Simon Bay	Diorite	Biotite	3.72±0.07	0.86	2.221	145±8
T68-33 (24)	Simon Bay	Diorite	Plagioclase	1.78±0.01	0.70	1.007	138±6
T66-22 (25)	Simon Bay	Qtz. Monzonite	Biotite	6.76±0.105 6.76±0.105	0.78 0.85	4.313 4.317	155±6 155±6
T66-28 (26)	Late dike	Dacite	Biotite	6.25±0.04 6.25±0.04	0.58 0.65	1.264 1.277	50±2 51±2
T65-1 (27)	Fraser	Qtz. Monzonite	Biotite	5.23±0.02 5.23±0.02	0.58 0.40	2.424 2.385	114±4 112±4

* Potassium analyses by Wm. H. White, T. Richards, and I. Semple using KY-1 and KY-3 flame photometers. s-standard deviation of quadruplicate analyses.

** Argon analyses by J. E. Harakal using MS-10 mass spectrometer.

*** Constants used in model age calculations: $\lambda_e = 0.585 \times 10^{-10} y^{-1}$, $\lambda_\beta = 4.72 \times 10^{-10} y^{-1}$, $^{40}K/K = 1.181 \times 10^{-4}$.

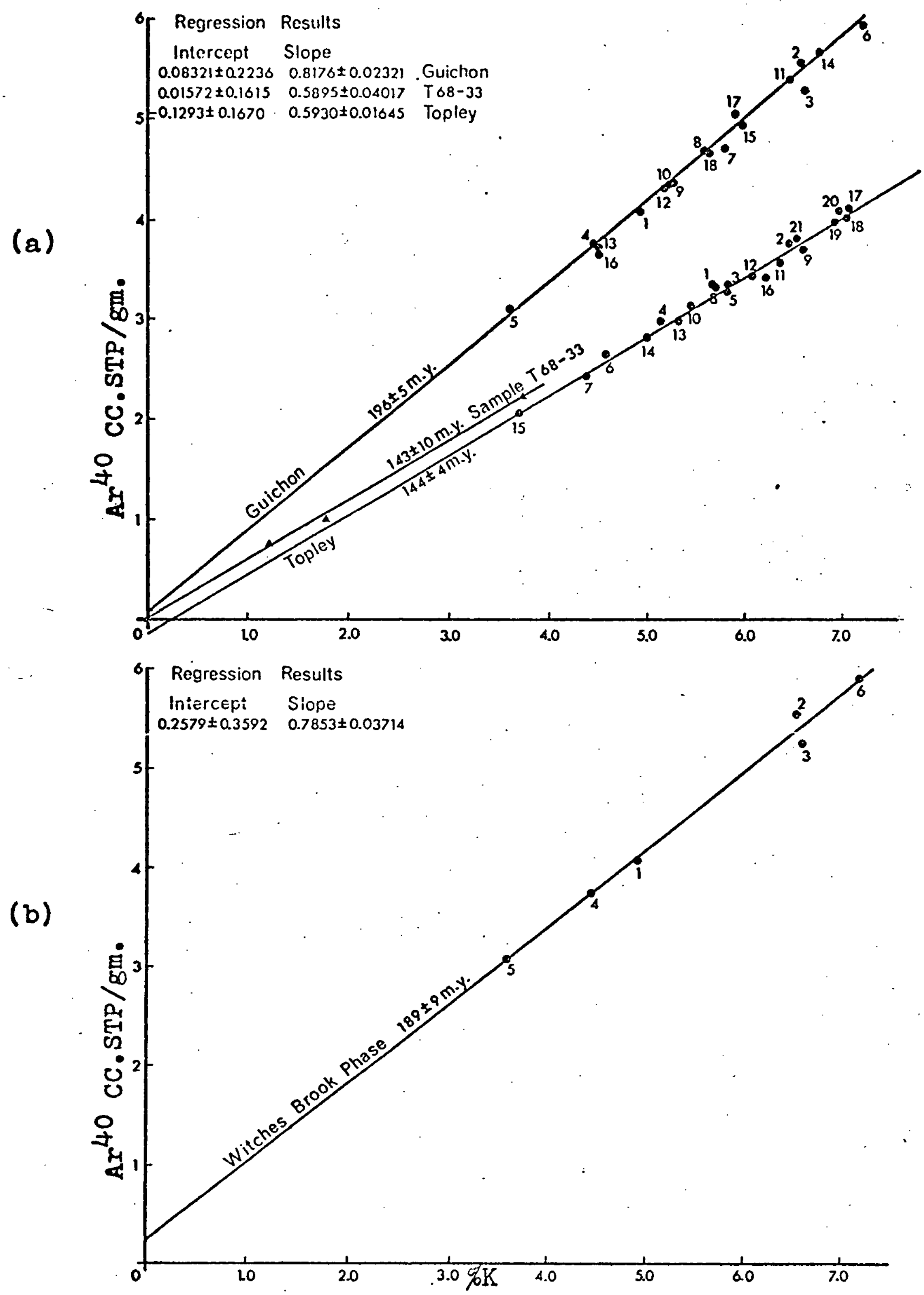

Fig. B - 2

a. Isochron plots for data from the Guichon Batholith, Topley Intrusions, and sample T68-33 from the Topley Intrusions.

b. Isochron plot for the Witches Brook Phase of the Guichon Batholith.

phase of the batholith . .

B.4.2 Topley Intrusions

K-Ar data for the Topley Intrusions near Endako, British Columbia has been interpreted by White et al. (1970) to indicate either one protracted perhaps intermittent magmatic event culminating in early Late Jurassic or three separate and unrelated events. Isochron plots of the Topley data were attempted in order to evaluate the two alternatives. The Triangle, Stellako, Francois, Casey, Tatin, Glenannon, Nithi and Endako phases of the Topley Intrusions have biotite K-Ar ages ranging from 133 m.y. to 143 m.y. and a mean age of 138 $\pm$ 3 m.y. The Simon Bay phase has a 155 m.y. age for biotite from sample T66-22 and from sample T68-33 discordant ages of 155, 145 and 138 m.y. The Topley isochron shown in Figure B-2a is from data (Table B-2) used to obtain the 138 $\pm$ 3 m.y. mean age and the isochron age of 144 $\pm$ 4 m.y. is consistent with the mean age. Hornblende, biotite and plagioclase data for sample T68-33 plots on an isochron that is parallel to the Topley isochron and has an isochron age of 143 $\pm$ 10 m.y.

For both the Topley isochron and sample T68-33 isochron, the isochron age and mean age of the conventional K-Ar determinations are consistent. Since the isochron and mean ages overlap, the isochron plots cannot be used to distinguish between continuous igneous activity or an intrusive pulse model.

B.4.3 Summary

Application of Ar^{40} (rad) vs %K isochron plots to data from the Topley Intrusions and Guichon Batholith supports the conventional age determinations. In both cases the mean age of the conventional determinations is consistent with the isochron age. For both the Topley Intrusions and the Guichon Batholith the initial argon ratio is essentially the same as the present-day value (Ar^{40}/Ar^{36} = 295.5).

APPENDIX C - FISSION TRACK DATING

C.1 INTRODUCTION

Fission track dating provides a method for using normal laboratory equipment for determining the age of nonconductors. Once polished section mounts are obtained, track counting and age determination takes only a few hours for materials with suitable age to uranium ratios. Unfortunately, in this study pre-counting steps consumed a majority of the time.

C.2 PROCEDURE

Fission track dating involves:

(a) determining the spontaneous fission track density (ρs) on an etched interior surface of a mineral or other nonconductor,

(b) using the calculated value for fission decay of U^{238} (λ_F), and

(c) determining the U^{238} content.

Step 1. MINERAL SEPARATION

Concentrates of the mineral to be used for fission track dating are obtained using standard mineral separation methods (see flow sheet Fig. C-1 and Table C-1). Care must be taken during mineral separation and subsequent steps to ensure that tracks are not annealed by heating.

Step 2. DIVISION OF SAMPLE

The mineral concentrates (65-95%) pure are split to obtain two portions. One portion is used to obtain the spontaneous (natural) track density, and this sample is saved till Step 6.

Figure C-1 Flowsheet for mineral separating

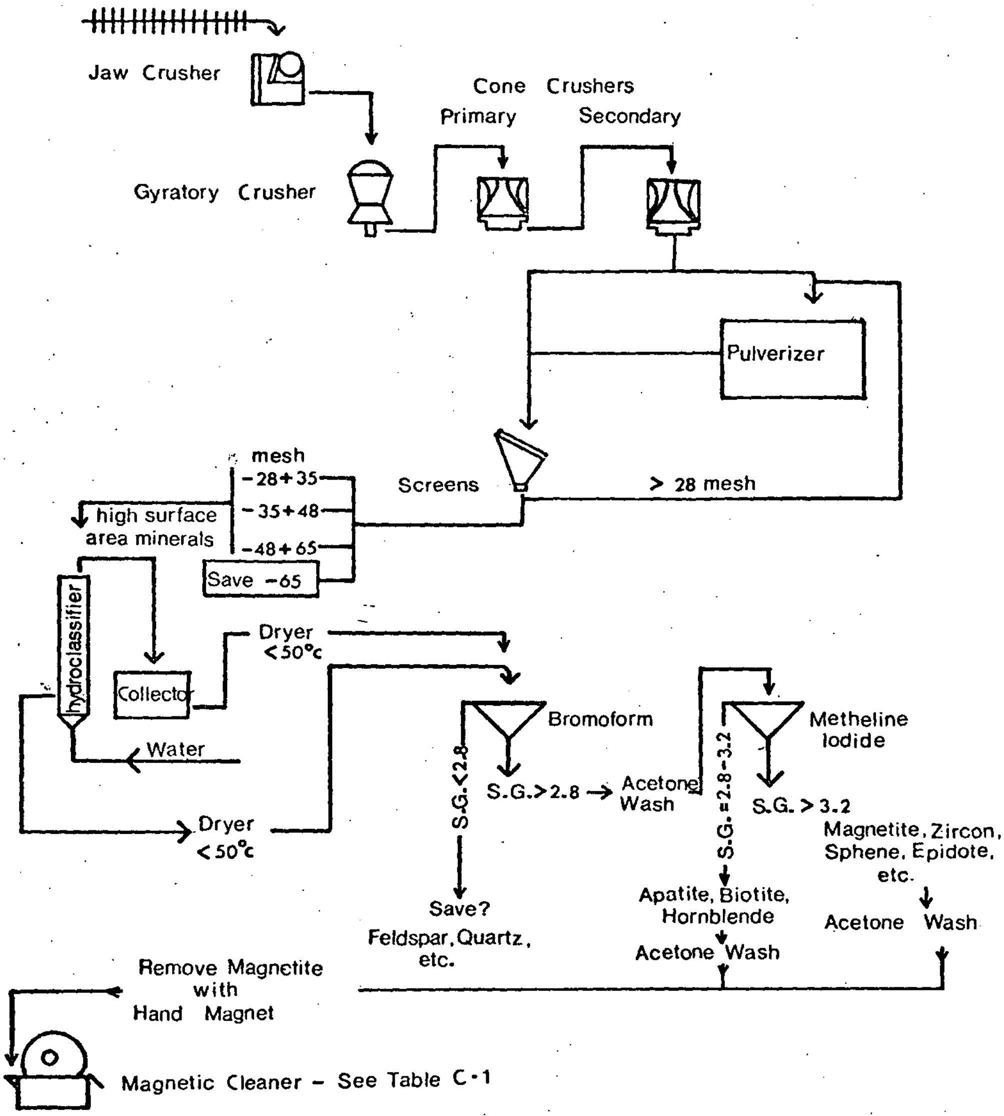

TABLE C-1 FRANTZ SEPARATION SETTINGS FOR DESIRED MINERAL SEPARATION (ROSENBLUM, 1958, p. 171)

Mineral	Cross tilt	Flow tilt	Current amps	Fraction used
Magnetite	18°	25°	less 0.2	heavies
Ilmenite	"	"	"	"
Pyrrhotite	"	"	"	"
Hornblende	"	"	0.2-0.5	"
Pyroxene	"	"	"	"
Biotite	"	"	"	lights
Sphene	"	"	0.6-1.0	heavies
Zircon	"	"	greater 1.2	"
Molybdenite	"	"	"	"
Pyrite	"	"	"	"
Fluorite	"	"	"	lights
Apatite	"	"	"	"

Step 3. PREPARATION OF SAMPLES FOR IRRADIATION

The second portion obtained from the split is placed in a porcelain crucible. This portion of each sample was annealed in an electric oven for 24 hours at 650 ± 25°C. Naeser (1967 p. 54) determined that annealing for one hour at 350°C and 625°C for apatite and sphene respectively will cause 100% track destruction. Therefore it is assumed that all spontaneous tracks were destroyed in the annealing procedure used by the writer.

Annealed apatite and sphene samples weighing between 0.01 and 0.2 gm. (minimum of 100 grains but generally several hundred) were next wrapped in high purity aluminum foil (provided by Mr. F.T. Murphy of AECL).

Glass standards* weighing between 0.1 and 0.2 gm. (1mm x 5mm x 5mm)

* Standard glass used to calibrate UBC reactor run 1 was provided by Dr. Charles Naeser of the U.S. Geological Survey.

were prepared in two different ways. One standard was in aluminum foil. A second standard was cleaned in a sequence of reagent grade solutions, including 50% ammonium hydroxide, acetone benzene and rinsed in deionized water, and then wrapped in a plastic detector which has been cleaned in reagent grade nitric acid, and rinsed in deionized water (Lahoud et al., 1966). The sample with the plastic detector was also wrapped in aluminum foil.

Step 4. SAMPLE IRRADIATION

Wrapped mineral samples and glass standards were placed in an aluminum capsule. The capsule was sealed and irradiated by Atomic Energy of Canada Limited in the self-serve unit of a NTX Reactor. A flux of 1.2×10^{15}nvt was requested and a cobalt tag included in the run was calibrated by the laboratory to have received a flux of 1.05×10^{15}nvt (1.35×10^{12}n/cm^2/sec for 13 minutes).

Step 5. FLUX DETERMINATION

Mr. F.T. Murphy of AECL (personal communication) suggested that the flux determined using the cobalt tag should be within 5% of the actual value, but Dr. C.W. Naeser (personal communication) has found that standards containing known uranium contents provided a more accurate determination. Three separate determinations provide independent support for a flux value of 1.31×10^{15}nvt $\pm$ 5%. These determinations include:

(1) count of induced tracks produced in standard glass included in the reactor run,

(2) comparison of the ratio of tracks/area in the standard glass included in the U.B.C. reactor run with the ratio of tracks/area in a piece of the same.

standard glass included in the Dartmouth reactor run 1 (flux of 1.46 x 10^{15}nvt was calculated by Dr. C.W. Naeser for the Dartmouth reactor run) and

(3) count of induced tracks/area produced in standard apatite Mc/G-1 that has a mean fission track apatite age of 120 m.y. and a concordant biotite K-Ar age of 120 m.y. (Christopher 1968).

Step 6. MOUNTING AND POLISHING

In order to handle 28-100 mesh mineral grains during fission track analysis, it is necessary for them to be mounted. The sample preparation procedure described by Naeser (1967, pp. 75-76 and 1967b, p. 1524) was used as a guide in preparing mounts.

At least 100 grains from each mineral concentrate are placed on a teflon sheet. The grains are then covered with a few drops of freshly mixed epoxy resin, and a labelled glass microscope slide is placed on top of the resin. The thickness of the epoxy wafer is gauged by placing a 0.1 to 0.5mm spacer at each end of the slide. Placing an iron weight on each mount eliminates bubbles from the mounts and produces an epoxy wafer of uniform thickness. After allowing the resin to dry for about 12 hours, the mounted sections are removed from the teflon sheet.

The mineral grains in the epoxy wafer must be polished to expose a fresh smooth interior surface. The grinding and polishing employed standard manual methods. An attempt was made to produce identical mounts of natural and irradiated mineral samples. Lack of a mechanical method for producing polished thin sections is considered to be one of the major problems in application of the fission track method. After spending over two hours (average) per polished section, variability in sections is considered to be one of the major sources of error.

The glass standard is mounted and polished in the same manner as the mineral grains. Other laboratories (Rensselaer and General Electric) have used fracturing methods for preparing the glass standard.

Step 7. ETCHING

Two slides of each mineral concentrate must be used to obtain an age. One slide is made from the natural mineral concentrate (Plates 1 and 3). A second slide is made from the annealed and irradiated portion (Plates 2 and 4). The two slides are placed back to back and dipped in an appropriate etchant (see Tables C-2 and C-3). For minerals with variable composition (e.g. apatite, epidote or micas), the etching has to be done in steps and the tracks examined at intervals to obtain the proper etch time.

The track density in the glass before irradiation is essentially zero, and therefore only the irradiated glass standard is mounted, polished to expose an interior surface and etched (Plates 5 and 6). A Makrofol KG plastic detector (polycarbonate) was also used to detect induced fission in the glass. Unfortunately the plastic detector was over etched.

Step 8. COUNTING TRACKS

Track densities for etched apatite and sphene samples were determined by observation using a polarized-light-microscope at about 1500x (magnification obtained from Zeiss 100x oil immersion objective, 12.5x eyepiece and 1.25x

TABLE C-3. ETCHING CONDITIONS FOR FISSION-TRACK COUNTING.

Material	Etchant	Temp.	Time	Reference	Comments
Apatite	HNO_3(65%)	25°C	15 sec.	Reimer et al. 1970	
Zircon (prism face)	NaOH (100N)	220°C	9 hrs.	" "	
Glass (microscope slide)	HF (48%)	25°C	5 sec.	" "	
Muscovite (001)	HF (48%)	25°C	15 min.	" "	
Sphene	1HF, $2HNO_3$, 3HCl, $6H_2O$	25°C	14 min.	" "	
Sphene	6:3:2:1 H_2O:HCl:HNO_3:HF	20°C	1-5 min.	Naeser and McKee, 1970	
Muscovite	HF (48%)	20°C	7-9 min.	" "	
Zircon	100M NaOH	220°C	4-6 hrs.	" "	
Apatite	HNO_3 (5%)	20°C	25 sec.	" "	
Apatite	HNO_3	23°C	5-30 sec.	Fleischer and Price, 1964d	
Glass	HF (48%)	23°C	5 sec.	" "	
Fluorite	H_2SO_4 (98%)	23°C	10 min.	" "	
Makrofol (KG)	NaOH 6N	23°C	2-2-1/2 hrs.	Lahoud et al., 1966	
Apatite	HNO_3 (70%)	20°C	5-20 sec.	Naeser and Dodge, 1969, unpublished	
Sphene	HCl (37%)	90°C	15-60 min.	" "	
Muscovite	HF (48%)	20°C	5-15 min.	" "	
Epidote	NaOH 50N	140°C	1/2-2 hr.	Naeser, Engels and Dodge, 1970	
Allanite	NaOH 50N	140°C	2-60 min.	" "	
Garnet	50N NaOH	140°C	30-120 min.	" "	
Glass	24% HBF_4, 5% HNO_3, 0.5% CH_3CO_2H	25°C	35-50 min.	Macdougall, 1971	compares other etchants
Pyroxene	6 g. NaOH, 4 co H_2O	boiling point	50 min.	Wilkening et al., 1971	
Plagioclase	6 g. NaOH, 8 co H_2O	boiling point	12 min.	" "	

setting on an optivar magnification changer). Track densities for etched glass standards were determined by observation using a reflected-light microscope at about 1000x (magnification obtained from a Zeiss 40x objective, 12.5x eyepiece and 2.0x setting on an optivar magnification changer). Tracks are counted in the field of view covered by a square reticle (Plate 7). The number of fields counted varied with the track density. Since the counting error decreases with increase in the number of tracks counted, a minimum of 400 counts is desirable. The standard deviation of the track counts is taken as the square root of the number of tracks counted (Naeser 1967b). This formula yields a counting error of ± 5% for 400 counts.

TABLE C-2 ETCHING TECHNIQUES USED FOR MATERIALS STUDIED

Material	Etchant	Etch Time	Temp.	Reference	Comments
Apatite	65-70%	5-30 sec.	23°C	Fleischer and Price, 1964d	Time varies with composition
Glass slide (standard)	48% HF	5 sec.	23°C	"	
Sphene	6:3:2:1 H_2O:HCL:HNO_3:HF	1-5 min.	20°C	Naeser et al. 1970	
Zircon	100M. NaOH	4-6 hrs.	220°C	Naeser and McKee, 1970	
Makrofol (K6)	6N NaOH	2-2-1/2 hr.	23°C	Lahoud et al. 1966	

Step 9. URANIUM DETERMINATION

By using a ratio of spontaneous tracks to induced tracks, the determination of absolute uranium content can be bypassed in the age calculation. Lahoud et al. (1966) suggest that the fission-track method is 10,000x more sensitive than other analytical methods of determining uranium content. In theory, it is possible to determine concentrations as low as 10^{-5}ppb. The only limitation on the sensitivity is the effect of extremely large neutron doses on the sample and the availability of standards for determining the flux.

In order to calculate the uranium concentration in a mineral phase, it is necessary to know the induced track density and the neutron dose which produced the tracks. The formula is (Naeser 1967a):

$$C(\text{ppm } U^{238}) = F \; \rho_i / \phi \; N_v \sigma \; IR_o$$

where

$$F = \frac{238 \text{ (atomic weight of } U^{238}) \times \text{No. atoms in mineral formula} \times 10^6}{\text{molecular weight of mineral}};$$

ρi = induced track density:

I = U^{235}/U^{238}, (7.26×10^{-3});

σ = thermal neutron cross section for fission of U^{235} $(5.83 \times 10^{-22} cm^2)$;

N_v = number of atoms per cm^3 of sample;

R_o = average fission fragment range (either 8×10^{-4} if new surface is exposed and etched after irradiation, or 4×10^{-4} cm if an old surface is used.

By substituting values for constants, the equation reduces to:

$$C = \frac{3.61 \times 10^{10} \quad \rho_i}{\phi}$$

for apatite when

$$F = 9.80 \times 10^{6} \text{ and}$$

$$N_v = 0.8010 \times 10^{23} \text{ atoms/cc}$$

and to:

$$C = \frac{3.33 \times 10^{10} \ \rho_i}{\phi}$$

for sphene when

$$F = 9.71 \times 10^{6} \text{ and}$$

$$N_v = .8603 \times 10^{23} \text{ atoms/cc.}$$

Plate 1. Microphotograph showing spontaneous (natural) fission-tracks in standard apatite sample Me/G-1. Apatite from this sample has a spontaneous track density of 8.73 $\pm$ 1.12 x 10^5 tracks/cm^2 and a uranium content of 15.5 $\pm$ 1.9 ppm. Scale 1 inch = 22 microns

Plate 2. Microphotograph showing induced tracks in standard apatite Me/G-1. Annealed apatite grains were exposed to a thermal neutron flux of 1.535 x 10^{15}. The induced track density produced was about 6.96 x 10^5 tracks/cm^2. Scale 1 inch = 22 microns.

Plate 3. Microphotograph showing spontaneous (natural) fission-tracks in sphene sample JH5. Cracks in sphene grains cause counting problems but can generally be distinguished from tracks of uniform size and characteristic shape. Scale 1 inch = 15 microns.

Plate 4. Microphotograph showing faint induced fission-tracks in sphene sample JH5. Lines which cross entire plate are scratches produced during polishing. Scale 1 inch = 15 microns.

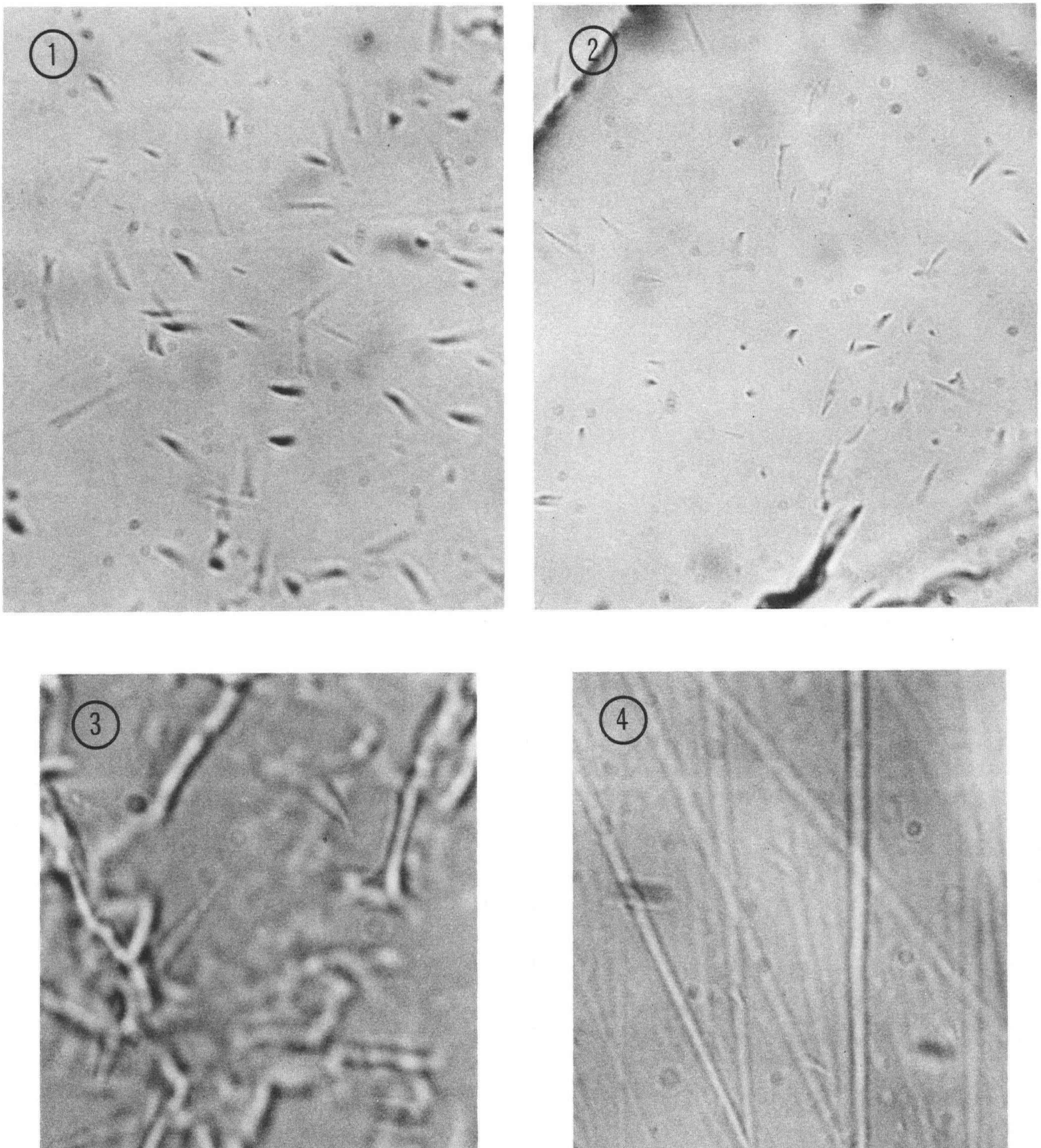
1
2
3
4

Plate 5. Microphotograph showing induced fission-tracks produced in standard glass used to calibrate U.B.C. reactor run. Glass contains 0.4 ppm uranium and was radiated to a flux of 1.31 x 10^{15} nvt. Scale 1 inch = 22 microns.

Plate 6. Microphotograph showing induced fission-tracks produced in standard glass used to calibrate a reactor run. Glass contains 0.44 ppm uranium and was irradiated to a flux of 8 x 10^{16} nvt (flux determined by S. Barr). Scale 1 inch = 22 microns.

Plate 7. Microphotograph showing central part of a reticle used for measuring area from which track count was obtained. Scale 1 inch = 15 microns.

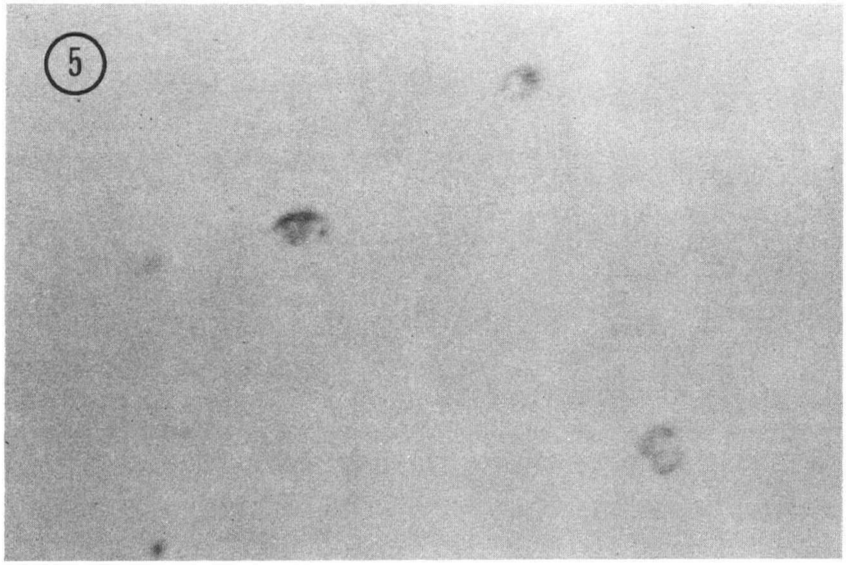
5

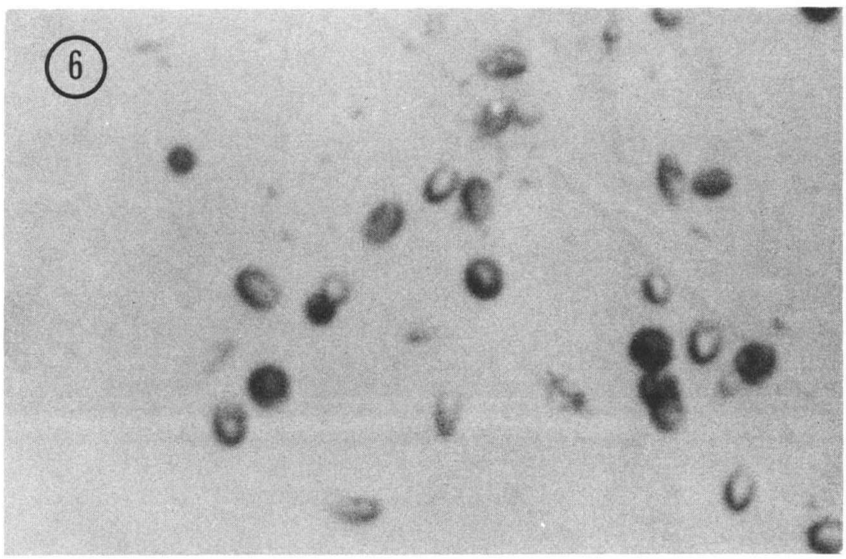
6

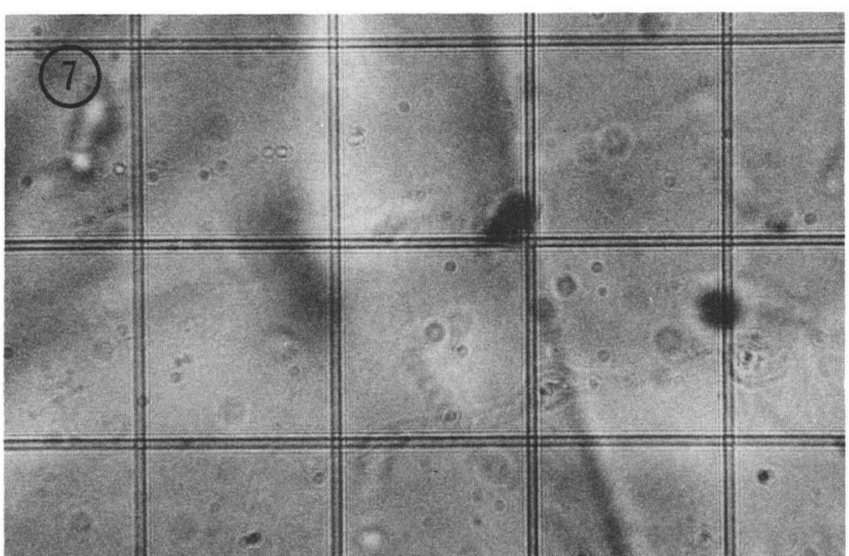
7

APPENDIX D

TABLE OF PUBLISHED K-Ar AGES REVIEWED FOR THIS REPORT

TABLE D-1 Published K-Ar ages referred to in this report.

Report No.	Reference Number and Mineral Dated		Age in m.y.	Rock Type	Unit	Location	Reference
			CASSIAR BATHOLITH - MEAN AGE 102 ± 3 m.y.				
1	AK50	Bio	101	Quartz monzonite	Cassiar Batholith	60°04'N. 130°29'W.	Baadsgaard, et al., 1961
2	GSC60-28	Bio	98	Biotite-granodiorite	Cassiar Batholith	60°32'N. 131°29'W.	GSC Paper 61-17, p. 17
3	GSC67-12	Musc	105±5	Granitic gneiss	margin of Cassiar Batholith	60°00'N. 130°44'W.	GSC Paper 69-2A, p. 9-10
4	GSC67-15	Bio	105±5	Quartz monzonite	Cassiar Batholith	58°49'N. 129°52'W.	GSC Paper 69-2A, p. 11
5	GSC70-35	Bio	102±5	Quartz monzonite	Cassiar Batholith	58°42.5'N. 128°43.5'W.	GSC Paper 71-2, pp. 21-22
			LATE CRETACEOUS AGES - WEST OF CASSIAR BATHOLITH				
6	GSC67-14	Bio	78±4	Granite	Parallel Creek Batholith	59°13.5'N. 130°23.5'W.	GSC Paper 69-2A, p. 10
7	GSC66-1	Hb	79±11	Granite	Glundebery Batholith	59°14'N. 130°49'S.	GSC Paper 67-2A, p. 11
8	GSC70-4	Hb	74±4	Granite	Glundebery Batholith	60°12'N. 131°06'W.	GSC Paper 71-2, pp. 7-8
9	GSC60-25	Bio	71	Quartz monzonite	unnamed	58°53'49"N. 130°01'28"W.	GSC Paper 61-17, p. 15
10	GSC70-49 (replaces GSC59-14)	Bio	98±5	Leuco-quartz monzonite	Seagull Batholith	60°02'32"N. 131°10'11"W.	GSC Paper 71-2, p. 31
11	GSC70-50	Bio	97±5 92±4	Leuco-quartz monzonite	Seagull Batholith	60°04.5'N. 131°09'W.	GSC Paper 71-2, pp. 32-33
			EARLY TERTIARY AGES - WEST OF CASSIAR BATHOLITH				
12 13	GSC67-9 GSC67-10	Hb Bio	48±4 46±2	Quartz diorite	unnamed	59°23'45"N. 131°40'30"W.	GSC Paper 69-2A, pp. 8-9
14	GSC70-19	Bio	58±18	Quartz diorite	Mount McMaster Stock	59°22'N. 133°12'W.	GSC Paper 71-2, p. 14
			EARLY TERTIARY AGES - BODY INTRUDES CASSIAR BATHOLITH				
15	GSC67-1	Musc	58±3	Quartz monzonite	unnamed stock?	59°39'N. 130°20.5'W.	GSC Paper 69-2A, p. 6
16	GSC67-2	Musc	53±3	Pegmatite	*	59°39'N. 130°27.5'W.	GSC Paper 69-2A, p. 6
			EARLY TERTIARY AGE - EAST OF CASSIAR BATHOLITH				
17	GSC62-74	Musc	57	Gneiss	Horse Ranch Group	59°30'40"N. 128°55'45"W.	GSC Paper 63-17, p. 48

* See reference.

TABLE D-1 (cont'd) Published K-Ar ages referred to in this report.

Report No.	Reference Number and	Mineral Dated	Age in m.y.	Rock Type	Unit	Location	Reference
				NOME LAKE AND SIMPSON PEAK BATHOLITHS, NORTHERN B.C.			
18	GSC67-3	Hb	181±14	Quartz monzonite	Simpson Peak Batholith	59°44'N. 131°26'45"W.	GSC Paper 69-2A, pp. 6-7
19	GSC67-4	Bio	165±8				
20	GSC67-5	Hb	183±9	Quartz monzonite	Nome Lake Batholith	59°37'N. 130°53.5'W.	GSC Paper 69-2A, p. 7
21	GSC67-6	Bio	183±8				
				PLATE CREEK STOCK, NORTHERN B.C.			
22	GSC70-23	Hb	184±10	Quartz diorite	Plate Creek Stock	59°53'N. 130°45.5'W.	GSC Paper 71-2, p. 16
23	GSC67-11	Hb	159±10	Quartz diorite	Plate Creek Stock	59°52'30"W. 130°45'W.	GSC Paper 69-2A, p. 9
				PARALLEL CREEK, KLINKET AND TUYA BATHOLITHS, NORTHERN B.C.			
24	GSC70-24	Bio	87±4	Quartz monzonite	Klinket Batholith	59°28'N. 131°13'W.	GSC Paper 71-2, pp. 16-17
25	GSC67-13	Bio	92±5	Granite	Tuya Batholith	59°04.3'N. 130°43'W.	GSC Paper 69-2A, p. 10
6	GSC67-14	Bio	78±4	Granite	Parallel Creek Batholith	59°13.5'N. 130°23.5'W.	GSC Paper 69-2A, p. 10
				CHRISTMAS CREEK BATHOLITH, NORTHERN B.C.			
26	GSC70-20	Hb	177±9	Quartz diorite	Christmas Creek Batholith	59°18'N. 131°40.5'W.	GSC Paper 71-2, p. 15
27	GSC67-7	Hb	128±6	Quartz diorite	Christmas Creek Batholith	59°22'30"N. 131°44'W.	GSC Paper 69-2A, pp. 7-8
28	GSC67-8	Bio	56±3				
29	GSC66-2	Hb	146±17	Quartz diorite	Christmas Creek Batholith	59°16'N. 131°29'W.	GSC Paper 67-2A, pp. 11-12
30	GSC66-3	Bio	73±5				
				HOTAILUH BATHOLITH, NORTHERN BRITISH COLUMBIA			
31	GSC70-27	Hb	147±8	Grano-diorite	Hotailuh Batholith	58°09.6'N. 129°51.9'W.	GSC Paper 71-2, pp. 17-18
32	GSC70-28	Bio	139±6				
33	GSC70-29	Hb	166±8	Granite	Hotailuh Batholith	58°08'30"N. 129°52'00"W.	GSC Paper 71-2, p. 18
		Hb	157±11				
34	GSC62-71	Bio	193				GSC Paper 63-17, pp. 45-46
35	GSC70-30	Hb	155±8	Quartz monzonite	Hotailuh Batholith	58°10.5'N. 129°38.5'W.	GSC Paper 71-2, p. 19
36	GSC70-31	Hb	163±9	Quartz monzonite/ granodiorite	Hotailuh Batholith	58°07.5'N. 129°30'W.	GSC Paper 71-2, p. 19
37	GSC70-32	Bio	163±7				
38	GSC70-33	Hb	215±11	Monzonite/ quartz monzonite	Hotailuh Batholith	58°10'N. 129°39'W.	GSC Paper 71-2, p. 20
		Hb	215±11				
39	GSC70-34	Hb	217±11	Diorite	Hotailuh Batholith	58°04.5'N.	GSC Paper 71-2, p. 20
		Hb	217±11				
40	GSC70-25	Hb	161±8	Quartz monzonite	Hotailuh Batholith?*	58°15.5'N. 130°15.5'W.	GSC Paper 71-2, p. 17
41	GSC70-26	Bio	141±7				

* See reference.

TABLE D-1 (cont'd) Published K-Ar ages referred to in this report.

Report No.	Reference Number and Mineral Dated		Age in m.y.	Rock Type	Unit	Location	Reference
				EARLY CRETACEOUS STOCK, NORTHERN B.C.			
42	GSC70-21	Hb Hb	112±28 120±26	Biotite quartz diorite	Tachilta Lake stock	58°38.5'N. 130°56'W.	GSC Paper 71-2, p. 15
43	GSC70-22	Bio	137±6	Hornblende quartz diorite	Tachilta Lake stock	*	GSC Paper 71-2, pp. 15-16
				HOGEM BATHOLITH, NORTHERN B.C.			
44	GSC70-11	Bio	122±6	Granite	Hogem Batholith	56°20'113'N. 125°49'W.	GSC Paper 71-2, p. 11
45	K65-1	Bio	170±8	Syenite	Hogem Batholith	55°56'N. 125°28'W. Lorraine	White et al. 1968; Koo, 1968
				LATE CRETACEOUS AND EARLY TERTIARY AGES COAST INTRUSIONS, NORTHERN B.C. AND SOUTHEASTERN ALASKA			
46	GSC61-39	Bio	54	Biotite granodiorite	Coast Intrusions	59°44'N. 134°59'W.	GSC Paper 62-17, p. 23-24
47	GSC61-38	Bio	65	Biotite granodiorite	"	59°47'30"N. 135°00'30"W.	GSC Paper 62-17, p. 23
48	GSC61-46	Bio	65	Granite	"	59°34'N. 135°11'W.	GSC Paper 62-17, p. 29
49	GSC61-47	Bio	70	Biotite granodiorite	"	59°30'30"N. 135°13'30"W.	GSC Paper 62-17, p. 29
50	GSC60-26	Bio	61	Granite	"	59°37'N. 135°08"W.	GSC Paper 61-17, p. 15-16
51	GSC60-27	Bio	68	Biotite	"	59°50'30"N. 135°01'W.	GSC Paper 61-17, p. 16
52	GSC62-75	Bio	69	Quartz monzonite	"	58°34'24"N. 133°18'00"W.	GSC Paper 63-17, p. 49
53	GSC66-6	Bio	44±2	Granodiorite	"	mouth of Scud River	White et al. 1968
54	GSC60-34	Bio	30	Quartz diorite	"	59°18'N. 135°20'W.	GSC Paper 61-17, p. 20
				EARLY TERTIARY AGES - EAST MARGINAL PLUTON (ALASKA)			
55	PMS-1	Bio	48.7±1.8	Monzonite	East Marginal Pluton	58°44'N. 133°51'W.	Forbes and Engels, 1970
56	PMS-2	Bio	52.8±2.6	Quartz monzonite	"	58°43'30"N. 133°52'30"W.	
57	EN-2	Whole R	51.1±1.5	Quartz monzonite	"	58°43'N. 133°55'W.	
58	EN-3	Whole R	46.9±1.4	Quartz monzonite	"	58°43'N. 133°58'W.	
59	EN-4	Bio	49.6±1.4	Quartz monzonite	"	58°41'N. 133°59'W.	
60	EN-5	Whole R	51.0±1.0	Quartz monzonite	"	58°40'30"N. 134°04'W.	
61	EN-6	Bio	47.0±1.6	Quartz monzonite	"	58°39'N. 134°18'W.	

* See reference.

TABLE D-1 (cont'd) Published K-Ar ages referred to in this report.

Report No.	Reference Number and Mineral Dated		Age in m.y.	Rock Type	Unit	Location	Reference
				KING SALMON LAKE AREA, B.C.			
62	GSC62-76	Bio	227	Granodiorite boulder in cong.	*	58°34'40"N. 133°02'30"W.	GSC Paper 63-17, pp. 49-50
63	GSC62-77	Bio	206	"	*	"	GSC Paper 63-17, p. 50
				STIKINE COPPER, NORTHERN B.C.			
64	GC66-1	Bio	174±9	*	*	Central ore zone DDH GC193 @ 400'	White et al., 1968
65	GC66-2	Bio	189±9	*	*	Central ore zone DDH GC148 @ 519'	"
66	GC66-5	Bio (chloritic)	182±9	Granite	*	*	"
67	GC66-7	Bio	177±9	Syenite	Copper Canyon syenite	"	"
68	A64-1	Bio	198±7	*	*	Central ore zone	"
				BLUE RIVER ULTRAMAFIC INTRUSIONS, NORTHERN B.C.			
69	GSC64-1	Whole R	245±80	Amphibolite	*	59°32'N. 129°58'W.	GSC Paper 65-17, p. 7
				CASSIAR INTRUSIONS NEAR DALL LAKE, B.C.			
70 71	GSC62-68 GSC62-69	Musc Bio	139 123	Quartz monzonite	*	59°27'N. 127°42'W.	GSC Paper 63-17, pp. 44-45
72 73	GSC62-72 GSC62-73	Bio Musc	124 194	Gneiss	*	59°57"N. 131°58'W.	GSC Paper 63-17, pp. 46-47
74	GSC62-70	Musc.	178	Gneiss	Oblique Creek*	58°58'36"N. 130°01'24"W.	GSC Paper 63-17, p. 45
				SUSTUT GROUP, NORTHERN B.C.			
75	GSC70-9	Whole R	49±5	Tuff	Sustut Group	57°19'N. 127°40'W.	GSC Paper 71-2, pp. 9-10
76	GSC70-10	Whole R	53±6	Tuff	Sustut Group	56°54'N. 126°56'W.	GSC Paper 71-2, p. 10
				WOLVERINE COMPLEX, NORTHERN B.C.			
77 78	GSC70-14 GSC70-15	Musc Bio	47±3 43±3	Granite	Wolverine Complex	56°23'N. 125°21.5'W.	GSC Paper 71-2, p. 12
				INGENIKA GROUP, NORTHERN B.C.			
79 80	GSC70-12 GSC70-13	Musc Bio	128±6 124±6	Schist	Ingenika Group	56°23'N. 125°21.5'W.	GSC Paper 71-2, pp. 11-12

* See reference.

TABLE D-1 (cont'd) Published K-Ar ages referred to in this report.

Report No.	Reference Number and Mineral Dated		Age in m.y.	Rock Type	Unit	Location	Reference
				POLARIS ULTRAMAFIC COMPLEX, NORTHERN B.C.			
81 82	GSC66-18 GSC66-19	Hb Bio	152±15 164±9	Peridotite	Polaris Ultramafic Complex	56°26'N. 125°35'W.	GSC Paper 67-2A, p. 21-22
				CASSIAR BATHOLITH[1]			
83	GSC70-48	Musc	87±4	Granodiorite (cataclastic)	Cassiar Batholith	69°04'47"N. 130°49'35"W.	GSC Paper 71-2, pp. 30-31*
				MARKER LAKE BATHOLITH			
84	GSC61-45	Bio	126	Granodiorite	Marker Lake Batholith	60°33'N. 130°57'W.	GSC Paper 62-17, p. 28
85	GSC60-30	Bio	98	Schist	east of Marker Lake Batholith	60°37'N. 130°47'W.	GSC Paper 61-17, p. 17-18
86	GSC60-29	Bio	66	Granodiorite	unnamed stock *	61°07'N. 130°51'W.	GSC Paper 61-17, p. 17
				AGES SOUTHWEST OF TINTINA TRENCH, YUKON TERRITORY (NASINA SERIES, YUKON GROUP, BRICK CREEK SCHIST)			
87	GSC66-60	Hb	199±34	Granitic cobble in conglom.	Laberge Group	61°37'N. 135°53'W.	GSC Paper 67-2A, pp. 55-56
88	GSC59-9	Musc	214	Schist	*	60-61°N. 132-134°W.	GSC Paper 60-17, p. 7
89	GSC59-11	Bio	140	Schist	Yukon Group	61°17'N. 138°07'W.	GSC Paper 60-17, p.8
90	GSC61-41	Bio	147	Schist	Yukon Group	61°14'N. 136°57'W.	GSC Paper 62-17, pp. 25-26
91	GSC61-42	Musc	222	Schist	Yukon Group	60°00'30"N. 132°08'20"W.	GSC Paper 62-17, pp. 26-27
				KLONDIKE SCHIST			
92	GSC60-33	Musc	138	Schist	Klondike schist	63°54'N. 138°52'W.	GSC Paper 61-17, p. 19
93	GSC61-40	Musc	175	Schist	Kondike schist	64°07'N. 140°48'W.	GSC Paper 62-17, p. 25
				PELLY GNEISS			
94	GSC62-82	Bio	202	Granodiorite	Pelly gneiss	64°02'00"N. 140°23'20"W.	GSC Paper 63-17, pp. 53-54
95 96	GSC64-24 GSC64-25	Bio Hb	187 161	Gneiss	Pelly gneiss	62°53½'N. 138°51'W.	GSC Paper 65-17, p. 22
97 98	GSC64-26 GSC64-27	Musc Bio	178 182	Granitic gneiss	Pelly gneiss	63°06'45"N. 139°29'30"W.	GSC Paper 65-17, pp. 23-25

* See reference.

[1] This sample is not included in mean age since Poole (1972) considers the age to be young.

TABLE D-1 (cont'd) Published K-Ar ages referred to in this report.

Report No.	Reference Number and Mineral Dated		Age in m.y.	Rock Type	Unit	Location	Reference
				GRANITIC ROCKS			
99	GSC59-10	Bio	223	Granodiorite	*	60°53'N. 135°33'W.	GSC Paper 60-17, pp. 7-8
100	GSC59-12	Bio	176	Quartz monzonite	*	61°21'N. 138°03'W.	GSC Paper 60-17, pp. 8-9
101	GSC59-13	Bio	58	Granodiorite	Yukon Group	61°25'N. 138°45'W.	GSC Paper 60-17, p. 9
102	GSC60-31	Bio	65	Quartz monzonite	Ruby Range Batholith	61°05'N. 136°59'W.	GSC Paper 61-17, pp. 18-19
103	GSC60-32	Bio	58	Granodiorite	Ruby Range Batholith	61°01'N. 138°08'W.	GSC Paper 61-17, pp. 18-19
				NORTH-BIG SALMON RIVER CRYSTALLINE BELT			
104	GSC65-34	Bio	90±6	Quartz monzonite	Big Salmon R. Crystal-line Belt	61°35'30"N. 133°26'30"W.	GSC Paper 66-17, pp. 35-36
105	GSC65-35	Bio	90±6	Granite	"	61°46'N. 133°26'30"W.	GSC Paper 66-17, pp. 35-36
106	GSC65-36	Bio	91±5	Schist	"	61°40'N. 133°20'W.	GSC Paper 66-17, pp. 36-37
107	GSC65-37	Amphibole	83±26	Gneiss	"	61°41'N. 133°16'W.	GSC Paper 66-17, pp. 37-38
				CANADIAN CREEK, YUKON TERRITORY (CASINO DEPOSIT)			
108	CP-25-69		69±3	Porphyritic dacite	*	62°43'N. 138°49'W.	Phillips and Godwin, 1970, p. 3
109	CP-2-69		71±3	Porphyritic dacite	*	62°43'N. 138°49'W.	"
110	GSC67-45	Hb Bio	99±6 95±5	Granodiorite	*	62°42.9'N. 138°50.8'W.	GSC Paper 69-2A, p. 27
				SELWYN BASIN NEAR YUKON TERRITORY - MACKENZIE TERRITORY BOUNDARY			
111 112	GSC67-65 GSC67-66	Hb Bio	80±5 87±4	Quartz monzonite	*	62°51'25"N. 128°49'30"W.	GSC Paper 69-2A, p. 37
113	GSC67-49	Bio	88±4	Schist	*	61°39'40"N. 128°34'00"W.	GSC Paper 69-2A, pp. 28-29
114	GSC62-88	Bio	110	Quartz monzonite	Pyramid Mtn. stock	61°53'03"N. 127°58'52"W.	GSC Paper 63-17, p. 58
115	AK 125	Bio	96	Granodiorite	Itsi Mountains Pluton	65°55'N. 130°10'W.	Baadsgaard et al., 1961 a and b
116	AK 107	Bio	94	Quartz monzonite	Nahanni	62°05'N.	Baadsgaard et al., 1961b, pp. 458-465
117	GSC65-45	Bio	99±5	Schist	*	61°23'N. 130°33'W.	GSC Paper 66-17, pp. 43-44

* See reference.

TABLE D-1 (cont'd) Published K-Ar ages referred to in this report.

Report No.	Reference Number and Mineral Dated		Age in m.y.	Rock Type	Unit	Location	Reference
				NORTHERN YUKON TERRITORY			
118	GSC63-15	Bio	265±12	Porphyritic granite	Old Crow Batholith	67°42'N. 140°42'W.	GSC Paper 64-17 (Part 1), p. 22
119	AK 108		220		Old Crow Batholith	67°44'N. 139°50'W.	Baadsgaard et al., 1961b, pp. 458-465
120	GSC63-15	Bio	370±16	Porphyritic granite	Mount Filton stock	67°42'N. 140°42'W.	GSC Paper 64-17 (Part1), p. 22-23
121	AK 51	Bio	353	Quartz monzonite	"	68°30'N. 138°01'W.	Baadsgaard, et al., 1961a, pp. 689-702
122	GSC63-16	Hb	355	Porphyritic granite	Mount Sedgwick stock	68°55'N. 139°07'W.	GSC Paper 64-17 (Part 1), p. 23
123	AK 110	Bio (chloritic)	95	Porphyritic granite	"	68°51'N. 139°07'W.	Baadsgaard et al., 1961b, pp. 458-465
124	GSC65-51	Whole R	237±47	Basalt	*	69°01'N. 141°05'W.	GSC Paper 66-17, p. 49
125	AK 105	Whole R	312	Syenite dike	*	65°19'N. 130°48'W. (D. of Mackenzie)	Baadsgaard et al., 1961b, pp. 458-465
				KENO HILL AREA, YUKON TERRITORY			
126	GSC65-46	Musc	84±8	Schist	Yukon Group	63°55'15"N. 135°26'W. (Galena Hill)	GSC Paper 66-17, p. 44
127	GSC65-47	Musc	93±12	Schist	Yukon Group	64°11'N. 135°21'30"W.	GSC Paper 66-17, p. 45
128	GSC65-48	Musc	101±6	Schist	Yukon Group	63°47'30"N. 135°41'45"W.	GSC Paper 66-17, pp. 45-46
129	GSC70-47	Musc	64±3 70±3	Schist	Yukon Group	63°23'N. 136°40'W.	GSC Paper 71-2, p. 29
130	GSC65-49	Bio	81±5	Quartz porphyry	*	63°51'05"N. 135°51'20"W.	GSC Paper 66-17, p. 47
131	GSC65-50	Bio	85±7	Quartz monzonite	*	63°29'N. 136°58'W.	GSC Paper 66-17, pp. 47-48
132	GSC62-78	Bio	102	Quartz monzonite	*	64°01'50"N. 135°25'50"W.	GSC Paper 63-17, p. 51
133	GSC62-80	Bio	106	Granodiorite	*	64°02'N. 135°50'W.	GSC Paper 63-17, p. 52
134	GSC62-81	Bio	81	Porphyritic quartz diorite	*	63°53'55"N. 134°46'15"W.	GSC Paper 63-17, pp. 52-53
				TOMBSTONE STOCK (SIMILAR AGE BODIES) NORTH OF TINTINA TRENCH, YUKON TERRITORY			
135 136	GSC66-58 GSC66-59	Bio Hb	91±5 80±13	Quartz monzonite	Tombstone stock	64°27'13"N. 138°33'00"W.	GSC Paper 67-2A, pp. 54-55
137	GSC62-79	Bio	134	Bio-feldspar porphyry	*	64°09'25"N. 137°40'00"W.	GSC Paper 63-17, p. 51

* See reference.

TABLE D-1 (cont'd) Published K-Ar ages referred to in this report.

Report No.	Reference Number and Mineral Dated		Age in m.y.	Rock Type	Unit	Location	Reference
ANVIL AREA, YUKON TERRITORY							
138	GSC61-43	Bio	100	Porphyritic dacite	*	62°31'N. 131°51'W.	GSC Paper 62-17, p. 27
139	GSC61-44	Bio	117	Porphyritic dacite	*	62°27'N. 132°18'W.	GSC Paper 62-17, p. 27
140	GSC65-44	Bio	86±6	Dacite	Tay Formation	62°15'30"N. 132°03'30"W.	GSC Paper 65-17, pp. 42-43
MOUNT SELOUS PLUTON							
141	GSC65-38	Bio	83±7	Quartz monzonite	Mount Selous Pluton	62°57'N. 132°30'W.	GSC Paper 66-17, p. 38
142	GSC65-39	Bio	81±10	Granodiorite	"	62°54'N. 132°27'W.	GSC Paper 66-17, p. 9
143	GSC65-40	Bio	74±7	Quartz monzonite	"	62°56'N. 132°27'W.	GSC Paper 66-17, pp. 38-40
144	GSC65-41	Bio	90±5	Quartz monzonite	Anvil Batholith	62°27'N. 133°27'30"W.	GSC Paper 66-17, p. 40
145	GSC65-42	Musc	79±6	Quartz monzonite	Anvil Batholith	62°17'N. 133°03'W.	GSC Paper 66-17, pp. 40-42
146	GSC65-43	Bio	87±5				
147	GSC67	Musc	99±5	Schist	thermal metamorphosed contact zone	62°22'N. 133°23'W.	GSC Paper 69-2A, pp. 27-28
148	GSC67-48	Bio	93±4				
149	GSC70-45	Musc	94±5	Granodiorite (sheared)	Anvil Batholith	62°17.5'N. 133°16.5'W.	GSC Paper 71-2, pp. 28-29
150	GSC70-46	Bio	94±5				
INSULAR BELT (51°-56°N.) - QUEEN CHARLOTTE ISLANDS, B.C.							
JURASSIC AGES (SYNTECTONIC AND POST-TECTONIC?)							
151	GSC70-1	Hb	143±8	Granodiorite (gneissic)	Kano Batholith	53°17.5'N. 132°38.5'W.	GSC Paper 71-2, p. 6
152	GSC67-20	Hb	142±14	Quartz diorite	San Christoval Batholith	52°34'30"N. 131°40'W.	GSC Paper 69-2A, p. 13
153	GSC70-3	Hb	156±10	Quartz diorite	Chinukudl Pluton	53°19'N. 131°58'W.	GSC Paper 71-2, p. 7
154	GSC66-14	Hb	142±37	Granodiorite	Burnaby Island Pluton	52°22'N. 131°15'W.	GSC Paper 67-2A, p. 19
MID-TERTIARY (POST-TECTONIC)							
155	GSC70-2	Bio	30±3	Granodiorite	Central Kano Batholith	53°13'N. 132°29'W.	GSC Paper 71-2, pp. 6-7
156	GSC67-16	Hb	26±6	Granodiorite	"	53°17'N. 132°26'W.	GSC Paper 69-2A, pp. 11-12
157	GSC67-17	Bio	29±2				
158	GSC67-18	Hb	38±2	Granite	Pocket Batholith	52°34'N. 131°48'W.	GSC Paper 69-2A, pp. 12-13
159	GSC67-19	Bio	39±2				
TERTIARY ACIDIC VOLCANIC ROCKS							
160	AK 378	Bio	62±3	Porphyry sill(?)	Massett formation	53°24.2' 132°23.1'	Mathews, 1964, pp. 465-468

* See reference.

TABLE D-1 (cont'd) Published K-Ar ages referred to in this report.

Report No.	Reference Number and Mineral Dated		Age in m.y.	Rock Type	Unit	Location	Reference
				COAST CRYSTALLINE BELT OF BRITISH COLUMBIA BETWEEN LATITUDES 52°N to 56°N			
161 162	GSC66-11 GSC66-12	Hb Bio	133±22 139±7	Quartz diorite	*	53°09'N 129°35'W.	GSC Paper 67-2A, p. 16
163	GSC67-24	Bio	104±4	Quartz diorite	*	53°15'N. 129°35'W.	GSC Paper 69-2A, p. 15
164	GSC67-23	Bio	115±6	Quartz monzonite	*	53°03'N 129°27'W.	GSC Paper 69-2A, pp. 14-15
165 166	GSC64-5 GSC64-6	Bio	103±6 111±6	Granodiorite	*	53°31'N. 130°01'W.	GSC Paper 65-17, pp. 10-11
167 168	GSC66-17 GSC66-16	Bio Hb	88±5 87±11	Granodiorite	*	52°34'N. 128°41'W.	GSC Paper 67-2A, p. 20
169	GSC67-21	Bio	84±4	Granodiorite	Melville Isl. stock	54°24'N. 130°44'W.	GSC Paper 69-2A, pp. 13-14
170 171	GSC66-4 GSC66-5	Bio Hb	96±5 101±15	Granodiorite	*	54°29'N. 130°57'W.	GSC Paper 67-2A, p. 12
172	GSC67-26	Bio	109±5	Granodiorite	*	52°45'30"N. 129°22'30"W.	GSC Paper 69-2A, pp. 16-17
173 174	GSC67-27 GSC67-28	Hb Bio	100±6 90±4	Gabbro	*	52°06'30"N. 128°17'00"W.	GSC Paper 69-2A, p. 17
175 176	GSC67-29 GSC67-30	Hb Bio	87±5 81±4	Andesite	*	52°13'00"N. 127°50'30"W.	GSC Paper 69-2A, pp. 17-18
177	GSC64-11	Bio	67±5	Quartz diorite	*	53°28'N. 128°51'W.	GSC Paper 65-17, pp. 13-14
178 179	GSC66-13 GSC66-12	Bio Hb	70±4 87±15	Granodiorite	Ecstall Pluton	53°41'N. 129°30'W.	GSC Paper 67-2A, p. 17-18
180 181	GSC67-33 GSC67-34	Hb Bio	79±5 75±5	Granodiorite	*	52°10'N. 128°00'W.	GSC Paper 69-2A, pp. 20-21
182	GSC65-31	Bio	64±8	Quartz diorite	*	54°13'N. 130°04'W.	GSC Paper 66-17, pp. 32-33
183	GSC64-8	Bio (-4+14 mesh)	77±5	Quartz diorite	*	52°32'N. 128°02'W.	GSC Paper 65-17, p. 11
184	GSC64-7	Bio (-100+150 mesh)	77±5	Quartz diorite	*	52°32'N. 128°01'55"W.	GSC Paper 65-17, pp. 11-12
185	GSC67-25	Bio	49±4	Quartz diorite	*	53°16'N. 128°16'W.	GSC Paper 69-2A, p. 16
186	GSC64-12	Bio	48±5	Biotite schist	*	53°38'N. 128°52'W.	GSC Paper 65-17, p. 14
187	GSC66-15	Bio	47±4	Granodiorite	*	54°54'N. 129°25'W.	GSC Paper 67-2A, pp. 19-20
188 189	GSC66-9 GSC66-8	Bio Hb	44±5 49±7	Quartz diorite	Quottoon Pluton	54°35'N. 130°11'W.	GSC Paper 67-2A, p. 15
190 191	GSC66-6 GSC66-7	Bio Hb	50±5 48±9	Quartz diorite	Quottoon Pluton	54°21'N. 129°52'W.	GSC Paper 67-2A, pp. 13-14
192	GSC65-29	Bio	43±5	Quartz diorite	*	54°17'N.	GSC Paper 66-17, pp. 30-31
193	GSC65-30	Bio	44±4	Granodiorite	Alastair Lake Pluton	54°05'N. 129°01'W.	GSC Paper 66-17, pp. 31-32
194	GSC65-32	Bio	46±10	Granodiorite	*	54°38'N. 129°02'W.	GSC Paper 66-17, pp. 33-34

* See reference.

TABLE D-1 (cont'd) Published K-Ar ages referred to in this report.

Report No.	Reference Number and Mineral Dated		Age in m.y.	Rock Type	Unit	Location	Reference
195	GSC64-9	Bio	45±12	Quartz monzonite	Labouchere Pluton	55°13'N. 129°51'W.	GSC Paper 65-17, p. 12
196	GSC65-19	Bio	47±5	Granodiorite	*	52°49'N. 126°38'W.	GSC Paper 66-17, p. 23
197	GSC65-28	Bio	70±14	Granodiorite	War Drum Pluton	52°07'N. 126°18'W.	GSC Paper 66-17, p. 30
198	GSC64-10	Bio	57±6	Quartz monzonite	Labouchere Pluton	52°25'N. 127°14'W.	GSC Paper 65-17, p. 13
199	GSC66-20	Musc	51±6	Quartz monzonite	*	52°25'N. 127°14'W.	GSC Paper 67-2A, pp. 22-23
				BERG "Cu-Mo" PROPERTY			
200	NC67-8	Bio	54±3	Quartz diorite	*	53° 127°	White, Harakal and Carter (1968)
201	NC67-12	Whole R	53±3	Hornfels	*	"	"
202	NC67-10	Bio	48±2	Quartz monzonite (porphyry)	*	"	"
203	NC67-9	Bio	44±2	Latite porphyry dike	*	"	"
204	GSC67-22	Bio	37±2	Pegmatite	*	53°47'N. 129°02'W.	GSC Paper 69-2A, p. 14
205	GSC67-31	Whole R	14.5±1	Gabbro	*	52°09'15"N. 128°04'00"W.	GSC Paper 69-2A, p. 18
206	GSC67-32	Whole R	12.5±2.7	Diabase	*	52°12'15"N. 128°08'00"W.	GSC Paper 69-2A, pp. 19-20
207	NC67-15	Bio	179±8	Granodiorite	*	Lucky Ship (54°N, 127°W.)	White, Harakal and Carter (1968)
208	Serb Creek	Bio	41±3	Porphyritic Quartz monzonite	*	54°N. 127°W. N.W.	Amax Expl. Ltd., Det. by Geochron Labs., Inc.
				INTERMONTANE BELT 52° - 56°N.			
				TOPLEY INTRUSIONS (see Table)			
209	AK23	Bio	163	Granite	Topley	54°04'N. 124°41'W.	Baadsgaard et al., 1961a
210	GSC61-34	Bio	63	Diorite (non-folicated)	*	53°42'N. 124°02'W.	GSC Paper 62-17, p. 21
211	GSC61-35	Bio	178	Diorite	Topley	54°31'N. 124°52'W.	GSC Paper 62-17, p. 22
212	GSC61-36	Bio	138	Granite	Topley	54°05'N. 125°02'W.	GSC Paper 62-17, p. 22
213	GSC61-37	Bio	154	Granite	Topley	54°02'N. 125°02'W.	GSC Paper 62-17, p. 22
				GLACIER GULCH MOLYBDENUM DEPOSIT - SMITHERS, B. C.			
214	GSC67-35	Bio	67±5	Quartz monzonite (porphyry)	*	54°49'30"N. 127°18'W. 2,782-2,851' DDH28*	GSC Paper 69-2A, p. 21
215	GSC67-36	Bio	60±5	Quartz latite (porphyry)	*	54°49'30"N. 127°18'W.	GSC Paper 69-2A, p. 22

* See reference.

TABLE D-1 (cont'd) Published K-Ar ages referred to in this report.

Report No.	Reference Number and Mineral Dated		Age in m.y.	Rock Type	Unit	Location	Reference
216	GSC67-37	Bio	63±4	Qtz-Bio veinlets	*	54°49'30"N. 127°18'W.	GSC Paper 69-2A, pp. 22-23
217	GSC67-38	Hb	65±6	Qtz-Hb-Sulphide veinlets	*	54°49'30"N. 127°18'W.	GSC Paper 69-2A, p. 23
218	NC67-41	Bio	69±3	Bio in quartz molybdenum seam	*	*	White et al., 1968
				BOSS MOUNTAIN MINE, B. C.			
219	BM65-1	Bio	105±4	Quartz diorite	*	5045 Level	White et al., 1968
220	BM65-3	Bio	98±4	Altered dike	*	"	White et al., 1968
221	BM65-4	Bio	104±4	Dike fragment in breccia ore	*	"	White et al., 1968
				TAKOMKANE BATHOLITH - CARIBOO DISTRICT, B. C.			
222	GSC62-64	Bio	187	Granodiorite	Takomkane Batholith	52°06'00"N. 120°55'03"W.	GSC Paper 63-17, p. 42
				CENOZOIC VOLCANIC ROCKS			
223	AK302	Bio	53±2	Dacite	T-Allin	54°03.5"N. 125°57.1"W.	Mathews, 1964, pp. 465-468
224	AK395	Bio	48±2	*	Endako Group	54°07.3'N. 125°19.0'W.	"
				SAM GOOSLEY PROPERTY, CENTRAL B.C.			
225	NC69-6		56.2±3	Biotite granitic stock	*	54°11'N. 126°16'W.	Church 1970, (G.E.M.) pp. 119-125
226	NC69-7		48.8±3	Syenomonzonite	*	54°11'N. 126°16'W.	"
				<u>OMINECA BELT 52° - 56°</u>			
				WOLVERINE METAMORPHIC COMPLEX			
227	GSC70-40	Bio	44±4	Gneiss	Wolverine Complex	55°07'35"N. 123°29'15"W.	GSC Paper 71-2, pp. 23-24
228	GSC70-41	Musc	46±3	Gneiss	Wolverine Complex	55°07'35"N. 123°29'15"W.	GSC Paper 71-2, p. 24
229	GSC70-43	Musc	40±2	Granite greisen	Wolverine Complex	55°07'35"N. 123°29'15"W.	GSC Paper 71-2, pp. 24-25
230	GSC70-42	Bio	43±4	Gneiss	Wolverine Complex	55°32'10"N. 123°52'40"W.	GSC Paper 71-2, p. 24
231	GSC70-44	Bio	45±2	Amphibolite	Wolverine Complex	55°32'10"N. 123°52'40"W.	GSC Paper 71-2, p. 25
232	GSC70-37	Musc	45±3	Schist	Wolverine Complex	55°23'30"N. 123°39'50"W.	GSC Paper 71-2, p. 22
233	GSC70-38	Musc	50±6	Pegmatitic granite	Wolverine Complex	55°23'30"N. 123°39'50"W.	GSC Paper 71-2, p. 23

* See reference.

TABLE D-1 (cont'd) Published K-Ar ages referred to in this report.

Report No.	Reference Number and Mineral Dated		Age in m.y.	Rock Type	Unit	Location	Reference
234	GSC70-39	Musc	47±3	Gneiss	Wolverine Complex	55°19'N. 123°30'W.	GSC Paper 71-2, p. 23
235 236	GSC61-31 GSC61-32	Musc Bio	75 77	Schist	Wolverine Complex	55°23'30"N. 123°39'50"W.	GSC Paper 62-17, p. 19-20
237	GSC61-30	Bio	69	Gneiss	Wolverine Complex	55°33'N. 123°56'W.	GSC Paper 62-17, p. 19
238	GSC61-33	Musc	71	Gneiss	Wolverine Complex	55°19'N. 123°30'W.	GSC Paper 62-17, p. 20-21
239	GSC60-23	Musc	22	Pegmatitic granite	*	55°24'N. 123°39'W.	GSC Paper 61-17, p. 14
240	GSC60-24	Bio	29	Marble	*	55°27'N. 123°34'W.	GSC Paper 61-17, p. 14
241	GSC62-67	Bio	78	Granite	*	55°5'20"N. 123°18'50"W.	GSC Paper 63-17, pp. 43-44
				MALTON COMPLEX			
242 243	GSC70-16 GSC70-17	Musc Bio	60±3 66±3	chips of gneiss and schist	Malton gneiss	55°25'N. 118°42'W.	GSC Paper 71-2, p. 13
244	GSC70-18	Bio	57±3	Granite	Malton gneiss	52°22.5'N. 118°38.5'W.	GSC Paper 71-2, p. 13-14
245	GSC67-43	Bio	53±4 59±5	Gneiss	Malton gneiss	52°36'00"N. 119°01'20"W.	GSC Paper 69-2A, p. 25
246	GSC67-44	Hb	114±12	*	*	*	GSC Paper 69-2A, p. 26
247	GSC65-24	Bio	72±5	Gneiss	*	52°38'N. 118°59'W.	GSC Paper 66-17, pp. 26-27
248	GSC67-40	Bio	36±3	Quartz diorite	*	54°06'N. 122°22'W.	GSC Paper 69-2A, p. 24
249	GSC67-41	Bio	93±4	Quartz monzonite	*	53°38'N. 122°38'W.	GSC Paper 69-2A, pp. 24-25
				MISINCHINKA SCHIST			
250 251	GSC62-65 GSC62-66	Bio Musc	143 136	Schist	Misinchinka schist	55°10'49"N. 122°45'55"W.	GSC Paper 63-17, pp. 42-43
				PRINCE GEORGE QUESNEL AREA*			
252	GSC66-21	Bio	105±6	Granite boulder	*	53°42'N. 122°41'W.	GSC Paper 67-2A, pp. 23-24
253	GSC66-22	Bio	98±5	Quartz monzonite	*	53°41'N. 122°41'W.	GSC Paper 67-2A, pp. 23-24
254	GSC66-23	Bio	104±5	Quartz monzonite	*	53°18'N. 122°22'W.	GSC Paper 67-2A, p. 24
255	GSC66-24	Bio	107±6	Quartz monzonite	*	53°25'N. 122°14'W.	GSC Paper 67-2A, p. 24-25
256	GSC66-25	Hb	176±20	Granite	*	53°44'N. 122°20'W.	GSC Paper 67-2A, pp. 25-26
257	GSC66-26	Bio	106±6	Granodiorite	*	52°04'N. 122°35'W.	GSC Paper 67-2A, p. 26

* See reference.

TABLE D-1 (cont'd) Published K-Ar ages referred to in this report.

Report No.	Reference Number and Mineral Dated		Age in m.y.	Rock Type	Unit	Location	Reference
				MIETTE GROUP			
258	GSC66-47	Bio	111±5	Quartzose phyllite	Miette Group	52°32'34"N. 118°41'56"W.	GSC Paper 67-2A, pp. 43-44
				KAZA GROUP			
259	GSC64-4	Musc	85±15	Granite pegmatite	Kaza Group	52°54'N. 119°31'W.	GSC Paper 65-17, p. 9
				CARIBOO GROUP			
260	GSC64-13	Bio	51±6	Quartz monzonite	Cariboo Group	52°21'40"N. 119°39'00"W.	GSC Paper 65-17, pp. 15-16
261	GSC64-14	Musc	54±6				
262	GSC63-6	Bio	143±14	Granodiorite	*	52°34'00"N. 120°02'30"W.	GSC Paper 64-17, Part 1, pp. 15-16
				INSULAR BELT - VANCOUVER ISLAND			
263	K-Ar-1652	Phlogopite	181±8 178±8	Skarn	*	Empire Dev.& Coast Copper	Carson et al., 1971
				BRYNNOR MINE			
264	GSC64-2	Bio	167±10	Granodiorite	*	49°03'N. 125°25'W.	GSC Paper 65-17, pp. 7-8
265	GSC64-3	Bio	121±35	Feldspar porphyry dyke	*	49°03'N. 125°26'W.	GSC Paper 65-17, pp. 8-9
266	K-Ar-1716 (GSC70-1716)	Bio	47±3	"	*	*	Carson et al., 1971
				UCONA BATHOLITH			
267	GSC65-18	Bio	166±8	Granodiorite	Ucona Batholith	49°43'30"N. 125°56'25"W.	GSC Paper 66-17, p. 22
268	GSC65-17	Bio	162±9	Granodiorite	Ucona Batholith	49°49'15"N. 125°58'25"W.	GSC Paper 66-17, p. 21
				NIMPKISH IRON MINE			
269	GSC65-14	Bio	151±14	Granodiorite	Nimpkish Batholith	50°16'35"N. 126°51'21"W.	GSC Paper 66-17, pp. 18-20
270	GSC65-15	Hb	143±60				
271	GSC66-27	Bio	150±8 152±7	Quartz monzonite	Nimpkish Batholith	50°22'15"N. 126°45'40"W.	GSC Paper 67-2A, p. 27
				ZEBALLOS IRON MINE			
272	GSC66-28	Phlogopite	148±8	Skarn	*	50°02'58"N. 126°49'56"W.	GSC Paper 67-2A, p. 28
				TEXADA MINES			
273	K-Ar-1698	Hb	165±9	Granodiorite	Gilles stock	49°42'N. 124°33'W.	Carson et al., 1971

* See reference.

TABLE D-1 (cont'd) Published K-Ar ages referred to in this report.

Report No.	Reference Number and Mineral Dated		Age in m.y.	Rock Type	Unit	Location	Reference
274	GSC67-39	Bio	120±6	Granodiorite	Pocahontas Stock	49°43'25"N. 124°24'30"W.	GSC Paper 69-2A, pp. 23-24
275	K-Ar-1541(2)	Bio	110±5	Granodiorite	Pocahontas Stock		Carson et al., 1971
276	K-Ar-1541A	Hb	114±15				
277	K-Ar-1778A	Bio	111±6	Granodiorite	East Stock	*	Carson et al., 1971
278	K-Ar-1778	Bio	106±4				
279	K-Ar-1777	Hb	155±8				
280	GSC66-33	Bio	160±8	Granodiorite	*	49°05'15"N. 124°16'15"W.	GSC Paper 67-2A, pp. 32-33
281	GSC66-34	Whole R	163±20	Schist	Sicker Group	48°52'00"N. 123°47'30"W. (Twin J)	GSC Paper 67-2A, pp. 33-34
282	GSC65-11	Bio	48±12	Quartz diorite	Catface Stock	49°14'35"N. 125°57'00"W. (Catface)	GSC Paper 66-17, p. 15
283	GSC66-31	Bio	50±5	Granodiorite	*	49°09'25"N. 125°55'30"W.	GSC Paper 67-2A, pp. 30-31
284	GSC66-32	Bio	59±3	Quartz monzonite	*	49°01'25"N. 125°29'10"W. (Brynnor Mine)*	GSC Paper 67-2A, pp. 31-32
285	GSC70-36	Hb	44±6	Orebody	*	48°27'N. 124°03'W. (Sunro Mine)	GSC Paper 71-2, p. 22
286	GSC65-13	Bio	39±10	Quartz diorite	*	48°26'55"N. 124°00'00"W. (Faith Lake)	GSC Paper 66-17, pp. 17-18
287	GSC65-12	Bio	38±4	Quartz diorite	Zeballos Batholith	50°02'07"N. 126°47'04"W.	GSC Paper 66-17, pp. 16-17
288	GSC66-29	Bio	39±7	Quartz diorite	*	49°39'12"N. 125°24'41"W. (Forbidden Plateau)	GSC Paper 67-2A, p. 29
289	GSC66-30	Bio	35±6	Quartz diorite	Mount Washington stock	49°46'04"N. 125°17'24"W. (Mt. Washington Mine)	GSC Paper 67-2A, pp. 29-30
290	GSC69-1653	Bio	38±2	Quartz diorite	*	49°01'N. 124°39'W. (Corrigan Creek)	Carson, D.J., 1969, p. 518

COAST CRYSTALLINE BELT AND CASCADE MOUNTAINS - 49° - 52°N.

CHILLIWACK BATHOLITH

Report No.	Reference Number	Mineral Dated	Age in m.y.	Rock Type	Unit	Location	Reference
291	10	Bio	29±1	Gabbro	Chilliwack Batholith	49°03'N. 121°19'W.	Richards & White, 1970, p. 1206
292	11	Bio	28±1	Quartz diorite	"	49°05'N. 121°26'W.	"
293	12	Bio	26±1	Quartz monzonite	"	49°06'N. 121°27'W.	"
294	13	Bio	26±1	Quartz monzonite	"	49°02'N. 121°23'W.	"
295	14	Bio	26±1	Quartz monzonite	"	49°02'N. 121°23'W.	"
296	15	Mafic conc.	24±1	Quartz diorite	Williams Peak Stock	*	"

* See reference.

TABLE D-1 (cont'd) Published K-Ar ages referred to in this report.

Report No.	Reference Number and	Mineral Dated	Age in m.y.	Rock Type	Unit	Location	Reference
297	16a b	Bio Bio	24±1 24±1	Quartz diorite	Hicks Stock	*	Richards & White, 1970, p. 1206
298	17	Bio	21±1	Granophyre	Mount Barr Batholith	49°19'N. 121°27'W.	"
299	18	Bio	18±1	Grano diorite	Mount Barr Batholith	49°14'N. 121°35'W.	"
300	19	Bio	16±1	Quartz monzonite	Mount Barr Batholith	49°15'N. 121°33'W.	"
301	AK-31	Bio	18	Quartz diorite	Mount Barr Batholith	49°15'N. 121°40'W.	Baadsgaard, 1961
302	AK-45	Bio	18	Quartz diorite	Mount Barr Batholith,	49°14'N. 121°40'W.	"
303		Bio	32		Chilliwack Batholith	48°38'N. 121°21'W.	UBC Guidebook, 1968
304		Bio	23	Granodiorite	*	49°20'N. 121°38'W.	Richards, 1971
305			20	Quartz diorite	Cascade Pass stock	49°30'N. 121°02'W.	Misch, 1966
306	GSC65-8	Bio	39±4	Granite	*	49°30'30"N. 121°10'W.	GSC Paper 66-17, p. 11
307	GSC65-26	Bio	40±5	Dacite	*	51°23'N. 120°58'W.	GSC Paper 66-17, p. 28
				HELL'S GATE STOCK			
308	AK-24	Bio	35	Granodiorite	Hell's Gate	49°47'N. 121°27'W.	Baadsgaard, 1961
309	GSC70-1736	Hb	40		Hell's Gate	49°46'N. 121°26'W.	reported by Richards, 1971
				HOPE PLUTONIC COMPLEX			
310	9	Hb	35±2	Quartz diorite	Silver Creek Stock	49°23'N. 121°20'W.	Richards & White, 1970, p. 1206
				YALE INTRUSIONS			
311	8	Bio	35±2	Quartz diorite	Ogilvie Stock	49°20'N. 121°27'W.	Richards & White, 1970, p. 1206
312	7	Bio	41±2	Quartz monzonite	Coquihalla Stock	49°22'N. 121°22'W.	"
313	4a b	Bio Bio	59±3 59±3	Granodiorite	Berkey Creek	49°19'N. 121°21'W.	"
				CUSTER RIDGE MICA-HORNBLENDE PERIDOTITE			
314	6	Hb	44±3	Hbite	Skagit Mica Peridotite	49°01'N. 121°18'W.	Richards & White, 1970, p. 1206
315	GSC70-1737	Bio	44			49°46'N. 121°26'W.	

*See reference.

TABLE D-1 (cont'd) Published K-Ar ages referred to in this report.

Report No.	Reference Number and Mineral Dated		Age in m.y.	Rock Type	Unit	Location	Reference
316	GSC70-1728	Bio	70			49°50'N. 121°41'W.	unpublished
317	GSC70-1731	Hb	72			49°55'N. 121°34'W.	"
318	GSC70-1734	Hb	73			49°41'N. 121°29'W.	"
319	GSC70-1735	Bio	74			49°41'N. 121°29'W.	"
320 321		Hb Bio	80 80	Quartz diorite	*	49°23'N. 121°28'W.	Richards, 1971
322		Bio	82	Quartz diorite	*	49°22'N. 121°29'W.	Richards, 1971
323	GSC65-10	Bio	84±6	Granodiorite	Dewdney Creek Group	49°12'N. 121°05'W.	GSC Paper 66-17, pp. 13-14
324	GSC65-9	Bio	98±6	Granodiorite	*	49°16'45"N. 120°46'W.	GSC Paper 66-17, pp. 12-13
325		Bio	92	Granodiorite	*	49°14'N. 123°08'W.	White, 1968
326		Bio	95	Quartz diorite	*	49°51'N. 123°11'W.	"
327		Hb	97	Quartz diorite	*	49°43'N. 123°06'W.	"
328	KA-126	Bio	97	Granodiorite	*	49°22'N. 123°16'W.	Baadsgaard, 1961
329		Bio	102	Quartz diorite	*	49°21'N. 121°34'W.	Richards, 1971
330	GSC66-47	Bio	111±5	Quartzose Phyllite	Miette Group	52°32'34"N. 118°41'56"W.	GSC Paper 67-2A, p. 43-44
331		Bio	158	Quartz diorite		49°54'N. 123°07'W.	White, 1968
				SPUZZUM INTRUSIONS			
332	1a b	Bio Bio	103±5 103±5	Quartz diorite		*	Richards & White, 1970, p. 1206
333	2a	Bio	79±4	Quartz diorite		*	"
334	3	Bio	77±3	Quartz diorite		*	"
335 336	* *	Hb Bio	76 76	Quartz diorite		49°36'N. 121°27'W.	McTaggart & Thompson, (1967)
337		Bio	253	*	Orcas Island	48°39'N. 12 °01'W.	UBC Guidebook, 1968
338		Whole R	258	*	Vedder Mountain	49°04'N. 122°03'W.	Ross in UBC Guidebook, 1968

* See reference.

TABLE D-1 (cont'd) Published K-Ar ages referred to in this report.

Report No.	Reference Number and Mineral Dated		Age in m.y.	Rock Type	Unit	Location	Reference
				INTERMONTANE BELT - 52° - 49°			
				TERTIARY AGES			
339	AK-116		10±2	Basalt	*	50°58.5'N. 120°58.8'W.	Mathews, 1964
340	AK-268		12±2	Basalt	*	51°54.9'N. 123°01.9'W.	"
341	AK-100		13±2	Basalt	*	51°53.2'N. 122°49.5'W.	"
342	GSC65-26	Bio	40±5	Dacite	*	51°23'N. 120°58'W.	GSC Paper 66-17, pp. 28-29
343	AK-117	Bio	45±2	Trachyte	Kamloops Group	50°43'N. 120°49'W.	Mathews, 1964
344		Bio	46	Quartz diorite	Castle Peak Stock	48°59'N. 120°52'W.	GSC Paper 67-2A, p. 39
345	AK-149		47±2	Breccia	Kamloops Group	50°08.3'N. 119°37.5'W.	Mathews, 1964
346		Bio	47	Basalt	*	49°29'N. 120°46'W.	UBC Guidebook, 1968 (map)
347	AK-99	Bio	48±2	Volcanic ash	Princeton Group	49°27'N. 120°32'W.	Mathews, 1964
348		Bio	49	Basalt	*	50°48'N. 121°10'W.	Mathews, 1964
349	AK-118	Bio	49±2	Dolerite	Kamloops Group	50°44'N. 120°33'W.	"
350		Bio	50	*	*	49°26'N. 120°30'W.	UBC Guidebook, 1968 (map)
351		Bio	50		*	49°14'N. 120°36'W.	"
352	GSC69-1444	Bio	64	*		51°28'N. 122°58'W.	unpublished
353	AK-625	Andesine	50	Hornblende-andesite	*	Sunday Summit	Hills & Baadsgaard, 1967
354	AK-626	Hb	48	Andesite	*	"	"
355	AK-627	Hb	52	Andesite	*	"	"
356	AK-628	Bio	50	Ash	*	McAbee	"
357	AK-629	Andesine	48	Ash	*	"	"
358	AK-631	Glass shards	22	Bentonite	*	Quilchena	"
359	AK-632	Bio	50	Rhyolite Lava	*	Allenby	"
360	AK-633	Andesine	49	"	*	"	"
361	AK-634	Sanidine (fine)	47	Lapilli Tuff	*	Sunday Creek	"
362	AK-635	Sanidine (coarse)	50	Lapilli Tuff	*	Sunday Creek	"
363	AK-636	Andesine	51	Ash	*	McAbee	"
364	AK-637	Bio	57 56	Ash	*	"	"
365	AK-638	Sanidine	67 56	Ash	*	"	"

* See reference.

TABLE D-1 (cont'd) Published K-Ar ages referred to in this report.

Report No.	Reference Number and Mineral Dated		Age in m.y.	Rock Type	Unit	Location	Reference
366	AK-640	Oligo-clase	51	Ash	*	Battle Bluff	Hills & Baadsgaard, 1967
367	AK-641	Sanidine	50	Ash	*	"	"
368	AK-642	Bio	50	Ash	*	"	"
369	AK-656	Bio	48	Ash	*	"	"
370	AK-643	Bio	47	Bentonite	*	Collins Gulch	"
371	AK-630	Sanidine	79*	Bentonite	*	Quilchena	"
372	GSC67-42	Hb	73±4	Granodiorite	China Head Mtn. stock	51°10'N. 122°23'W.	GSC Paper 69-2A, p. 25
				MAGGIE MINE (Cu-Mo Porphyry)			
373	MM16	Whole R	61.2±2	Biotite porphyry	*	50°52.3-55.5'N. 121°23.1-23.7'W. (Maggie)	McMillian, 1970, (G.E.M.) pp. 324-325
				Unmineralized volcanic strata that unconformably overlie mineralized Nicola rocks - Craigmont			
374 375	GSC61-29	Bio	80 (108)*	Lava	*	50°12'N. 120°55'W.	GSC Paper 62-17, p. 19 unpublished
376	GSC65-27	Bio	100±6	Quartz diorite	boulder in conglomerate	51°11'N. 122°35'W.	GSC Paper 66-17, p. 29
377	GSC65-25	Bio	166±11	Quartz diorite	*	51°15'N. 120°58'W.	GSC Paper 66-17, p. 28
378	GSC65-23	Bio	105±9	Quartz monzonite	*	51°41'20"N. 120°07'25"W.	GSC Paper 66-17, p. 26
				EAGLE GRANODIORITE			
379	GSC65-9	Bio	98±6	Granodiorite	*	49°16'45"N. 120°46'W.	GSC Paper 66-17, pp. 12-13
380	GSC62-56	Bio	143	Granodiorite	*	49°31'N. 120°55'W.	GSC Paper 63-17, p. 38
381	E-1a b	Bio Bio	103±1.6 106.2±1.7	"	*	*	Roddick, 1970
382	E-2-1 2	Bio Bio	99.1±1.6 96.4±1.5	"	*	*	"
383	E-3	Musc Musc	71.7±1.2 71.8±1.2	Pegmatite	*	*	"
384	E-4	Bio	85.4±1.4	Granodiorite	*	*	"
385	E-5	Bio	102.±1.6	"	*	*	"
386	E-6	Hb	104.5±1.7	"	*	*	"
387	E-7	Bio	106.2±1.7	"	*	*	"

*See reference.

TABLE D-1 (cont'd) Published K-Ar ages referred to in this report.

Report No.	Reference Number and	Mineral Dated	Age in m.y.	Rock Type	Unit	Location	Reference
388	E-8-1	Hb	111.4±1.8 111.7±1.7	Granodiorite	*	*	Roddick, 1970
	2	Bio	112.1±1.8	"	*	*	"
389	GSC65-22 (see 378)	Bio	140±9	Quartz monzonite	*	51°49'N. 120°03'30"W.	GSC Paper 66-17, p. 25
390	GSC65-25	Bio	166±11	Quartz diorite	*	51°15'N. 120°58'W.	GSC Paper 66-17, p. 28
				IRON MASK BATHOLITH			
391	GSC66-41	Bio	176±8	Pegmatite	Iron Mask	50°35'N. 120°21'W. (Fargo Mineral Claim)	GSC Paper 67-2A, p. 39
				BRENDA MINES (see Oriel 1972)			
392	W67-3	Bio Hb	148±6 168±8	Granodiorite	Okanagan Batholith	Brenda Pit	White et al. 1968
393	W67-4	Bio Hb	148±5 166±8	Granodiorite	Okanagan Batholith	Brenda Pit	"
				SIMILKAMEEN BATHOLITH			
394	H-1	Bio	154.5±2.4	Granodiorite	Similkameen	*	Roddick, 1970
395	H-2	Hb Bio	152.2±2.4 149.5±2.3	"	"	*	"
396	H-3	Bio	156.9±2.4	"	"	*	"
397	H-4	Bio	156.4±2.4	"	"	*	"
398	H-10	Bio	156.1±2.4	"	"	*	"
				HEDLEY COMPLEX			
399	H-6 H-6a	Hb Hb	170.7±2.7 179.5±3.7	Diorite	Hedley Complex	*	Roddick, 1970
400	H-8	Hb	183.2±2.9	Diorite	"	*	"
401	H-11L	Hb	170.8±2.6	Diorite	"	*	"
402	H-11H	Hb	176.2±2.9	Diorite	"	*	"
403	H-12	Hb	188.3±3.0	Gabbro	"	*	"
404	H-14	Hb	190.2±3.0	Diorite	"	*	"
				TULAMEEN COMPLEX			
405	GSC62-55	Bio	186	Pyroxenite	Tulameen	49°34'N. 120°54'W.	GSC Paper 63-17, p. 38
406	T-1a	Bio	68.0±1.2	Pyroxenite	"	*	Roddick, 1970
407	1B	Bio	81.9±1.3	Pyroxenite	"	*	Roddick & Farrar, 1971
405a	GSC62-57	Hb	286	Pyroxenite	"	49°26'N. 120°48'W.	GSC Paper 63-17, p. 39

* See reference.

TABLE D-1 (cont'd) Published K-Ar ages referred to in this report.

Report No.	Reference Number and Mineral Dated		Age in m.y.	Rock Type	Unit	Location	Reference
408	2H-1	Hb	192.5±2.9	Diorite	Tulameen	*	Roddick & Farrar, 1971
	2	Hb	191.5±2.9				
	3	Hb	191.6±2.9				
409	3B	Bio	127.4±2.0	Diorite	"	*	"
410	5H-1	Hb	201.5±3.0	Hornblendite	"	*	"
	2	Hb	200.4±3.0				
	3	Hb	196.6±3.0				
	4	Hb	199.1±3.0				
411	7W	Whole R	178.1±7.2	Amphibolite	"	*	"
412	8B	Bio	151.5±2.3	Hb clinopyroxenite	"	*	"
413	8W	Whole R	198.2±3.2		"	*	"
414	8P	Pyrox	922.3±13.2	Hb clinopyroxenite	"	*	"
415	8H-1	Hb	206.4±3.1	"	"	*	"
	-2	Hb	203.5±3.1				
416	9H	Hb	209.6±3.5	"	"	*	"
417	10B	Bio	171.5±2.6	Pyroxenite	"	*	"

COPPER MOUNTAIN, B.C.

Report No.	Reference Number and Mineral Dated		Age in m.y.	Rock Type	Unit	Location	Reference
418	CM-ore-65	Bio	194±7	Biotite veinlet with chalcopyrite	Wolf Creek	49°19'N. 120°32'W.	Sinclair & White, 1968
419	CM-F20a-65	Bio	199±7	Monzonite	Copper Mtn. Stock	"	"
420	CM-AL7-65	Bio	194±8	Monzonite	"	"	"
421	CM-E2a-65	Bio	151±6	Diorite hydrothermally altered	" *	"	"
		Clino-pyroxene	150±9				
422	CM-12-65	Bio	182±8	Gabbro	"	"	"
423	VP-69KA-1	Bio	194±8	Latite porphyry	Lost Horse	49°19'N.* 120°32'W.	Preto et al., 1971
424	VP-69KA-2	Bio	197±8	Diorite	Smelter Lakes	"	"
425	VP-69KA-3	Bio	200±8	Diorite	"	"	"
426	VP-69KA-4	Bio	101±4	Quartz monzonite	Verde Creek	"	"
427	VP-69KA-5	Bio	98±4	Quartz monzonite	Verde Creek	"	"
428	VP-69KA-6	Bio	181±7	Diorite	Voigt	"	"
429	VP-69KA-7	Bio	194±7	Diorite	Voigt	"	"
430	VP-69KA-8	Bio	194±8	Micromonzonite porphyry	Lost Horse	"	"
431	VP-69KA-9	Bio	197±8	Latite porphyry	Lost Horse dike	"	"
432	VP-69KA-10	Bio	195±8	Micromonzonite porphyry	Lost Horse	"	"
433	VP-69KA-13	Bio	189±8	Biotite-sulphide pegmatite vein		"	"

* See reference.

TABLE D-1 (cont'd) Published K-Ar ages referred to in this paper.

Report No.	Reference Number and Mineral Dated		Age in m.y.	Rock Type	Unit	Location	Reference
				GUICHON BATHOLITH - HIGHLAND VALLEY, B. C.			
434	1DB70	Sericite	196±6	Quartz diorite	Bethsaida	*	Blanchflower, 1971
435	2DB70	Sericite	195±6	"	"	*	"
436	3DB70	Bio	189±6	"	"	*	"
437	4DB70	Bio	203±6	"	"	*	"
438	5DB70	Bio	198±6	"	"	*	"
439	K63-240	Bio	199±8	Breccia	Iona Breccia	*	White in Northcote, 1969
440	GSC66-37	Bio	184±8	Quartz diorite	Guichon Batholith	50°29'20"N. 120°51'55"W.	GSC Paper 67-2A, pp. 35-36
441	GSC66-38	Hb	189±20	Quartz diorite	"	50°29'20"N. 120°51'55"W.	GSC Paper 67-2A, pp. 36-37
442 443	GSC66-40 GSC66-39 (Replaces GSC63-3)*	Hb Bio	187±27 197±10	Quartz diorite	"	50°34'45"N. 121°13'25"W.	GSC Paper 67-2A, pp. 37-38
444	AK-44	Bio	186	Quartz diorite	"	50°29'N. 120°58'W.	Baadsgaard, 1961
445	GSC62-63	Bio	224**	Granodiorite	"	50°29'10"N. 121°03'20"W.	GSC Paper 63-17, pp. 41-42
446	GSC62-59	Bio	227**	Quartz diorite	"	50°29'25"N. 120°55'05"W.	GSC Paper 63-17, p. 40
447	GSC62-61	Bio	230** 237**	Quartz diorite	"	50°28'55"N. 120°55'40"W.	GSC Paper 63-17, pp. 40-41
448	GSC62-60	Bio	237**	Quartz diorite	"	50°29'N. 120°55'W.	GSC Paper 63-17, p. 40
449	GSC62-62	Bio	242**	Granodiorite	"	59°29'10"N. 121°03'30"W.	GSC Paper 63-17, p. 41
450	GSC62-58	Bio	245**	Quartz diorite	"	50°30'03"N. 120°56'25"W.	GSC Paper 63-17, p. 39
451	GSC63-2	Bio	242±12 **	Granodiorite	"	50°36'N. 121°14'20"W.	GSC Paper 64-17, (Pt. 1), p. 12
452	GSC63-3	Bio	265±14**	Quartz diorite	"	50°34'45"N. 121°13'25"W.	GSC Paper 64-17, (Pt. 1), pp. 12-13
453	GSC63-4	Bio	240±12**	Quartz diorite	"	50°29'20"N. 120°51'55"W.	GSC Paper 64-17, (Pt. 1), p. 13
454	GSC63-5	Bio	248±12 **	Granodiorite	"	50°13'10"N. 120°55'00"W. (Craigmont Open Pit)	GSC Paper 64-17, (Pt. 1), pp. 13-15
455	GSC66-35 GSC66-36 (see 389)	Bio Hb	194±10 198±12	Granodiorite	*	51°20'40"N. 120°24'00"W.	GSC Paper 67-2A, pp. 34-35

* See reference.

** Values considered to be high (see reference).

TABLE D-1 (cont'd) Published K-Ar ages referred to in this report.

Report No.	Reference Number and Mineral Dated		Age in m.y.	Rock Type	Unit	Location	Reference
				OMINICA BELT - 52° - 49°N.			
				TERTIARY AGES			
456	AK-25	Bio	36	Granite	Cascade	49°01'N. 118°18'W.	Baadsgaard, et al., 1961
457	AK-27	Bio	55 56	Granite	Nelson(?) Batholith	50°00'N. 118°06'W.	"
				CORYELL			
458	AK-28	Bio	54	Syenite	Coryell	49°03'N. 118°03'W.	"
459	AK-26	Bio	58	Syenite	"	49°04'N. 117°58'W.	"
460	GSC60-20	Bio	27	Leucrosyenite	"	49°24'N. 118°02'30"W.	GSC Paper 61-17, pp. 12-13
461	GSC61-13	Bio	32	Granite	"	49°50'30"N. 117°56'30"W.	GSC Paper 62-17, p. 11
462	GSC61-12	Bio	53	Granite	"	49°49'15"N. 117°56'20"W.	GSC Paper 62-17, p. 10
463	CX70-17	Bio	50.6±1.5	Monzonite	"	49°05'N. 117°15'W.	Macdonald, 1972, in preparation
464	CX70-21	Bio	49.5±1.5	Lamprophyre dike	"	49°05'N. 117°15'W.	"
465	R70-1	Bio	48.9±1.4	Monzonite	"	*	Fyles, et al., 197[illegible]
466	R70-5	Bio	49.0±1.5	Monzonite	"	*	"
467	R70-18	Bio	48.3±1.4	Syenite	"	*	"
468	R70-12	Bio	48.1±1.5	Gabbro	Diorite dyke	*	Fyles, et al., 197[illegible]
469	R70-3	Bio Hb	46.4±1.5 48.4±1.5	Lamprophyre	Spokane dyke	*	"
470	R70-4	Whole R	58.1±2.0 60.5±2.0	Lamprophyre	Conglomerate dyke	*	"
471	R70-7	Bio	49.0±1.4	Lamprophyre	Mayflower dyke	*	"
472	R70-9	Bio	48.8±1.6	Lamprophyre	Nickel Plate dyke	*	"
473	R70-11	Bio	49.2±1.4	Lamprophyre	Dyke	*	"
474	R70-13	Bio	48.1±1.6	Lamprophyre	Headwall dyke	*	"
475	R70-14	Whole R	47.0±1.8	Hornfels	*	*	"
476	R70-15	Bio	48.7±1.5	Quartz diorite	Rainy Day Stock	*	"
477	R70-16	Bio	50.5±1.5	Granodiorite	Trail Batholith	*	"
478	R70-17	Bio	49.5±1.4	Granodiorite	Trail Batholith	*	"
479	R70-2	Bio	47.3±1.5	Monzonite	Rossland Monzonite	*	"

* See reference.

TABLE D-1 (cont'd) Published K-Ar ages referred to in this report.

Report No.	Reference Number and Mineral Dated		Age in m.y.	Rock Type	Unit	Location	Reference
480	R70-6	Bio Bio	89.7±2.8 90.8±2.0	Monzonite	Rossland Monzonite	*	Fyles, et al., 1973.
481	R71-1	Bio	58.8±1.8	Monzonite	Rossland Monzonite	*	*
				POST-TECTONIC INTRUSIONS			
482	GSC66-46	Bio	46±3	Quartz monzonite	*	49°07'24.4"N. 118°23'14"W.	GSC Paper 67-2A, pp. 44-45
483	GSC66-45	Bio	39±5	Quartz monzonite	*	49°02'49.3" . 118°21'43"W.	GSC Paper 67-2A, pp. 41-42
484	GSC63-1	Phlogo-pite	41±10	Lamprophyre	*	51°17'N. 118°28'W.	GSC Paper 64-17, (Pt. 1), p. 11
485	GSC63-7	Bio	56±8	Granite	*	50°00'N. 123°58'W.	GSC Paper 64-17, (Pt. 1), p. 16
				TERTIARY VOLCANICS			
486	F69-203	Whole R	51.6±1.7	Latite	OK Volcanic	*	Fyles, et al., 1973.
487	AK-112	Bio	49±2	Ash	Midway	49°03.8'N. 118°58.4'W.	Mathews, 1964
488	AK-150	Bio	48±2	Pulaskite porphyry	Kettle River	49°02.8'N. 118°53.1'W.	"
489	AK-151	Bio	46±2	Dacite	Kettle River	49°48'N. 119°06.1'W.	"
490	*	Bio	51.6±1.8	*	Marron Formation (Kitley Lake member)	East of Yellow Lake*	Church, 1970, in (GEM), p. 397
				OKANAGAN			
491	W65-6	Musc	139±5	Granite	Okanagan	*	White et al., 1968
492	W65-5	Musc	144±6	Granite	"	*	"
493	W65-7	Sericite	140±6	Footwall alteration	"	*	"
494	W65-4	Bio	82±3	Granite	"	*	"
495	W66-7	Bio	99±4	Granite	"	*	"
496	W65-3	Bio	118±4	Granite	"	*	"
497	W67-1	Sericite	114±5	*	"	*	"
				NELSON BATHOLITH			
498 499	GSC66-50 GSC63-10	Hb Bio	141±16 123±20	Quartz diorite	Ruby Stock	50°04'57.5"N. 117°43'59"W.	GSC Paper 67-2A, pp. 46-47
500	GSC66-51	Hb	136±14	Granodiorite	Nelson	49°47.0'N. 117°22.4'W.	GSC Paper 67-2A, p. 47
501	GSC66-52	Hb	146±10	Granodiorite (porphyritic)	Nelson	49°49'N. 117°12'W.	GSC Paper 67-2A, pp. 47-48
502	GSC66-53	Hb	141±24	"	Nelson	49°46.4'N. 117°04.5'W.	GSC Paper 67-2A, p. 48
503	GSC62-27	Bio	159	"	Nelson	"	GSC Paper 67-2A, p. 20
504	GSC66-54 GSC62-5	Hb Bio	152±10 128	Granodiorite	Porcupine stock	49°15'N. 117°05'W.	GSC Paper 67-2A, pp. 48-49 GSC Paper 63-17, pp. 7-8

* See reference.

TABLE D-1 (cont'd) Published K-Ar ages referred to in this report.

Report No.	Reference Number and Mineral Dated		Age in m.y.	Rock Type	Unit	Location	Reference
505	GSC62-5	Bio	128	Granodiorite	Porcupine stock	49°15'N. 117°05'W.	GSC Paper 63-17, pp. 7-8
506	C	Bio	150±6	Quartz monzonite	Nelson	49°53'45"N. 117°14'23"W.	Nguyen, et al., 1968
507	D	Bio	169±6	Lamprophyre	Dike (cuts Nelson)	49°53'49"N. 117°14'23"W.	"
508	K	Hb	161±6	Quartz monzonite	Mt. Carlyle stock	49°54'58"N. 117°04'18"W.	"
509	L-236	Bio	135±5	Hornfels	Zenolith in Nelson Batholith	49°52'20"N. 117°06'57"W.	"
510	R-11	Bio	120±5	Granodiorite (porphyritic)	Nelson	49°53'15"N. 117°6'25"W.	"
511	R-12	Bio	146±5	Quartz diorite	"	49°52'56"N. 117°6'38"W.	"
512	R-13	Bio	130±5	Granodiorite (porphyritic)	"	49°43'58"N. 117°9'45"W.	"
513	S	Hb	150±5	Quartz monzonite	"	49°57'29"N. 117°21'16"W.	"
514	GSC61-17	Bio	131	Granodiorite	"	49°51'30"N. 117°02'48"W.	GSC Paper 62-17, p. 13
515	GSC62-27	Bio	159	Granodiorite	"	49°46'24"N. 117°04'30"W.	GSC Paper 63-17, p. 20
516	GSC62-29	Bio	163	Granodiorite	"	49°46'54"N. 117°20'18"W.	GSC Paper 63-17, p. 21
517	GSC62-26	Bio	165	Granodiorite	"	49°45'48"N. 117°13'30"W.	GSC Paper 63-17, p. 20
518	GSC62-28	Bio	171	Granodiorite	"	49°47'N. 117°22'24"W.	GSC Paper 63-17, pp. 20-21
519	GSC62-30	Bio	171	Granodiorite	"	49°56'N. 117°08'W.	GSC Paper 63-17, p. 21

AGES PREVIOUSLY ASSIGNED TO NELSON BATHOLITH

Report No.	Reference Number and Mineral Dated		Age in m.y.	Rock Type	Unit	Location	Reference
520	GSC60-21	Bio	49	Quartz monzonite	Nelson	49°42'N. 117°19'W.	GSC Paper 61-17, p. 13
521	GSC60-22	Bio	55	Granodiorite (porphyritic)	"	49°36'N. 117°15'W.	GSC Paper 61-17, pp. 13-14
522	GSC62-32	Bio	63	Granodiorite	"	49°29'18"N. 117°20'30"W.	GSC Paper 63-17, pp. 22-23
523	GSC59-1	Bio	86	Granodiorite	"	49°29'N. 117°20'W.	GSC Paper 60-17, p. 5
524	GSC62-31	Bio	105	Leucogranite	"	49°36'36"N. 117°07'54"W.	GSC Paper 63-17, p. 22

POST TECTONIC INTRUSIONS (see 482-485 and reference)

Report No.	Reference Number and Mineral Dated		Age in m.y.	Rock Type	Unit	Location	Reference
525	GSC64-22	Bio	52±6	Syenite	*	51°55.5'N. 118°10.5'W.	GSC Paper 65-17, p. 20
526	GSC64-15	Bio	96±5	Quartz monzonite	*	51°27'N. 119°56'W.	GSC Paper 65-17, p. 16
527	GSC64-16	Bio	80±6	Granodiorite	*	51°17'20"N. 119°29'40"W.	GSC Paper 65-17, pp. 16-17

* See reference.

TABLE D-1 (cont'd) Published K-Ar ages referred to in this report.

Report No.	Reference Number and Mineral Dated		Age in m.y.	Rock Type	Unit	Location	Reference
				CHINA HEAD MOUNTAIN STOCK			
528	GSC67-42	Hb	73±4	Granodiorite	*	51°10'N. 122°23'W.	GSC Paper 69-2A, p. 25
				FRY CREEK BATHOLITH			
529	GSC60-18	Bio	45	Quartz monzonite	Fry Creek	50°05'N. 116°51'W.	GSC Paper 61-17, p. 11
530	GSC60-19	Musc	63				
531	GSC62-12	Bio	76	Quartz monzonite	"	49°52'N. 116°34'W.	GSC Paper 63-17, pp. 10-11
532	GSC62-8	Musc	83	Quartz monzonite	"	49°59'N. 116°44'12"W.	GSC Paper 63-17, p. 9
533	GSC62-11	Bio	86	Quartz monzonite	"	50°05'24"N. 116°33'24"W.	GSC Paper 63-17, p. 10
534	GSC62-10	Musc	91				GSC Paper 63-17, p. 9-10
535	GSC62-9	Musc	97	Quartz monzonite	"	50°01'54"N. 116°39'42"W.	GSC Paper 63-17, p. 9
				BAYONNE BATHOLITH			
536	GSC62-7	Bio	33	Granodiorite	Bayonne Batholith	49°16'30"N. 116°39'W.	GSC Paper 63-17, pp. 8-9
537	KA 118	Bio	77	Granodiorite	Kootenay Lake	49°15'N. 116°39'W.	Baadsgaard et al., 1961
538	GSC62-6	Bio	100	Quartz monzonite	Bayonne Batholith	49°24'30"N. 116°44'18"W.	GSC Paper 63-17, p. 8
				ANGUS CREEK STOCK			
539	GSC62-43	Bio	118	Granodiorite	Angus Creek	49°33'N. 116°08'36"W.	GSC Paper 63-17, p. 30
				LOST CREEK STOCK			
540	GSC62-4	Bio	119	Quartz monzonite	*	49°05'36"N. 117°10'12"W.	GSC Paper 63-17, p. 7
				DODGER STOCK			
541	CX-70-19	Bio	100±3	Granite	Dodger Stock	49°05'N. 117°15'W.	Macdonald, 1972, in prep.
				KUSKANAX BATHOLITH			
542	GSC62-33	Bio	66	Quartz monzonite	Kuskanax	50°41'N. 117°53'W.	GSC Paper 63-17, pp. 24-25
543	GSC62-34	Musc	90				
544	GSC66-48	Musc	137±7	Feldspar porphyry	"	50°25'15"N. 117°20'50"W.	GSC Paper 67-2A, pp. 44-45
				ICE RIVER COMPLEX			
545	AK 46	Bio	355	Jacupirangite	Ice River	51°10'N. 116°23'W.	Baadsgaard, et al., 1961a
546	AK 83	Bio	360	Minette	"	51°08'N. 116°24'W.	"
547	AK 84	Bio	304	Pegmatite	"	51°11'N. 116°27'W.	"

* See reference.

TABLE D-1 (cont'd) Published K-Ar ages referred to in this report.

Report No.	Reference Number and	Mineral Dated	Age in m.y.	Rock Type	Unit	Location	Reference
548	GSC59-7	Bio	340	Syenite	Ice River	51°12'N. 116°29'W.	GSC Paper 60-17, pp. 6-7
549	GSC59-8	Bio	330	*	"	51°12'N. 116°29'W.	GSC Paper 60-17, p. 7
550		Pyroxenite	392	Biotite pyroxenite	*	*	Rapson, 1963, pp. 116-124
551		Bio	336	Biotite pegmatite	*	*	"
552		Bio	327	Minette sill	*	*	"
				TOBY STOCK			
553	GSC66-49	Hb	162±8	Granodiorite	Toby	50°13'N. 116°34'W.	GSC Paper 67-2A, pp. 45-46
554	GSC62-14	Bio	179	Granodiorite gneiss	Toby	50°11'N. 116°34'W.	GSC Paper 63-17, pp. 12-13
555	GSC62-13	Bio	232	Granodiorite	Toby	50°12'36"N. 116°33'24"W.	GSC Paper 63-17, pp. 13-14
				ADAMANT BATHOLITH			
556	GSC64-23	Whole R	97±12	Monzonite	Adamant Pluton	51°44'N. 117°55'W.	GSC Paper 65-17, pp. 20-21
557	GSC61-24	Bio	90	Granodiorite	Adamant	51°46'8"N. 117°54'20"W.	GSC Paper 62-17, pp. 16-17
558	GSC62-24	K-feldspar	92	Granodiorite	Adamant	51°44'30"N. 118°44'W.	GSC Paper 63-17, pp. 18-19
559	GSC61-22	Bio	131	Pegmatite	Adamant	51°42'40"N. 117°50'30"W.	GSC Paper 62-17, p. 15
560	GSC61-23	Bio	200	Granodiorite	Adamant	51°46'8"N.	GSC Paper 62-17, pp. 15-16
561	GSC62-25	Hb	116			117°51'30"W.	GSC Paper 63-17, p. 19
562	GSC61-21	Bio	281	Granodiorite	Adamant	51°42'40"N. 117°50'30"W.	GSC Paper 62-17, p. 15
				WHITE CREEK BATHOLITH			
563	GSC60-3	Bio	18	Quartz monzonite	White Creek	49°53'N. 116°22'W.	GSC Paper 61-17, p. 6
564	GSC60-4	Bio	29	Quartz monzonite	"	49°50'N. 116°17'W.	GSC Paper 61-17, pp. 6-7
565	GSC60-5	Bio	56	Mafic-rich inclusion	"	49°48'N. 116°16'W.	GSC Paper 61-17, p. 7
566	GSC60-6	Bio	60	Quartz monzonite	"	49°51'N. 116°14'W.	GSC Paper 61-17, p. 7
567	GSC61-9	Bio	73	Granodiorite	"	49°48'33"N. 116°13'10"W.	GSC Paper 62-17, p. 9
568	GSC60-7	Bio	79	Granodiorite	"	49°48'N. 116°13'W.	GSC Paper 61-17, pp. 7-8
569	GSC61-11	Musc	80	Quartz	"	49°51'10"N.	GSC Paper 62-17, p. 10
570	GSC61-10	Bio	82	monzonite		116°16'40"W.	" , p. 9
571	GSC62-2	Bio	126	Meta-diorite	"	49°47'18"N. 116°18'54"W.	GSC Paper 63-17, p. 5

* See reference.

TABLE D-1 (cont'd) Published K-Ar ages referred to in this report.

Report No.	Reference Number and Mineral Dated		Age in m.y.	Rock Type	Unit	Location	Reference
572	GSC62-3	Bio	138	Quartz diorite sill	White Creek	49°45'42"N. 116°19'48"W.	GSC Paper 63-17, pp. 7-8
				HORSETHIEF CREEK BATHOLITH			
573	GSC62-16	Bio	108	Quartz monzonite	Horsethief Creek	50°36'12"N. 116°30'42"W.	GSC Paper 63-17, p. 14
574	GSC61-19	Bio	205	Granite	"	50°38'6"N. 116°35'42"W.	GSC Paper 62-17, pp. 13-14
575	GSC65-21	Bio	96±16	Schist	*	51°48'N. 117°58'W.	GSC Paper 66-17, pp. 24-25
576	GSC65-20	Musc	55±8				
				FANG CREEK STOCK			
578	GSC62-23	Bio	168	Granodiorite	Fang stock	51°20'N. 117°50'W.	GSC Paper 63-17, p. 18
579	GSC70-5	Hb	164±9				GSC Paper 71-2, p. 8
				BATTLE BATHOLITH			
580	GSC62-21	Musc	91	Quartz monzonite	Battle Batholith	51°03'N. 117°30'W.	GSC Paper 63-17, p. 17
581	GSC62-20	Bio	92				" , p. 16
582	GSC62-19	Bio	94	Quartz monzonite	"	51°03'N. 117°30'W.	GSC Paper 63-17, p. 16
583	GSC62-22	Musc	120	Pegmatite	"	51°03'N. 117°30'W.	GSC Paper 63-17, pp.17-18
				BUGABOO BATHOLITH			
584	GSC61-20	Bio	100	Granodiorite	Bugaboo Batholith	50°44'6"N. 116°55'30"W.	GSC Paper 62-17, p. 14
585	GSC62-17	Bio	132	Quartz monzonite	"	50°45'36"N. 116°49'6"W.	GSC Paper 63-17, p. 15
586	GSC62-18	Musc	138				" , pp. 15-16
				GLACIER CREEK STOCK			
587	GSC61-18	Bio	127	Granodiorite	Glacier Creek	50°23'12"N. 116°47'49"W.	GSC Paper 62-17, p. 13
588	GSC62-15	Bio	145	Granodiorite	"	50°23'12"N. 116°47'42"W.	GSC Paper 63-17, p. 13
				SHUSWAP METAMORPHIC COMPLEX (After Gabrielse & Reesor, 1964)			
				VALHALLA COMPLEX			
589	GSC59-5	Bio	11	Granite-gneiss	Valhalla	49°51'N. 117°41'W.	GSC Paper 60-17, p. 6
590	GSC59-4	Bio	13	Granodiorite gneiss	"	49°51'N. 117°37'30"W.	GSC Paper 60-17, p. 6
591	GSC60-8	Bio	15	Granite-gneiss	"	49°57'N. 117°35'10"W.	GSC Paper 61-17, p. 8
592	GSC59-6	Bio	16	Granodiorite gneiss	"	49°51'30"N. 117°37'W.	GSC Paper 60-17, p. 6
593	GSC60-9	Bio	25	Granitic gneiss	"	49°52'30"N. 117°41'15"W.	GSC Paper 61-17, p. 8

* See reference.

TABLE D-1 (cont'd) Published K-Ar ages referred to in this report.

Report No.	Reference Number and Mineral Dated		Age in m.y.	Rock Type	Unit	Location	Reference
594	GSC60-10	Bio	28	Quartz monzonite (gneiss)	Valhalla	49°37'N. 117°48'W.	GSC Paper 61-17, pp. 8-9
595	GSC60-11	Bio	31	Granite gneiss	"	49°47'30"N. 117°37'W.	GSC Paper 61-17, p. 9
596	GSC60-12	Bio	42	Granite	"	49°48'N. 117°49'40"W.	GSC Paper 61-17, p. 9
597	GSC60-13	Bio	46	Pegmatite	"	49°42'53"N. 117°42'20"W.	GSC Paper 61-17, pp. 9-10
598	GSC60-14	Bio	47	Gneiss	"	49°46'N. 117°29'W.	GSC Paper 61-17, p. 10
599	GSC60-15	Bio	58	Gneissic Granite	"	49°53'13"N. 117°42'W.	GSC Paper 61-17, p. 10
600	GSC61-16	Bio	58	Granite	"	49°48'N. 117°54'W.	GSC Paper 62-17, p. 12
601	GSC61-15	Bio	59	Granite-gneiss	"	49°42'25"N. 117°54'W.	GSC Paper 62-17, p. 12
602	GSC60-16	Bio	60	Granite-gneiss	"	40°53'47"N. 117°37'20"W.	GSC Paper 61-17, pp. 10-11
603	GSC60-17	Bio	62	Gneiss	"	49°42'N. 117°36'W.	GSC Paper 61-17, p. 11
604	GSC61-14	Bio	66	Granite	"	49°44'N. 117°58'W.	GSC Paper 62-17, p. 11
605	GSC62-39	Bio	69	Quartz monzonite	"	49°59'14"N. 117°50'W.	GSC Paper 63-17, pp. 28-29
606	GSC63-11	Bio	107±6	Quartz monzonite	*	50°1'23"N. 117°42'23"W.	GSC Paper 64-17, Pt. 1, p. 19
607	GSC63-10	Bio	123±20	Diorite	*	50°04'57.5"N. 117°43'59"W.	GSC Paper 64-17, Pt. 1, p. 18
608	GSC63-12	Bio	74±4	Quartz monzonite	*	50°2'17"N. 117°35'19"W.	GSC Paper 64-17, Pt. 1, p. 20
609	GSC63-8	Bio	110±6	Granite*	*	*	GSC Paper 64-17, Pt. 1, pp. 16-17
610	A	Bio	149±5	Granodiorite (porphyritic)	Fennell Cr. Stock	49°53'12"N. 117°14'11"W.	Nguyen, et al., 1968
611	GSC66-43	Hb	61±6	Granodiorite gneiss	Shuswap	50°34'N. 118°9'W.	GSC Paper 67-2A, pp. 40-41
612	GSC66-44	Hb	79±8	Granodiorite	Shuswap	50°33'12"N.	GSC Paper 67-2A, p. 41
613	GSC62-35	Bio	64	gneiss		118°04'54"W.	GSC Paper 63-17, pp. 25-26
				MONASHEE GROUP			
614	AK 25	Bio	36	Gneissic granite	Monashee	49°1'N. 118°18'W.	Baadsgaard et al., 1961
615	GSC61-5	Bio	52	Gneiss	"	50°34'N. 118°43'W.	GSC Paper 62-17, p. 6
616	GSC61-4	Bio	57	Pegmatite	"	50°34'N. 118°43'W.	GSC Paper 62-17, p. 6
617	AK 29	Bio	57	Granodiorite	"	51°08'N. 118°11'W.	Baadsgaard et al., 1961
618	GSC60-1	Bio	62	Gneiss	"	50°15'N. 119°09'W.	GSC Paper 61-17, p. 5

* See reference.

TABLE D-1 (cont'd) Published K-Ar ages referred to in this report.

Report No.	Reference Number and Mineral Dated		Age in m.y.	Rock Type	Unit	Location	Reference
619 620	GSC62-45 GSC62-44	Musc Bio	65 70	Quartzite	Monashee	50°49'13"N. 118°15'9"W.	GSC Paper 63-17, p. 31
621	GSC61-6	Bio	71	Pegmatite	"	50°56'N. 118°27'W.	GSC Paper 62-17, p. 7
622	GSC62-46	Musc	73	Quartzite	"	50°49'N. 118°15'30"W.	GSC Paper 63-17, pp. 31-32
623	GSC62-47	Bio	76	Granite	"	50°47'24"N. 118°15'16"W.	GSC Paper 63-17, p. 32
624	GSC61-8	Musc	81	Pegmatite	"	50°49'3"N. 118°15'48"W.	GSC Paper 62-17, pp. 8-9
625	GSC62-48	Bio	81	Paragneiss	"	50°46'44"N. 118°14'16"W.	GSC Paper 63-17, pp. 32-34
626	GSC62-36	Bio	89	Gneiss	"	50°32'N. 118°2'W.	GSC Paper 63-17, p. 26
627	GSC61-7	Bio	102	Paragneiss	"	50°56'N. 118°27'W.	GSC Paper 62-17, pp. 7-8
628	AK 27	Bio	55 56	Granite	"	50°00'N. 118°06'W.	Baadsgaard et al., 1961
629	AK 47	Bio	96	Granite (porphyritic)	"	49°58'N. 118°18'W.	Baadsgaard et al., 1961
				MT. IDA GROUP			
630	GSC62-37	Bio	127	Leucocratic rock	"	50°46'N. 119°20'W.	GSC Paper 63-17, p. 26
631 632	GSC61-2 GSC61-3	Bio Musc	136 140	Schist	"	50°48'N. 118°42'W.	GSC Paper 62-17, p. 5 " , p. 6
633	GSC61-1	Bio	140	Gneiss	"	50°47'30"N. 118°40'W.	GSC Paper 62-17, p. 5
				METAMORPHIC ROCKS NORTH AND SOUTH OF ADAMANT BATHOLITH			
634 635	GSC62-49 GSC62-50	Bio Musc	73 72	Schist	*	51°54'10"N. 117°56'8"W.	GSC Paper 63-17, p. 34
636	GSC61-28	Musc	107	Pegmatite	*	51°48'N. 117°57'W.	GSC Paper 62-17, p. 18
637 638	GSC62-51 GSC62-52	Bio Musc	119 124	Schist	*	51°34'55"N. 117°38'4"W.	GSC Paper 63-17, p. 35
639 640	GSC62-53 GSC62-54	Bio Musc	146 205	Schist	*	51°34'5"N. 117°33'30"W.	GSC Paper 63-17, p. 36 " , pp. 37-38
				UNDIFFERENTIATED METAMORPHICS			
641	GSC64-18	Phlogopite	51±10	Marble	Chancellor Formation	51°58'N. 118°1.5'W.	GSC Paper 65-17, p. 18
642 643	GSC64-19 GSC64-20	Bio Musc	58±6 67±10	Quartzite	*	51°47'N. 117°43'W.	GSC Paper 65-17, p. 18

TABLE D-1 (cont'd) Published K-Ar ages refered to in this report.

Report No.	Reference Number and	Mineral Dated	Age in m.y.	Rock Type	Unit	Location	Reference
			Vancouver Island (Supplement)				
644	KN-68-158	Whole R	32.3±1.6	Dike		E. Straggling Island	Unpublished K. Northcote B.C. Dept. Mines & Pet. Res.
645	PN-70-124A	Bio	50.6±1.7	Intrusive		Hepler Creek	"
646	KN-69-10	Whole R	103±4	Rhyodacite		East side of mouth of Hansons Lagoon	"
647	KN-69-8	Whole R	135±4 134±4	Rhyolite		Cape Scott	"
648	KN-69-98 VI	Whole R	139±4	Rhyodacite		East side of mouth of Hansons Lagoon	"
649	PN-70-124A	Bio	145±5	Intrusive		Helper Creek	"
650	KN-69-327	Whole R	145±6	Rhyodacite		Radar Domes San Josef	"
651	KN-68-177A	Bio	154±6	Intrusive		East End Rupert Inlet	"
652	CN-70-152	Bio	159±5	Intrusive		Southeast of Nahwitti Lake	"
653	KN-68-168	Whole R	161±6		Bonanza	Apple Bay	"
654	KN-69-234	Bio	163±6			North of Nahwitti Lk.	"
655	CN-70-204B	Bio	166±5	Granitic intrusive		Ridge east of Stranby & south of Irony	"
656	KN-69-264A	Bio	169±6			North of west end of Nahwitti Lake	"
657		Whole R	182±6			Shaft Creek (Liard Copper)	unpublished age B.C. Dept. Mines & Pet.